Macrocycle functionalized supramolecular gels and the host-guest chemistry of dendrimers in the gas phase

Dissertation Zur Erlangung des akademischen Grades des
Doktors der Naturwissenschaften
(Dr. rer. nat.)

eingereicht im Fachbereich Biologie, Chemie und Pharmazie
der Freien Universität Berlin

vorgelegt von

Zhenhui Qi

aus Zhejiang, V. R. China

June, 2013

The research results presented in this thesis were achieved during the period from September 2009 to June 2013 at the Institut für Chemie und Biochemie of Freie Universität Berlin under the supervision of Prof. Dr. Christoph A. Schalley.

1st Reviewer: Prof. Dr. **Christoph A. Schalley**
2nd Reviewer: Prof. Dr. **Rainer Haag**

Date of Defense: June 18, 2013

Dedicated to my wife and my parents

人之云 非知之难 行之惟难 非行之难 终之斯难

— 吴兢（唐，公元 670-749）

The difficult thing is not just to know something, but to do it;

The difficult thing is not even to do something, but to be persistent in doing it.

— Jing Wu（A.D. 670-749, China）

Table of contents

1. Preface

In the past two decades, the fast development of supramolecular chemistry has greatly expanded the knowledge of chemistry beyond the molecule itself. The supramolecular method represented by self-assembly has become one of most fashionable synthetic methods to make highly complicated hierarchical structures which closely resemble their natural counterparts. Artificial membranes, enzymes and ion channels among other biological structures have been successfully realized by supramolecular synthesis. Supramolecular gel is an intriguing supramolecular synthetic entity as it exhibits selective environmental responsiveness, thus serving as a novel means for creating “smart” materials. The highly dynamic nanostructures (e.g. fibers) in supramolecular gels provide ideal scaffolds to mimic the natural molecular networks and their functions. However, one prerequisite to achieve all these conceptions requires endowing the precise responsive sites on these gel or nanostructures. Obviously, macrocycles and their host-guest chemistry should be excellent candidates for this purpose. The large numbers of macrocycles with diverse conformation, geometry, topology, solubility, biocompability etc. can be utilized as design elements for creation of target objects. Furthermore, a vast knowledge of the host-guest chemistry of macrocycles as well as their explored functionality is available to bestow the gels/nanostructures with innovative responsiveness and functionalities. Nowadays, growing evidence has shown the great potential of incorporating macrocycles in supramolecular gels. Interestingly, the joint force of extra supramolecular building blocks and characterization technologies such as dendrimers and mass spectrometry, respectively, provides an additional dimension to the understanding of highly dynamic assembly processes. When looking at the past achievements in the concerned fields, one must marvel that the most interesting part of macrocycle-functionalized supramolecular synthetic entities is yet to come.

2. Aim of the research

In this thesis, I attempt to expand the macrocycles and their host-guest chemistry into two different dimensions: 1) The construction of novel crown ether-functionalized supramolecular gels and utilizing the host-guest chemistry of crown ethers plus other supramolecular interactions to equip new soft materials with unprecedented properties; 2) Development of crown ether-functionalized dendrimers and study of their host-guest chemistry in solution and the gas phase.

Macrocycles like crown ethers have attracted considerable attention in the past decades, and their host-guest chemistry has been well developed, too. Until now, there are many supramolecular gels based on macrocycles reported.[1, 2] However, most of them only focused on the construction of macrocycle-containing supramolecular gels. And the design of new supramolecular gels mainly arises from serendipitous discovery or from extension of previously discovered basic gelation elements. This problem is especially prominent for low-molecular-weight gelators. For this reason, attempts to rationalize the gelling power between molecular structure and solvents are highly welcome. Therefore, more macrocycle-functionalized supramolecular gels should be invented, and enhanced functionality of macrocycle-containing supramolecular gels need to be further explored. Many interesting properties of macrocycles have not been fully used in gel chemistry. Recently, the development of systems chemistry has pushed the research paradigm to systems with multiple components. The orthogonal self-assembly of supramolecular gels with surfactants reported by Jan van Esch et al.[3, 4] can be used in the construction of cell architecture mimics. Therefore, employing the systems approach may afford gel materials with unprecedented properties.

Since two dendrimer components interact with each other, their binding mode is close related to multivalency behaviors in nature (e.g. virus particles docking to the corresponding receptors on the cell surface). We hope the unique environment within the mass spectrometer and powerful tandem mass spectrometric experiments could unravel some valuable information concerning these multivalent systems. Our group recently found that crown ether ([18]crown-6) can move like “spacewalk” upon the surface of

larger molecular scaffolds featuring many binding sites for it, e.g. oligolysine peptides[5] as well as the periphery of polyamino propylene amine (POPAM) dendrimers[6] with all its amino termini. Now, the question is: what if we synthesize a POPAM dendrimer that has crown units on all its branches and mix it with an amino-terminated POPAM dendrimer? They should form complexes by bridging more than once through crown/ammonium interactions. As the crown moves around different ammonium termini, we could visualize the rolling behavior of the two dendrimers utilizing the H/D exchange experiment. Consequently, there would be a new kind of intermolecular movement in the gas phase.

3. Introduction

3.1 Macrocycle-functionalized supramolecular gels

Gels

Gels are a type of solid, jelly-like material (Figure 1a). They not only represent an intriguing case of self-assembly and phase separation, but also serve as a novel means for creating "smart" materials.[7-11] In microscopic views, gels usually consist of three dimensional (3D) networks that span the volume of a liquid medium and entrap the solvent through the surface tension effect.[12] Principally, as depicted in Figure 1b, these internal 3D-network structures can be constructed either by chemical bonds (chemical gels) or by non-covalent interactions (physical gels).[9] In this context, any gelating species that use non-covalent interactions such as hydrogen bonds, π-π interactions, metal coordination, or host-guest inclusion can also be described as supramolecular gels,[13] Hence, this definition includes gels composed of macromolecular and low-molecular-weight building blocks. Therefore, the supramolecular gels can be further divided into supramolecular polymeric gels[14] and low-moleulcar-weight gels (LMWGs),[7, 8, 13, 15, 16] depending on the molecular weight of the gel's building blocks.

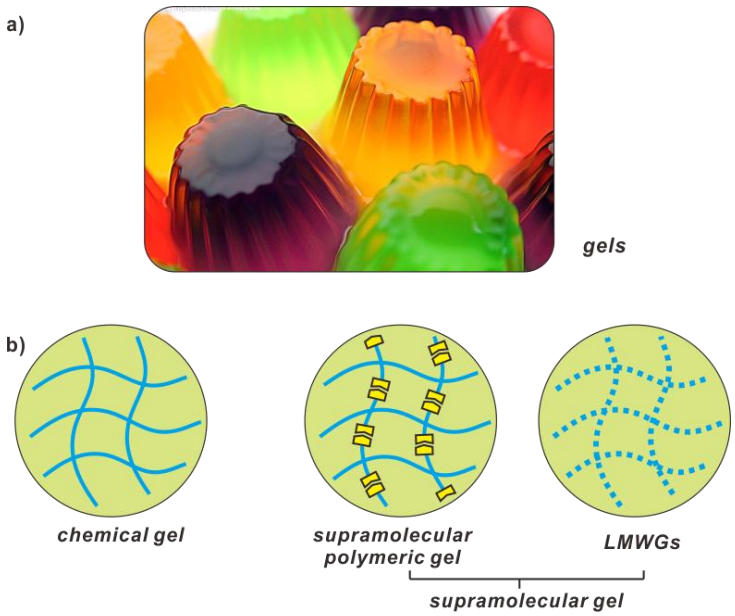

Figure 1. a) Photography of puddings, one of most common gels in daily life (pic source: internet[17]); b) illustration of the difference of chemical gels and supramolecular gels.

Why supramolecular gels?

Since chemical gels are interconnected by persistent non-reversible bonds, they are mechanically stable and can be considered permanent on an experimental timescale. This feature is favorable for applications that require tough polymer materials, but it is detrimental if these materials shall be further processed or recycled. Therefore, the usage of chemical gels for encapsulation and controlled release applications is limited. In contrast, supramolecular gels are particularly responsive and a tunable form of soft matter.[10, 18] The reversibility of supramolecular interactions in gel networks greatly facilitates their processing and recycling (Figure 2).[19] A wide range of external stimuli can dramatically affect the physical properties of the resulting gels (e.g. viscosity).[18] These stimuli include temperature variation, mechanical force (sonication), oxidation, change of the pH value, addition of specific chemical compounds as well as light irradiation.[20-24] Therefore, the environmental responsiveness makes the supramolecular gels well suitable as 'smart media' for immobilizing cargo (drugs, proteins, etc.) and releasing it on demand. Some supramolecular gels based on macromolecular building blocks not only retain the mechanical characteristics of chemical gels,[25] but also possess responsive de-crosslinking behavior under certain stimuli,[26] which significantly promotes the utility of supramolecular gels.

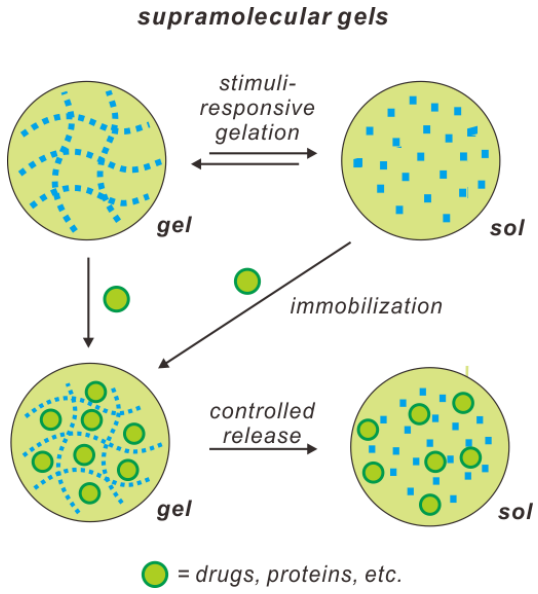

Figure 2. Illustration of the responsiveness of supramolecular gels to changes in the environment making application for immobilization and controlled release possible.

Why should macrocycles be introduced into supramolecular gels?

Macrocycles are important and useful building blocks for supramolecular chemistry.[27-30] They provide a range of hosts that can encapsulate guest molecules often with selectivity and can be chemically modified to fine-tune their properties. Until now, a vast number of macrocyclic compounds with different constitutions, size, shapes and polarities have been developed (Figure 3). Such examples of compounds include porphrins,[31-34] crown ethers,[35-41] calixarenes,[42-46] cucurbituriles,[47-49] cyclophanes,[50] cyclodextrins (CDs),[51-60] and arylene ethynylenes.[61, 62] Moreover, the large family of macrocycles, nonetheless, continues to rapidly increase due to the constant discovery of new macrocycles like pillararenes,[63, 64] asararenes,[65] metallocavitands,[66] and many natural bioactive macrocycles isolated from soil bacteria or marine organisms etc.[67] With a rising number of macrocycles available, investigations of host-guest chemistry of macrocycles can be carried out in more detail.[68] Over the last decades, a plentiful knowledge of host-guest chemistry of macrocycles has been obtained. As a result, the macrocycles and their host-guest chemistry were broadly utilized as supramolecular synthons for constructing complicated architectures and to unravel the underlying rules which govern the natural systems. This contribution also includes the conception birth of supramolecular chemistry itself.[69, 70] Moreover, based on the unique host-guest chemistry of macrocycles, numerous applications were explored, such as catalysis,[71] drug delivery,[60, 72-74] cosmetics,[75] photochemistry,[33, 34] gas separation,[76] molecular sensing[37, 45] and others.[39, 77]

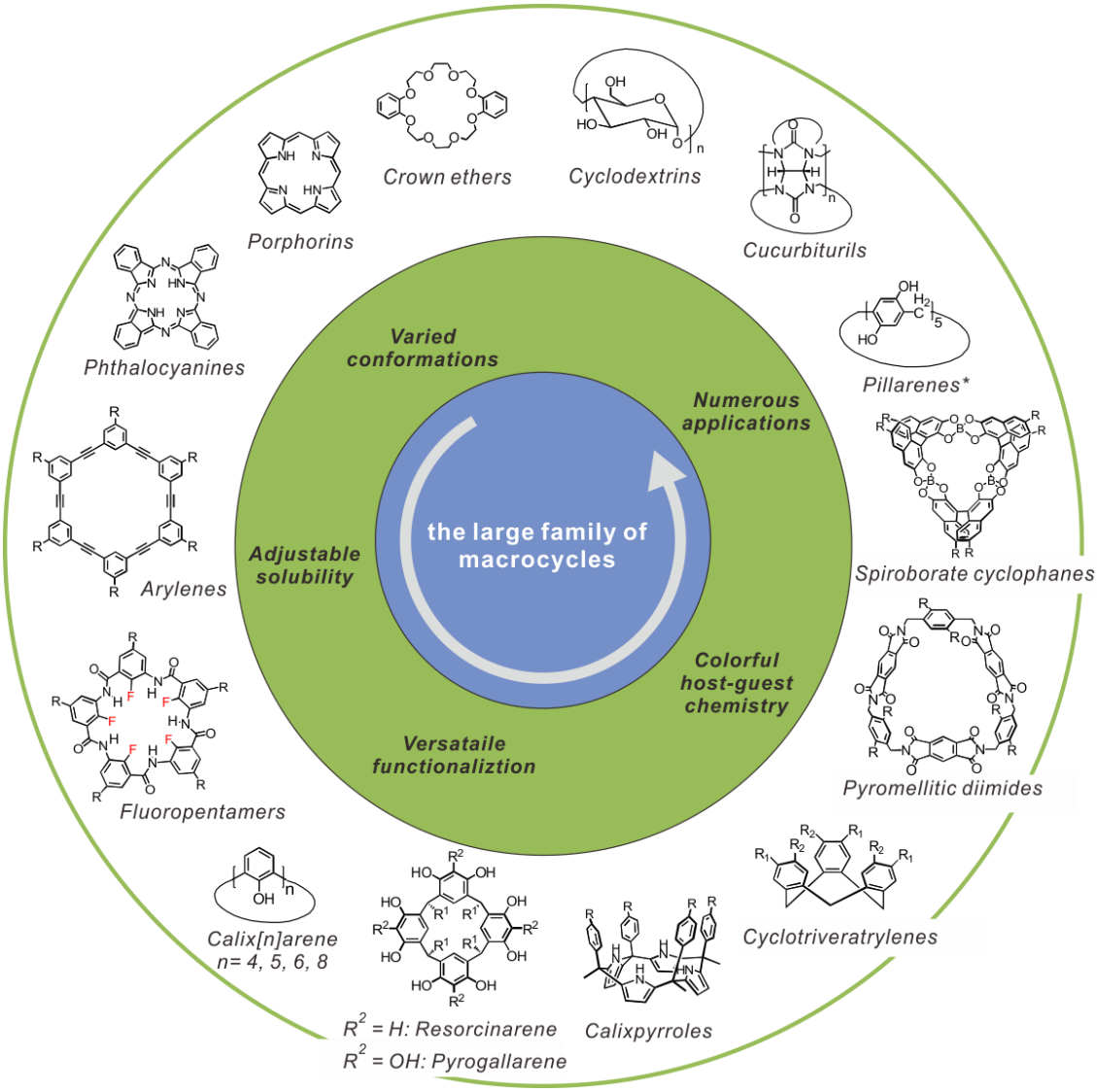

Figure 3. The large family of macrocycles: all the macrocycles (except pillarenes) shown in the picture have been already utilized to design supramolecular gels. The inner green circle lists some typical advantage of macrocycles.

Therefore, the introduction of macrocycles into supramolecular gels opens up unprecedented opportunities which are impossible to obtain with other gel systems. Large numbers of macrocycles with diverse conformation, geometry, topology, solubility, and biocompability etc. can be used as design elements in order to create novel gelators. Furthermore, the vast knowledge of host-guest chemistry of macrocycles as well as their explored functionalities is available to furnish the gel materials with innovative function in combination of their unique physical properties.

The role of macrocycles for the formation of supramolecular gels

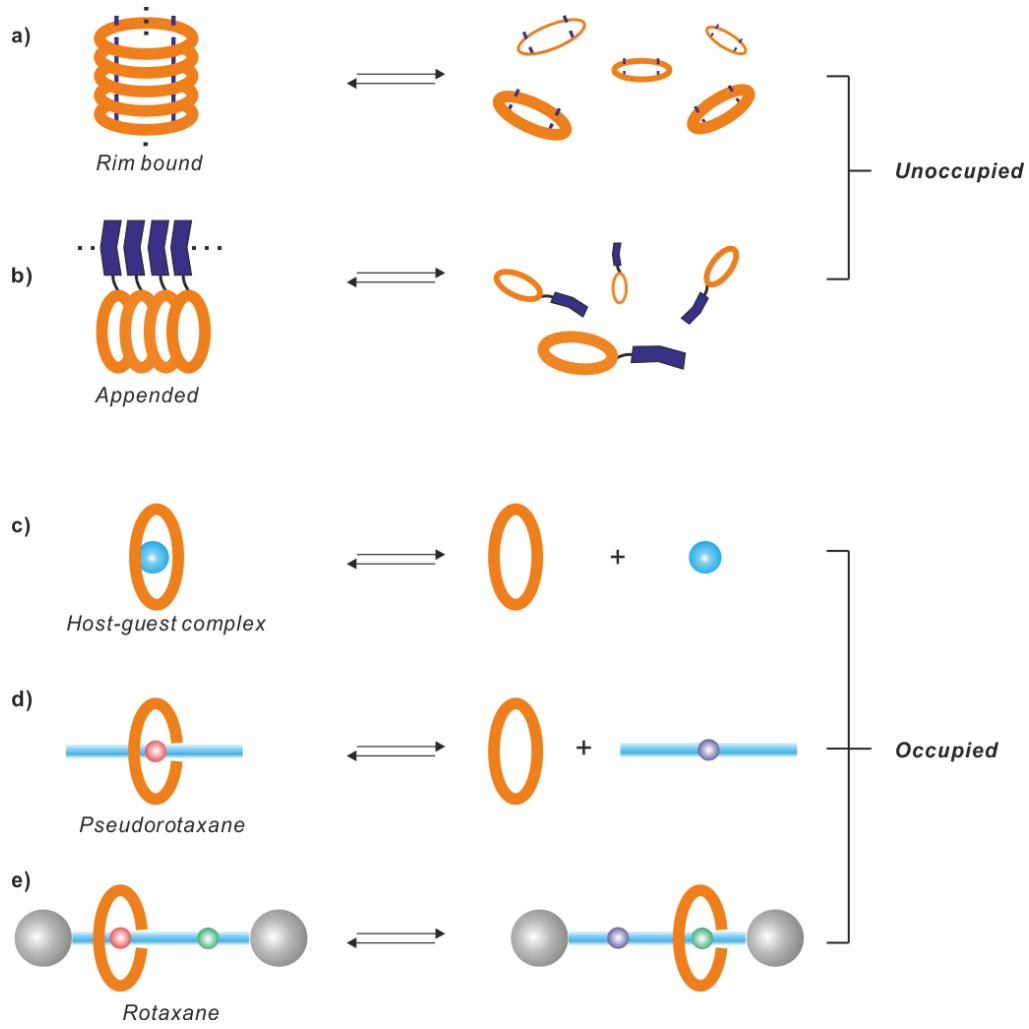

Scheme 1. Illustration of five different types of incorporation of macrocycles in supramolecular gels: a) - b) unoccupied macrocycles; occupied macrocycles with different complexation motifs: c) host-guest complex; d) *pseudo*rotaxane; e) rotaxane.

According to the role of macrocycles in the gel formation，macrocycle-functionalized supramolecular gels can be classified into two categories: the unoccupied form and the occupied one (Scheme 1). In the first category, the macrocycle contributes only the skeleton. Its binding site/cavity remains unexploited (Scheme 1a, 1b). Interactions between the rims of macrocycles or side chains appended to the cavity constitute the main driving force for the formation of gels. In the second category, the macrocycle is occupied by a guest molecule to form a host-guest complex (Scheme 1c),

*pseudo*rotaxanes (Scheme 1d) or rotaxanes (Scheme 1e). In each case, the interaction between macrocycle and guest is of critical importance for the construction of structures with a higher order. The complexed guest molecule can leave or dethread the macrocycle host under certain stimuli, which leads to the disruption of pre-organized structures resulting in the macroscopic collapse of the gel phase. In cases where rotaxanes are used for gel formation, the structure is mechanically interlocked by large bulky groups. Hence, the macrocycle can only slide along the axle but never dethread. Such a sliding movement still can result in the macroscopic change (e.g. gel-sol transition), although the 3D-networks still exist. Overall, the roles of macrocycles in the gel formation largely determine the strategies used to design stimuli for gels.

3.2 Characterization of macrocycle-functionalized supramolecular gels.

In principle, any analytical methods used in supramolecular chemistry can be applied to characterize (macrocycle-functionalized) supramolecular gels.[78] Spectroscopic techniques like FT-IR, UV-vis absorption, luminescence and NMR spectroscopies are frequently utilized in probing the molecular organization of the gels. It is worth to note that circular dichroism (CD) spectroscopy is particularly useful to investigate if the gelator molecules self-assemble in a specific chiral arrangement.[79] However, special care has to be taken when one evaluates the obtained CD signal, since potential artificial signals resulting from linear dichroism (LD)[80] might lead to the wrong conclusion.

For the characterization of the morphology of gels, microscopic techniques, including atomic force microscopy (AFM), scanning electron microscopy (SEM) and transmission electron microscopy (TEM) are useful tools. In order to determine cross-sectional profiles and directional anisotropy of fibers like aggregates, scattering techniques, like small angle X-ray (SAXS) or neutron (SANS) scattering, are often used.[81]

Since gels are kind of soft materials, it is essential to evaluate their mechanical properties. Therefore, rheology is the method of choice to study the deformation or the flow of gel sample under a given stress. Depending on the angular frequency of the applied stress, the elasticity of gel can be measured by the storage modulus (G') and loss modulus (G''). For solid-like gels, the G' values usually are constantly larger than the loss modulus *G*'' over the whole range of frequency. The interesting feature of rheology is that it even can provide valuable information on the junction zones,[82] number and energetics of the entanglement of fibers in the 3D-networks.[83] Recently, Bouteiller et al. summarized various kinds of application of rheology in characterizing supramolecular gels.[84]

For LMWGs, the gel-sol transition temperature (T_{gs}) and the critical gelation concentration (CGC) are two important data for a given LMWG. T_g provides a thermal stability criterion in a appointed solvent at a specified concentration.[85] The CGC value depicts the minimum LMWG concentration to induce gel formation, thus reflecting the gelation efficiency in a tested solvent.

3.3 Exploring novel applications of macrocycle-functionalized supramolecular gels

Selective responsiveness

Conferring responsiveness to gels is a prerequisite for the development of smart materials. Therefore, exploring macrocycle-containing supramolecular gels which are responsive to temperature, mechanical, light and chemical stimuli is virtually important and has been extensively studied.[20, 23, 24] Especially in regard to chemical stimuli, a diversity of responsive signals have been developed, such as host-guest interactions,[86] the addition of acid/bases[87-90] and/or ions,[91, 92] metal coordination,[93-95] CO_2 absorption,[96, 97] light,[95, 98-100] redox chemicals,[101-103] chiral recognition[104-106] and biomolecules insertion[21] (e.g. enzymes). Numerous reviews have extensively summarized supramolecular gels with one or several types of responsiveness.[19-24, 91, 93, 106-109] In the following paragraph, only a few unique examples are highlighted.

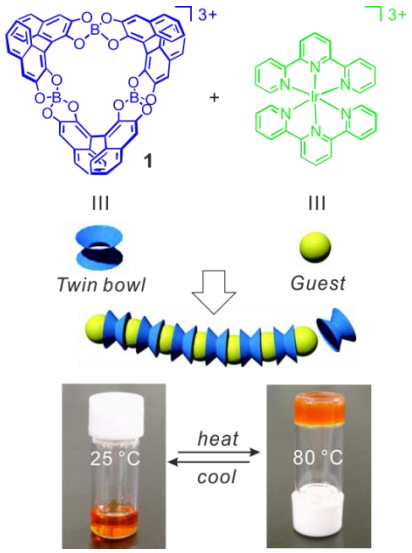

Figure 4. An example of gel formation while occurs upon the increase of temperature.[110] Copyright © 2009, American Chemical Society.

Thermo-responsibility is a universal characteristic of supramolecular gels, due to the temperature-dependent property of most supramolecular interactions. Normally, (macrocycle-containing) supramolecular gels show a gel-sol transition when the temperature increases. However, the gel formation which takes place when the temperature increases is quite rare.[104] Recently, Danjo et al. have reported a new class of

supramolecular gel based on D_3-symmetric tris(spiroborate) cyclophanes $\mathbf{1}^{3-}$ which shows gel formation only when the temperature is increased.[110] Macrocycle $\mathbf{1}^{3-}$ itself adopts a back-to-back, twin bowls shape, and exhibits molecular recognition of cationic metal compounds,[111] e.g. $[Ir(tpy)_2](PF_6)_3$, through π-π and electrostatic interactions at both sides of a symmetry plane (Figure 4). When equivalent amounts of host $\mathbf{1}^{3-}$ and guest $[Ir(tpy)_2](PF_6)_3$ were dissolved in DMF (10 mM), they can form supramolecular chain structures by iterative host-guest interaction, which was confirmed by ^{1}H NMR, CSI-MS and crystal characterization. Intriguingly, the resulting chain structure in *N*,*N*,*N*′,*N*′,*N*″,*N*″-hexamethylphosphoric triamide (HMPA) solution showed rapid gelation behavior when it was heated above the lower critical solution temperature (LCST, e.g. 78.5 ℃ at this concentration). After cooling to ambient temperature, the gel quickly returns to its solution phase (within 15 min). Thus a sol-gel transition is completely reversible.

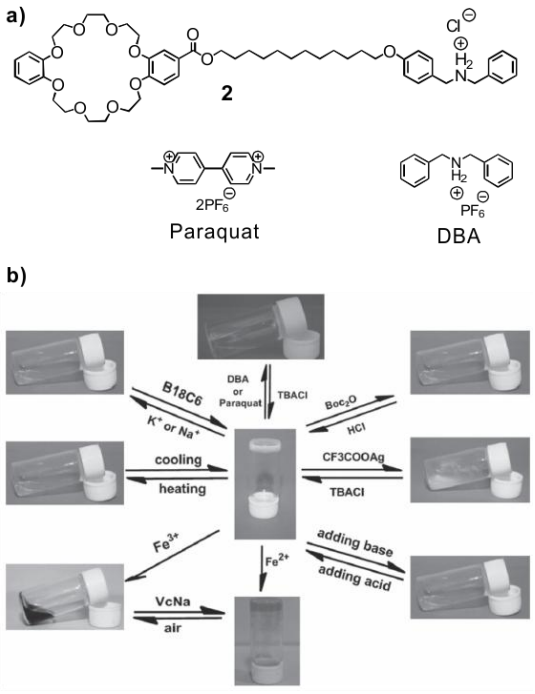

Figure 5. a) The chemical structure of the crown ether functionalized hetroditopic gelator **2** and organic cation stimuli; b) The reversible gel-sol transitions of supramolecular gel (gelator **2**/ acetonitrile) triggered by a variety of stimuli.[94] Copyright © 2012 WILEY-VCH Verlag GmbH & Co. KGaA, Weinheim.

Nowadays, a growing number of examples show that designing multiple responsive gel

materials is favorable trend, since a real smart material should be able to predictably adapt different external environmental stimuli. The combination of host-guest chemistry of macrocycles and other responsive elements provides a facile way to realize this purpose. Recently, Huang and his group reported a type of crown ether based supramolecular gel which was able to respond to up to eight types of stimuli.[26] The chemical structure of the heterotopic gelator they developed is shown in Figure 5. One terminal side of the gelator was functionalized with dibenzo 24-crown-8 (DB24C8) and the other side was equipped with dibenzylamine, a complementary guest for the DB24C8 unit. The crown ether moiety can form a *pseudo*rotaxane structure with the dibenzylamine, which results in the formation of long-range supramolecular polymeric structures. They found the gelator which was capable of gelation in 25 types of solvents. Here, the counteranion Cl^- plays a significant role for the improved gelation ability (the critical gelation concentration (cgc) of **2** in acetonitrile is only 0.6 wt.%) in comparison to its counterpart with PF_6^- (its cgc in acetonitrile is 4.6 wt.%).[112] By simply adjusting the chemical environment of crown ether moiety, secondary ammonium unit and chloride, up to eight types of stimuli can be designed. For example, the crown ether group can bind different cations, like K^+/Na^+, dibenzylammonium (DBA)/paraquat and Fe^{3+}, owing to the host–guest interactions. The addition of excess organic salts or metal ions is able to compete to complex with DB24C8 unit. Therefore, the internal structures would be destroyed and the gel phase switches to sol phase. Other stimuli which alter the properties of the secondary ammonium unit can also be used. These stimuli include triethylamine (base) and di-*tert*-butyl dicarbonate **(**Boc_2O). After adding one of them, the resulting ammonium is no longer capable of forming *pseudo*rotaxane with DB24C8, thus triggering the gel-sol transition. Moreover, a change of counteranions also can induce the gel-sol transition. For instance, the addition of $AgPF_6$ scavenges the Cl^- ion in the system due to the formation of AgCl precipitate leaving the gelator with PF_6^- as counteranion. Since the gelator **2** with PF_6^- cannot form a gel at the tested concentration, the gel-sol transition again occurs. However, if the Cl^- source is replenished into the system, the gel status is regained. This example nicely shows how macrocycles as well as their host-guest chemistry can enrich the stimuli to large extents, which would push forward the design of adaptive gel materials.

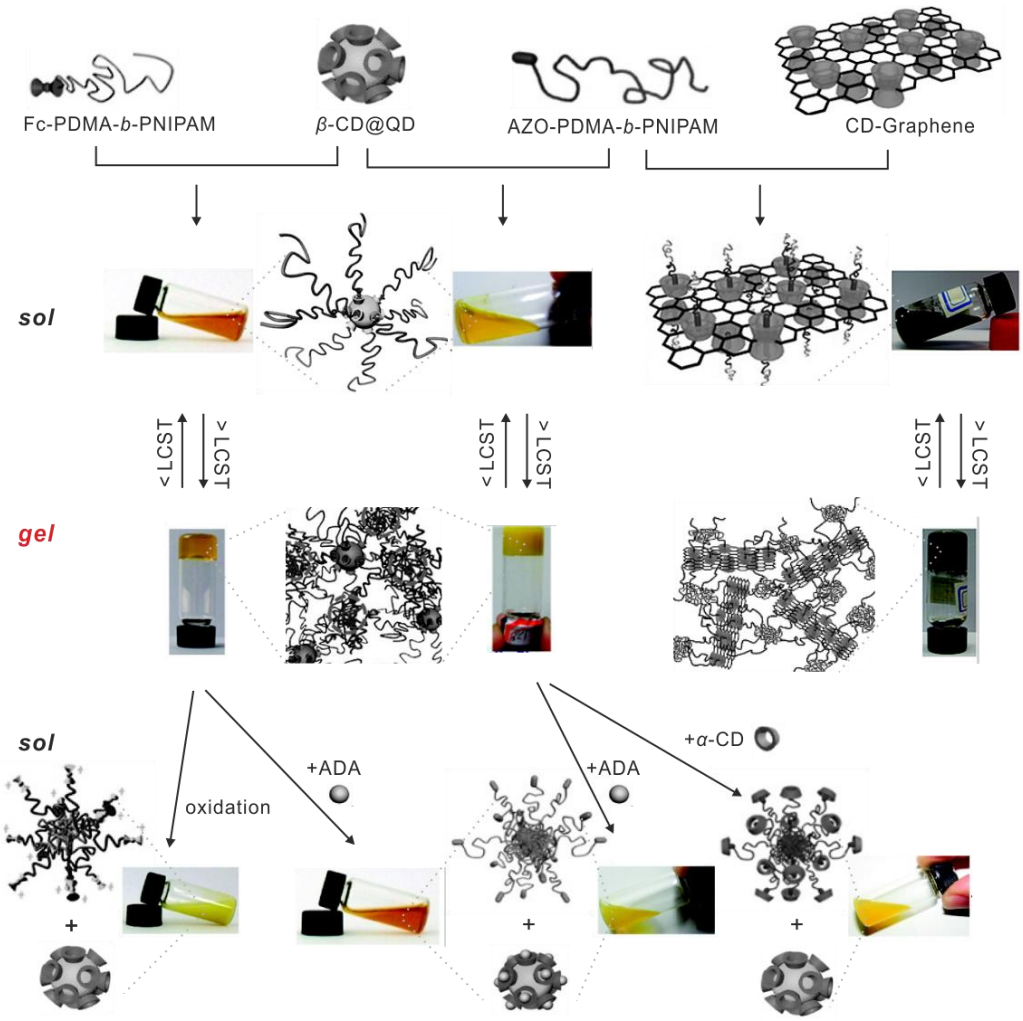

Figure 6. The hybrid supramolecular gel system developed in Jiang's group showed multiple gel-sol transitions and reverse sol-gel transitions triggered by different stimuli.[113-115] Copyright © 2010, Copyright © 2011, American Chemical Society.

Jiang and his colleague developed another versatile method utilizing the host-guest chemistry of macrocycles to construct hybrid supramolecular gels which are not only multiply responsive, but are also easily incorporated into different functional building blocks (like quantum dots and graphene oxide).[113-115] Figure 6 lists the synthesized *β*-CD modified CdS quantum dots (*β*-CD@QD) and azobenzene-and ferrocene-functionalized block copolymer AZO-PDMA-*b*-PNIPAM and Fc-PDMA-*b*-PNIPAM (PDMA-*b*-PNIPAM: poly-(*N*,*N*-dimethylacrylamide)-*b*-poly(*N*-isopropylacrylamide). The mixing of *β*-CD@QD and resultant block copolymers forms a hybrid complex due to the inclusion of *β*-CD and azobenezene/ferrocene. The *β*-CD@QD herein served as a

linker-hub, whereas the block copolymers served as a shell. Upon heating the mixture, the aggregation of PNIPAM (above its LCST) results in a domain interaction with adjacent PNIPAM moieties (Figure 6) eventually affording hydrogels. The corresponding supramolecular gels exhibit thermo-responsive properties. When the temperature is increased above the LCST, the gel-sol transition takes place. Beyond thermo-responsiveness, the gels also exhibit chemical-responsiveness. When the competitive guest adamantine or competitive host *α*-CD is added to the resultant gel, the gel-sol transition occurs. For the Fc-PDMA-*b*-PNIPAM, the oxidization of the Fc moiety also stimulated the gel-sol transition. The amazing part is the versatility of this method. Following the same strategy, other materials, like graphene oxide sheets, are able to be easily introduced when the surface of graphene was functionalized with *β*-CDs (CD-graphene). When the CD-graphene is mixed with AZO-PDMA-*b*-PNIPAM, graphene-functionalized hybrid supramolecular hydrogels are realized at elevated temperatures (Figure 6, right).

Sensors

The macrocycle cavities offer special advantages as they allow fabricating porous materials due to their alterable cavity. For macrocycle-containing supramolecular gels, the gelation process provides a facile way to pile up the macrocycle/cavity into a porous channel without any template assistance. Once the gel is formed, additional function may be added to the resultant porous structures due to the guest binding properties of macrocycles. Shinmyozu et al. showed an intriguing example employing the accommodation of macrocycles in supramolecular gel as chemsensors (Figure 7).[116] The pyromellitic diimide-based macrocycle **3** was found to selectively gelate *N*,*N*-dimethylaniline. After removing the solvent by drying the gel in vacuo, the resultant xerogel retained the nanofibrous structures also with the hollow tubular structures. High-resolution transmission electron microscopy (HR-TEM) revealed the tubular hollows along the fiber growth axis to have a diameter comparable to the size of **3** (ca. 1 nm). The single crystals obtained by the recrystallizing **1** from a mixture of *N*,*N*-dimethylaniline and 1,1,2,2-tetrachloroethane (*v*/*v*=1:1) further confirmed the packing mode of the inner macrocycles. X-ray analysis showed that the nanofibers of the xerogel had channel-type

empty cavities and the cross section of the bundles of nanofibers had a *pseudo*hexagonal nanoporous structure which was similar to a honeycomb (Figure 7b). Owing to the π-electron deficient cavities of **3**, the resultant xerogel was able to adsorb π-donating compounds (gas form) through charge transfer (CT) interactions. These π-electron donating guests include *N*,*N*-dimethylaniline, *N*-methylaniline, aniline, and 1,3-dimethoxybenzene. Shown in Figure 7c-g, the adsorption of gas molecules was rapidly reflected by the specific color change from original pale yellow to yellow or orange depending on the π-donating ability of the guests. Therefore, the results extend the application of macrocycle-containing supramolecular gels as new sensor which can easily be judged by the naked eye according to color changes.

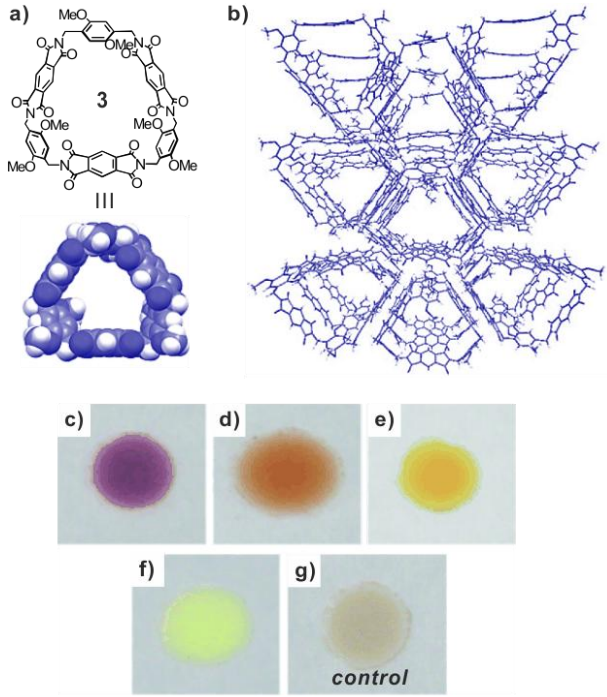

Figure 7. a) Chemical structure of pyromallitic diimide-based macrocycle **3** and its CPK representation. b) Crystal structure of **3** (*N*,*N*-dimethylaniline)$_2$ (1,1,2,2-tetrachloroethane)$_2$. Solvent molecules are omitted for clarity. Photographs of the xerogel after adsorption of c) *N*,*N*-dimethylaniline, d) *N*-methylaniline e) aniline, f) 1,3-dimethoxybenzene, and g) before adsorption. Copyright © 2010 WILEY-VCH Verlag GmbH & Co. KGaA, Weinheim.

Active electronic devices

The formation of long-range ordered structures plays a vital role for the effective fabrication of electronically active materials. Therefore, many efforts have been devoted to

control the self-assembly of electronically active molecules. The gelation process with these electronically active organic molecules was found to be particularly efficient to produce one-dimensional (1D) fibers *in situ* with improved electronic properties.[117, 118] Therefore, a number of supramolecular gels with electronic conductivity and charge-carrier mobility have been reported as prospective soft materials for developing organic electronic devices.[119-121] Macrocycles like porphyrins and phthalocyanines are good candidates as building blocks for photoelectronic materials, e.g. organic field-effect transistors (OFETs) and organic solar cells (OSCs).[33] In addition, their intrinsic, strong π-stacking tendency makes them extremely suitable for constructing electroactive supramolecular gels.

Early work reported by Terech[122] and Shinkai[123] proved that the strong intrinsic π-stacking tendency of porphyrin units assisted by lateral non-covalent interactions like hydrogen bonding can efficiently construct 1D nanowires. Following this concept, many porphyrin-based supramolecular gels have been developed by altering the binding mode of the attached groups.[124-127] Figure 7 shows three typical strategies used to produce these 1D nanostructures by gelation: a) applying the π-π stacking of porphyrin units plus the weak interaction at the side chain;[125] b) employing the unique host-guest recognition of porphyrin to immobilize other electroactive components like fullerene (C60) into the center of porphyrin without damaging the conjugated system;[124] c) equipping the periphery of porphyrin with polymerizable groups to increase the mechanical strength of the resulting porphyrin nanowires or nanosheets through post-polymerization. For example, Shinaki's group has developed tetraphenlporphyrin **7** functionalized with triethoxysilyl (TEOS) groups.[126] After so called 'sol-gel' condensation, the cross linking between adjacent TEOS afforded the gels with a very high thermal stability as well as a unique mechanical strength. Subsequently, these principles were applied to a number of other systems.[128]

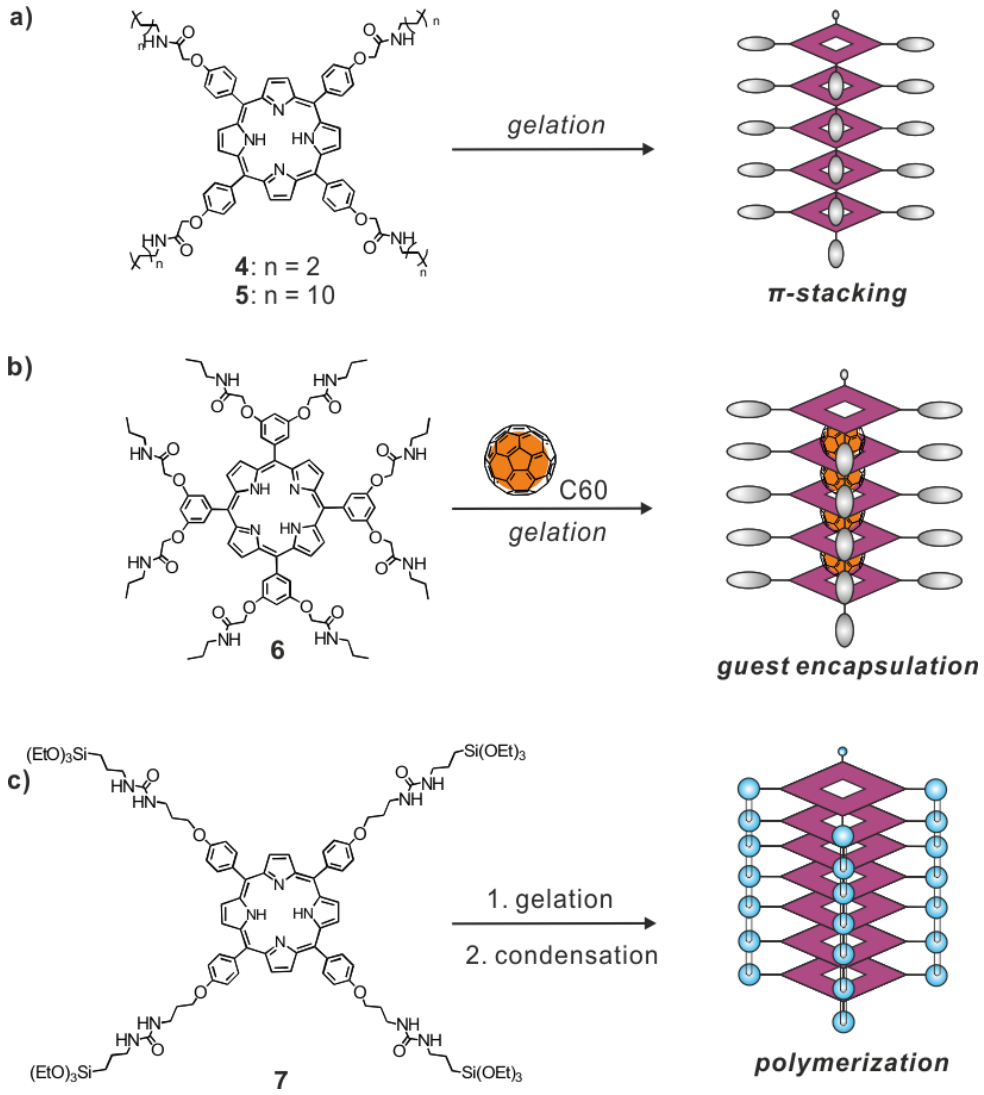

Figure 8. Three strategies to construct supramolecular gel-based nanowires utilizing the π-stacking of porphyrin and phthalocyanine derivatives.

Besides serving as electroactive building blocks, the macrocycles may also serve as a molecular skeleton to connect systems. Nakamura et al. reported a novel amphiphilic bis-tetrathiafulvalene (TTF) annulated macrocyclic derivative **8**[129] which formed redox-active organogels as well as electrically active nanowires and nanodots with controllable size (Figure 9). The intermolecular S-S and π-π interactions between terminal ethylenedithio-TTF groups promote the gelation process. Entangled fibrous structures formed in the resulting gels. When doping with an oxidant (I_2), the resulting surface of **8**/(I_2) produced nanodot structures either in linear or ring-like form (see Figure

9b, 9c). The conductance of single nanodots fabricated on highly ordered pyrolytic graphite (HOPG) substrates was measured by conducting AFM (C-AFM). The conductance of a single nanodot with an open-shell electronic structure was four to five orders of magnitude higher than that of fibers of **8** with a closed-shell electronic structure. This observation indicates that the high electronic conductivity is strongly dependent on the magnitude of intermolecular charge-transfer (CT) interactions and the length of the stacks.[130] The obtained nanostructures of molecular conductors can potentially be used in molecular electronic devices as electrically active units.

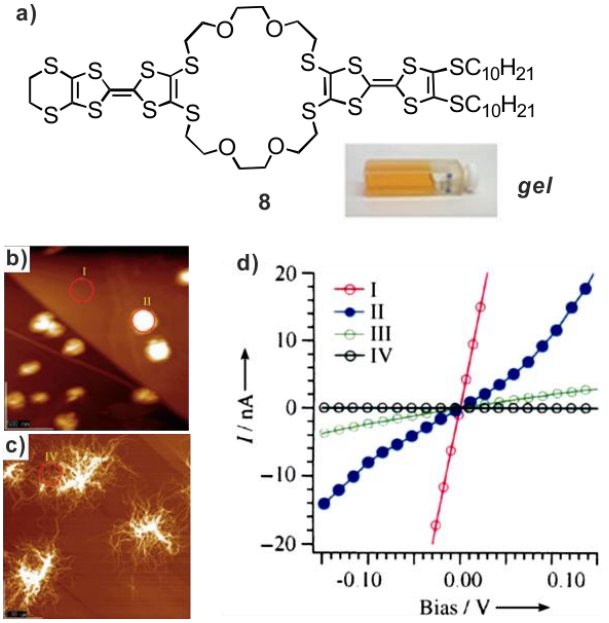

Figure 9. a) Chemical structure of amphiphilic bis-TTF annulated macrocyclic derivative **8** and the photograph of gel formed in $CHCl_3/CH_3CN$ (*v*/*v* = 6/4). AFM images of b) nanodots of **8**/$(I_2)_2$ and c) fibrous structures of **8** on HOPG (10×10 mm^2) prepared by spin casting of a 1 mm solution ($CHCl_3/CH_3CN$ 6:4). d) *I*-*V* characteristics at points I (HOPG), II (single nanodot in air), III (single nanodot in vacuum at 5×10^{-3} Pa), and IV (bundle of fibers).[129] Copyright © 2005 WILEY-VCH Verlag GmbH & Co. KGaA, Weinheim.

The macrocycles in supramolecular gels provide an additional strategy for controlling the aggregation mode of electroactive organic building blocks. Shinkai's group reported a unique class of oligothiophene-based organogelator **9** bearing two crown ethers at both ends.[131] This compound could gelate in several organic solvents, yielding 1D fibrous aggregates. Due to the terminal crown, the resulting gel shows alkali metal cation

responsiveness with enhanced fluorescence emission upon gel-to-sol phase transition (Figure 10). Moreover, the introduction of chiral guests of the crown ether allows controlling the helical handedness of oligothiophene-based fibrous structures.[132] The authors found that the addition of equivalent optically pure chiral guests with a 1,2-bisammonium ethylene skeleton not only bridged two adjacent crown ethers, while stabilizing the gel, but also could induce the twisted stacking of the oligothiophene units towards one direction due to steric effects (Figure 10). Consequently, the gels with chiral 1,2-bisammonium guests displayed mirrorsymmetric bisigned ICD spectra. This example nicely shows the advantage by which the induction of macrocycles permits the post-modification of the helicity of electroactive fibrous structures.

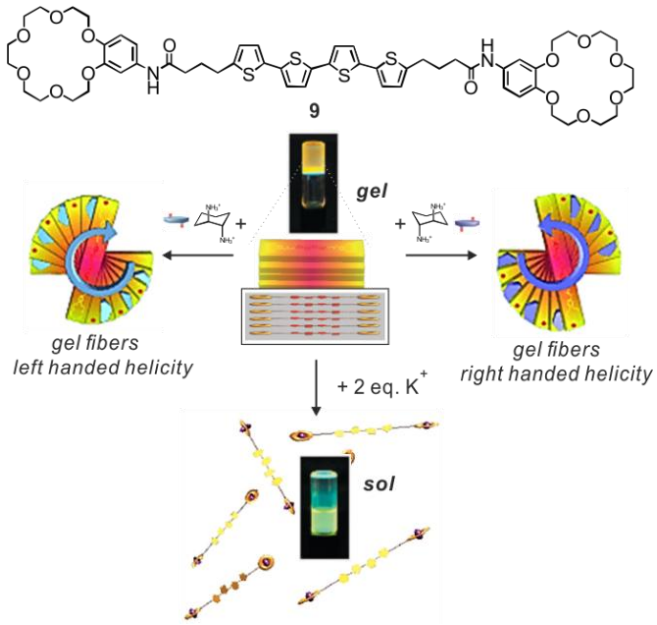

Figure 10. Top: Chemical structure of gelator **9** with oligothiophene core; bottom: graphical representation of the ICD mechanism in the gel phase and the gel–sol phase transition upon increasing concentration of K^+.[131, 132] Copyright © 2011, Royal Society of Chemistry, Copyright © 2012 WILEY-VCH Verlag GmbH & Co. KGaA, Weinheim.

Phenylacetylene macrocycles (PAMs) is recently developed carbon-rich macrocycle, which can be easily functionalized through chemical synthesis, allowing the fine-tuning of their cavity size and electronic properties.[61, 62] The face-to-face stacking of π-conjugated systems is a convenient and elegant way of building porous materials analogous to carbon nanotubes. The major driving force for gelation of PAM deviates are π-π interactions,

while other weak interactions such as van der Waals interactions between peripheral alkyl chains and intermolecular hydrogen bonds also play an important role. Zhang and Moore reported the first example concerning the formation of supramolecular gels based on arylene ethynylene macrocycle, affording internal nanofibrous structures.[133] Inspired by this seminal work, growing numbers of supramolecular gels based on PAM were reported.[134-138]

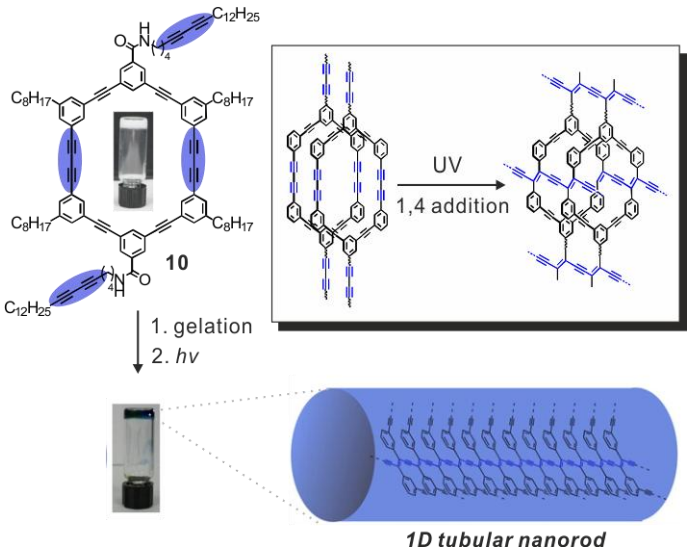

Figure 11. Chemical structure of phenylacetylene macrocycle **10** and the photographs of the gel before and after photopolymerization. The insert picture shows the proposed mechanism for the topochemical polymerization between macrocycles in the dried gel state.[136] Copyright © 2013, American Chemical Society.

Among these reports, Morin's group produced nongraphitic nanotubes using phenylacetylene macrocycle-based supramolecular gels.[136] They designed and prepared a kind of topochemically polymerizable phenylacetylene macrocycle **10**, which can form a supramolecular gel in ethyl acetate (Figure 11). The amide groups at the periphery play a vital role for the self-assembly in a columnar arrangement. The butadiyne moieties located both inside and outside the macrocycles' skeletons enhance the aggregation and allowing fix the pre-organized rod structure through post-photo-polymerization. Upon irradiation with UV light, topochemical polymerization in the gel state produces large shape-persistent nanorods. These nanostructures can be characterized by PXRD and HRTEM. These results inspire a novel strategy to fabricate nongraphitic semiconducting nanorods and nanotubes for electronic applications.

Reaction medium and template

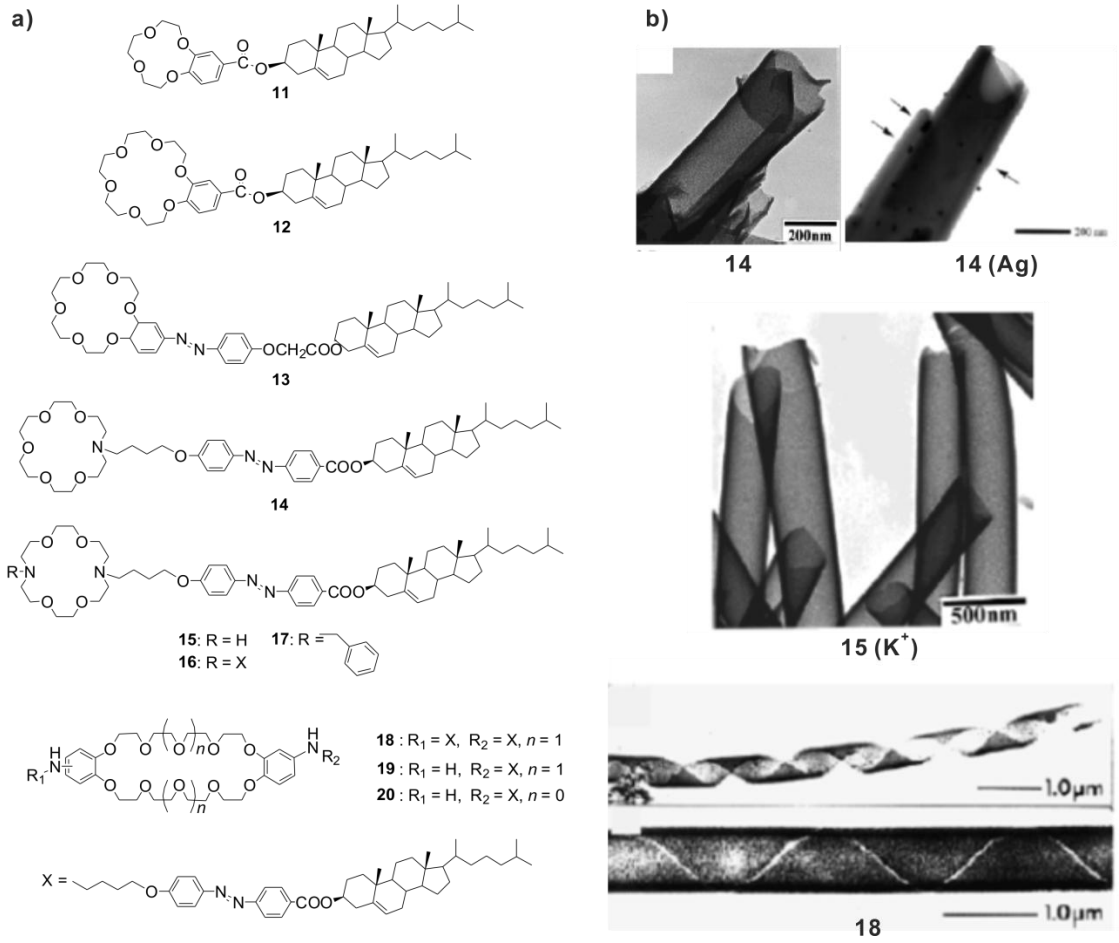

Figure 12. a) Chemical structures of various crown-appended cholesterol gelators. b) TEM images of selected silica nanofibrous morphologies templated through organogels. Top row: rolled-paper-like (multiwalled) tubules obtained with gelator **14** without metal,[139] and with Ag;[140] middle row: tubules obtained from **15** with K^+;[139] bottom row: Helical ribbons and double-layered tubes obtained with **18**.[141] Copyright © 2000, 2001 American Chemical Society, Copyright © 1969, Royal Society of Chemistry.

Currently, growing evidence shows the great potential of applying supramolecular gels as active media for organic reactions and catalysis.[19, 142-144] For the macrocycle-containing gels, Shinkai's group have successfully proved that the crown ether-coupled cholesterol gelators can be used as template to fabricate silica nanotubes.[144] They have designed and synthesized a series of gelators with minor structural variation (Figure 12a).[139, 141, 145-149] The crown ether unit cannot directly prompt the formation of supramolecular gels. Instead,

it is steroidal motifs provide the driving force for the gelation. A detailed gelation test revealed that the gelators **11**-**20** were able form thermally reversible gels. However, the cavity size of crown ethers determines the gelation ability as well as internal superstructures to a large extent. The tubular superstructures, which depend on the gelators, were found to be quite useful as a template to create hollow fibrillar silica (Figure 12b). By using a sol-gel polymerization of TEOS on the surface of formed superstructures, the silica was generated. After calcination, the gel template was removed affording hollow tubes. Particularly in the case of gelator **18**, the gel template facilitated the helical ribbon structure of the silica.[141] This is a very rare example of chiral inorganic materials. These results clearly indicate the versatility of the template method in the gel phase for the creation of various silica structures.

Biomedical application

Supramolecular hydrogels are of particular interest in biomaterials application due to their high water content, good compatibility with biomolecules, and tractable release kinetics. Since 2000, cyclodextrins were the first macrocycle approved by FDA to be used in food and drug application because of excellent biocompatibility.[150-152] Consequently, significant efforts have been made to develop cyclodextrins-containing supramolecular gels as biomaterials. As early as 1994, Li et al. reported the first necklace-like poly*pseudo*rotaxane (PPR) structure based on linear water-soluble polymers such as PEO which form a complex in the inner cavity of multiple α-CD.[153] They found the resulting PPR shows thixotropic nature and biocompatibility and were demonstrated to be suitable as injectable hydrogel drug delivery systems.[154] Afterwards, the development of α-CD-based supramolecular hydrogels using other block copolymers on the basis of PPR or polyrotaxanes flourished (Figure 13).[155] Many different hydrogels based on the triblock copolymers of poly(ethylene oxide) and poly(propylene oxide),[156] triblock copolymers of poly(ethylene oxide) and poly((R)-3-hydroxybutyrate),[157] block copolymers of poly(ethylene oxide) and poly(L-glutamic acid),[158] block copolymers of poly(ethylene oxide) and poly(ε-caprolactone),[159] poly(ethylene oxide)-grafted copolymers[160] have been broadly explored with varied topologies. A large amount of research results evidence that the resulting gels exhibit a sustained/controlled release

behavior and are capable to be employed under biological conditions.[161] So far, supramolecular hydrogels based on the self-assembly of inclusion complexes between CDs with biodegradable block copolymers are the most extensively explored macrocycle-containing gels.[162] A number of reviews comprehensively summarized this area from different aspects.[162-164] Therefore, only some recent examples besides the PPR and polyrotaxane structures are presented here. In addition, another macrocycles like cucurbiturils which also exhibit great potential to biomaterials shall be highlighted.

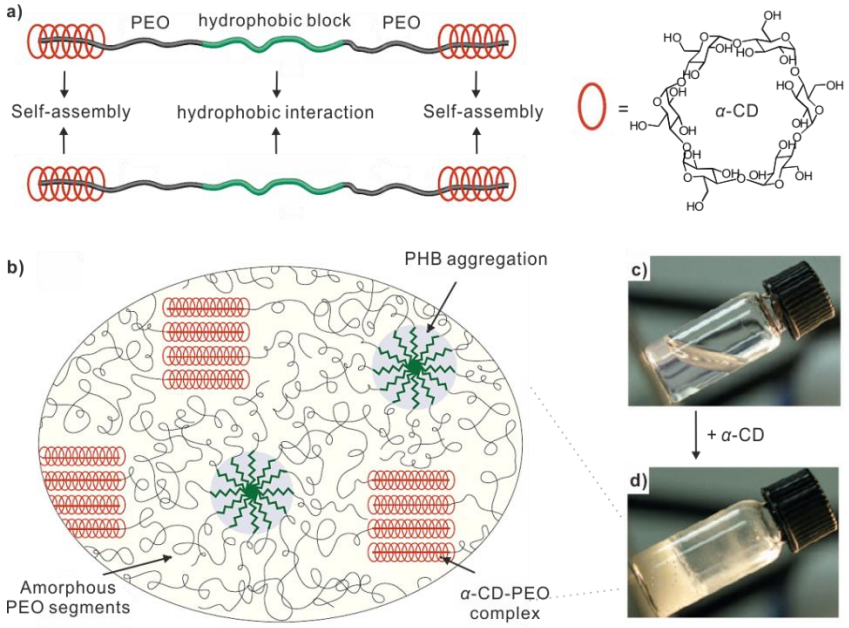

Figure 13. Example for a PPR based hydrogel:[155, 165] a) Schematic illustration of the supramolecular self-assembly of α-CD and a triblock copolymer consisting of two PEO blocks integrating a central hydrophobic block PEO-PHB-PEO (5000-1750-5000). (b) Schematic illustration of the structure of the α-CD/PEO-PHB-PEO hydrogel. c) Aqueous solution of PEO-PHB-PEO triblock copolymer. d) Supramolecular hydrogel formed after the addition of α – CD into c). Copyright © 2006, Elsevier, Copyright © 2010, Nature Publishing Group.

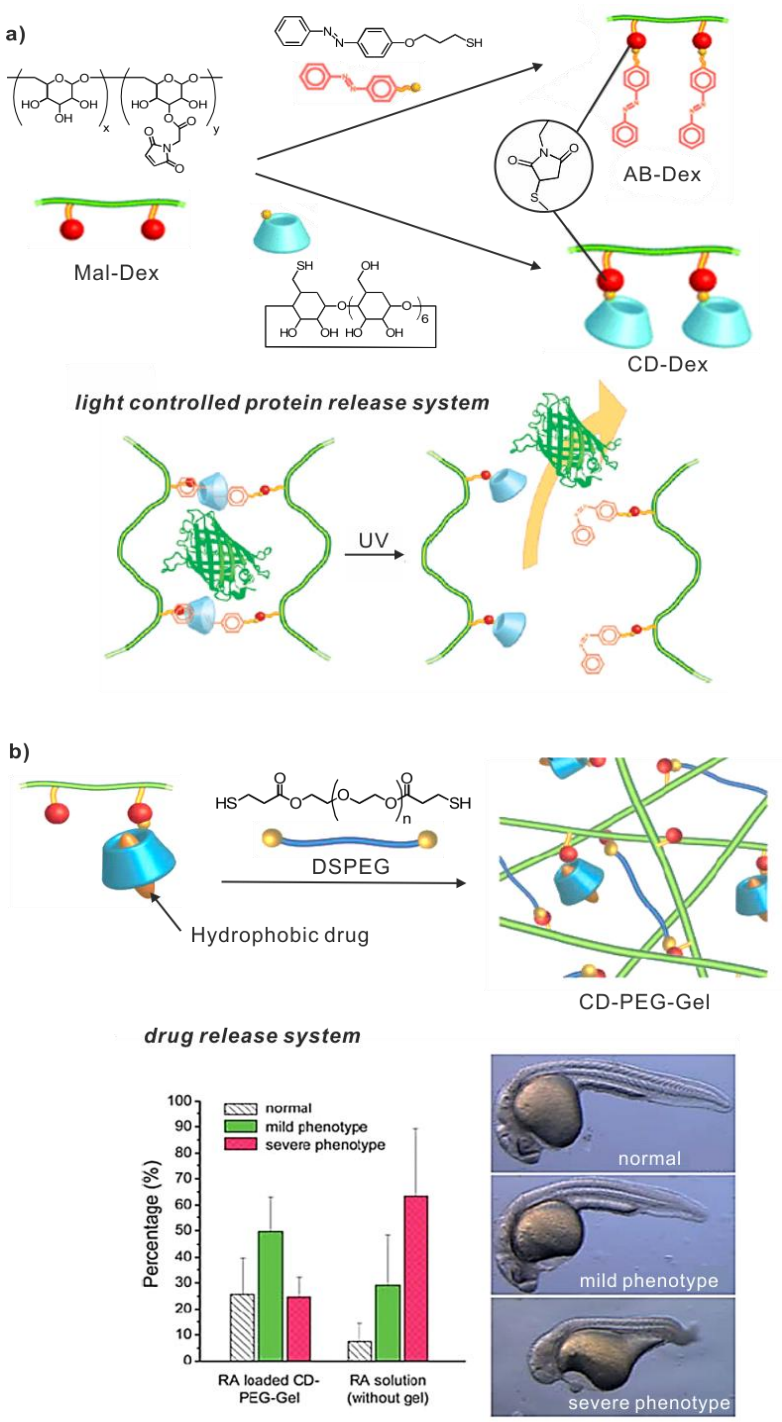

Figure 14. a) UV-light-sensitive azobenzene moieties isomerise from *trans* to *cis* configurations, resulting in the gel-sol transition and allow the light-controlled release of the entrapped protein into the media.[166] b) The inclusion complexes of hydrophobic drug (retinoic acid) and cyclodextrins are conjugated into the gel and the effects of drug-loaded gel injections on the development of zebrafish embryos was evaluated.[167] Copyright © 2010, Royal Society of Chemistry.

Recently, Kros and his coworkers synthesized and developed a cyclodextrins-based photo-responsive hydrogel.[166] Through Michael addition, they functionalized the side chain of dextran with *β*-CD (CD-Dex) and azobenzene (AB-Dex). The hydrogel can be obtained simply by mixing the *trans*-AB-Dex and CD-Dex solutions. Upon UV radiation, *trans*-AB moieties were isomerized to their *cis* configuration resulting in the dissociation of gel networks, and therefore, the release of entrapped green fluorescent protein (GFP) as model protein (Figure 14a). The Kros group further developed the CD-Dex into a biocompatible drug release system, through the addition of a dithiol linker DSPEG to the solution of CD-Dex (Figure 14b).[167] The hydrogel was able to form *in situ*, and thus was stable for direct injection. By changing the concentrations of the polymer solutions, the injectable, nanosized hydrogel particles were formed and showed high biocompatibility without affecting the development of zebrafish embryos. Retinoic acid (RA) was tested as a model hydrophobic drug and was able to be efficiently loaded into the CD-PEG-Gel due to the formation of inclusion complexes with CDs. The controlled release of RA from the CD-PEG-Gel particles was further confirmed both *in vitro* and *in vivo* in the zebrafish embryo assay (Figure 14b).

Besides the cyclodextrins, cucurbiturils (CB[n]) are macrocycles which also show great potential as biomedical materials.[168, 169] Similar to the CD family, the number of glycoluril units determines the size of the CB[n] cavity without affecting the height of the molecular container (~0.9 nm).[48] Several studies have demonstrated that the CB[n] family is generally non-toxic, thus promoting potential application in a wide variety of biomedical related fields.[73, 170] Therefore, growing attention has been paid in developing hydrogel systems based on CB[n] binding motifs.

Scherman's group has designed different types of hydrogels on the basis of cucurbit[8]urils (CB[8]s). One type of hydrogel-based triple components shows extremely high water content (up to 99.75% water).[171, 172] The detailed composition includes the naturally renewable cellulose derivatives which have been functionalized with a naphthalene moiety (HEC-Np), a poly(vinyl alcohol) polymer modified with viologen (PVAMV) and CB[8]. The naphthalene and viologen moieties can form strong

and highly specific hetero-ternary complexes with CB[8], thus providing the essential crosslinker for the formation of a 3D-network. The exceptionally low gelation concentration and high water content improves the obtained gels' biocompatibility and makes them suitable for biomedical applications. The authors conducted release studies of model protein therapeutics from supramolecular gels. The chosen model protein therapeutics includes bovine serum albumin (BSA) and lysozyme with different molecular weights (BSA, Mw: 67,000 g mol^{-1} versus lysozyme, Mw: 14,000 g mol^{-1}), thus the release rates could be compared. For both proteins, the sustained release effects were observed. As the level of polymer loading increased from 0.5 wt.% to 1.5 wt.%, a dramatic difference in the release rate can be observed: The larger protein BSA was released much slower than lysozyme. Therefore, the release rate is highly dependent on the density of network points. Moreover, further bioactivity test revealed that the released proteins retain most of their activity even after long periods (BSA: over 80% original activity preserved after 50 days), demonstrating that this newly developed cucurbit[8]uril containing gel material is suitable for sustained therapeutic applications.

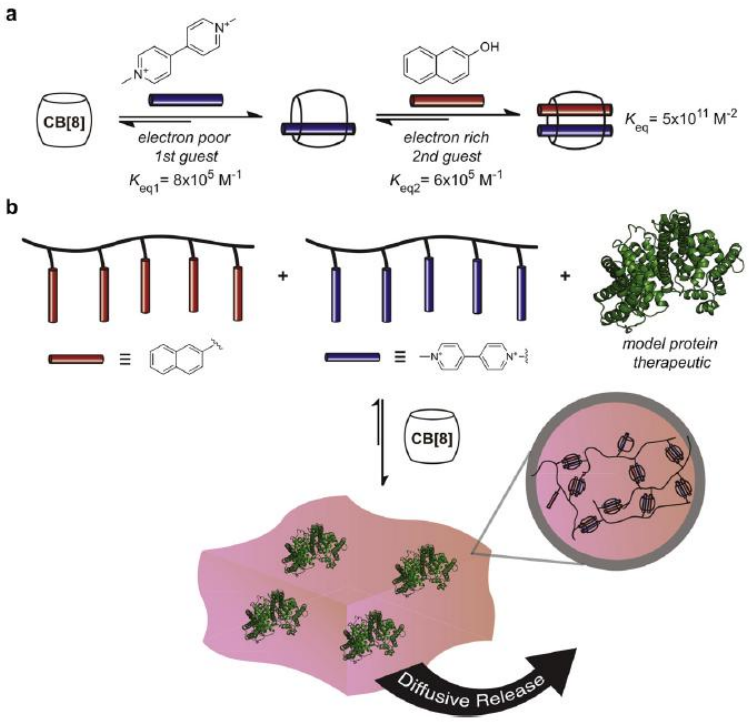

Figure 15. a) Two-step, three-component binding of cucurbit[8]uril (CB[8]) in water. b) Schematic representation of the preparation of extremely high water content hydrogels through strong host-guest interactions of CB[8].[172] Copyright © 2012, Elsevier.

Cellular engineering

In addition to sustained protein release systems, CB-based supramolecular gels can also serve as highly promising scaffolds for tissue engineering. Kim et al. reported an easy-to-prepare *in situ* prepared supramolecular biocompatible hydrogel using cucurbit[6]uril-conjugated hyaluronic acid (CB[6]-HA) and polyamines conjugated HA (PA-HA) (Figure 16a).[173] CB[6] can form ultrastable 1:1 host-guest complexes with protonated PAs like 1,5-diaminohexane (DAH) or spermine (SPM) (binding constants up to 10^{10} or 10^{12} M^{-1} respectively). Therefore, this strong host-guest interaction was used as a driving force for the cross-linking of biopolymer chains. By simple mixing CB[6]-HA, PA-HA, and NIH3T3 cells, the cell-entrapped gel formed *in situ* after 2 min. The consequent cytocompatibility studies showed that the resulting gels possess high cell viability, enzymatic degradability and negligible cytotoxicity, which are essential characteristics for their application to 3D cellular engineering. Intriguingly, some uncomplexed DAH moieties in the CB[6]/DAH-HA hydrogels provide additional groups for further modification of the obtained hydrogels by the simple addition of singly or multiply functionalized CD[6] derivatives, termed 'tags-CB[6]' (tags: FITC, rhodamine B derivatives and RGD-based adhesion peptides, shown in Figure 16b-d). Rheology experiment demonstrated that the physical stability of hydrogel was not significantly changed after treatment with tags-CB[6]s. The authors proved that a simple treatment of CB[6]/DAH-HA hydrogel with c(RGDyK)-CB[6] (c(RGDyk) is a promoter for cell adhesion) was able to modify the hydrogel as a stable RGD environment for efficiently proliferating the entrapped NHDF human fibroblast cells. As shown in Figure 16f, the modular modification of hydrogel *in vivo* by injection of a solution of FITC-CB[6] was even possible. The *in situ* preparation and modular modification of the hydrogels fully demonstrate the great potential of the CB[6]/PA-HA function as an effective 3D biocompatible platform for studying cellular behavior, therapy and tissue engineering.

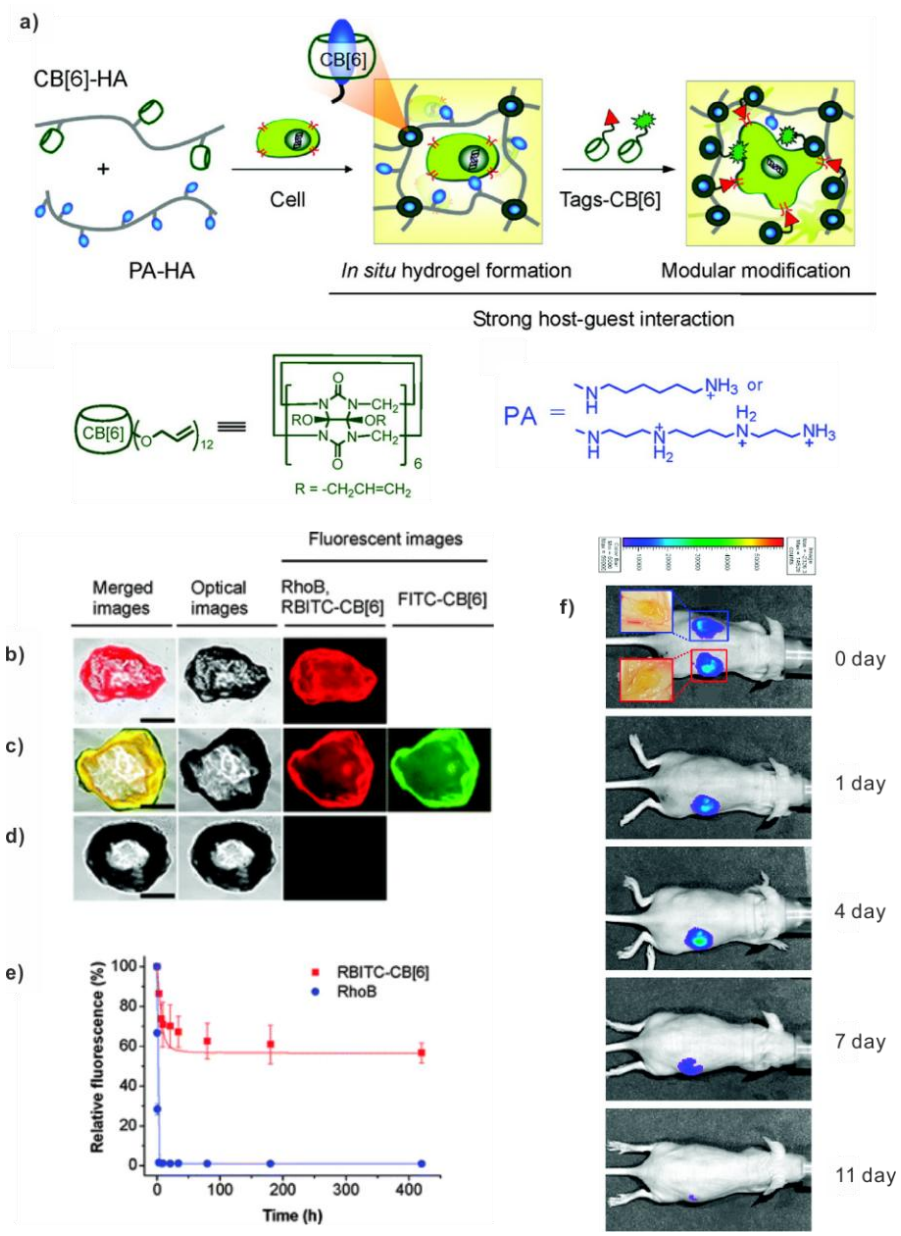

Figure 16. (a) Schematic representation for *in situ* formation of supramolecular biocompatible hydrogel and its modular modification using highly selective and strong host-guest interactions of CB[6] with PAs.[173] Modular modification of CB[6]/DAH-HA hydrogel with tags-CB[6]: (b) RBITC-CB[6], (c) RBITC-CB[6]tFITC-CB[6], and (d) RhoB (scale bar = 100 m). (e) Relative fluorescence intensity of RBITC-CB[6]@CB-[6]/DAH-HA hydrogel and RhoB@CB[6]/DAH-HA hydrogel in PBS with increasing time. f) *In vivo* fluorescence images of live mice were taken for 11 days to assess the modular modification and the complex stability on the back of mice. Copyright © 2012, American Chemical Society.

Self-healing

Self-healing and self-repair are crucial to the survival of living species. In contrast, the lifetime of synthetic man-made materials is limited by the occurrence of macroscopic damage or microcracks that severely decrease performance, eventually leading to failure. Fascinated by the beauty and efficiency of natural healing processes, scientists have developed a new research area focusing on synthetic self-healing materials aiming to extend their lifetimes, improve safety, and ensure sustainability.[174-176] Self-healing and self-repairing properties can also be achieved using supramolecular gels that consist of host-guest systems.

Harada et al. successfully realized a self-healing supramolecular hydrogel consisting of poly(acrylic acid) (pAA) possessing β-CD as a host polymer (pAA-6βCD) and ferrocene as a guest polymer (pAA-Fc) (Figure 17a).[101] Interestingly, when the resulting pAA-6βCD/pAA-Fc hydrogel (1 wt%) was cut in half, the two cut pAA-6βCD/pAA-Fc hydrogel pieces can self- heal after standing for 24 h to form one gel (Figure 17b). It is well known that the formation of the inclusion complex between cyclodextrin and ferrocene is redox sensitive. Based on this, the self-repairing property of hydrogel was able to be controlled by redox stimuli. Shown in Figure 17c, a hydrogel (2 wt%) was cut in half and the cut surfaces were coated with an aqueous solution of NaClO (7 mM, 20 μl) which oxidized the Fc unit into Fc^+. The oxidized Fc^+ does not form stable inclusion complexes with *β*-CD, thus resulting in the unsuccessful reattachment of the two pieces under the same timescale. In contrast, after spreading a reducing agent glutathione (GSH, aq. 20 mM, 20 μl) onto the oxidized cut surface, the healing process was observed again. This result clearly shows that the utilization of host-guest complexation of macrocycles can not only produce self-repair properties, but it can do this in a chemically controlled manner, if the inclusion complex formation is environmentally responsive.

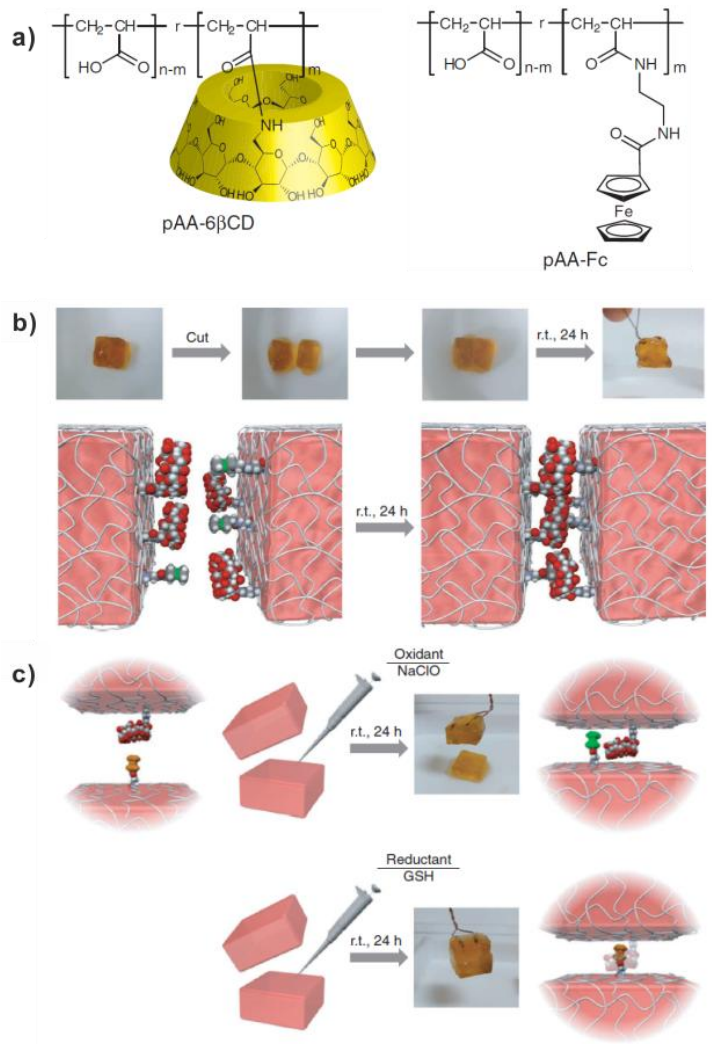

Figure 17. a) Chemical structures of the host polymers pAA-6βCD) and guest polymer (pAA-Fc). Self-healing experiments: b) After standing for 24 h, two cut pAA-6βCD/pAA-Fc hydrogel (1 + 1 wt%) pieces were rejoined and the cut sufficiently healed to form one gel. c) Redox-responsive healing experiment of the pAA-6βCD/pAA-Fc hydrogel using oxidizing/reducing agents. A pAA-6βCD/pAA-Fc hydrogel (2 wt%) was cut in half and aqueous NaClO was spread on the cut surface. After 24 h, the healing process did not occur. Re-adhesion was only observed after spreading aqueous GSH onto the oxidized cut surface.[101] Copyright © 2011, Rights Managed by Nature Publishing Group.

Very recently, Huang et al. showed that the construction of autonomous supramolecular self-healing materials was not merely restricted in cyclodextrin-based supramolecular gels. They developed self-healable supramolecular gels based on the host-guest complexation between DB24C8 and its secondary ammonium salt guest (Figure 18).[177]

The resulting gels exhibit excellent self-healing properties which can be visually observed (Figure 18b). A detailed rheological investigation revealed more quantitative information for the self-healing ability of the crown ether based gel. In less than ten seconds, 100% recovery even under 10 000% strain can be repeated over several cycles.

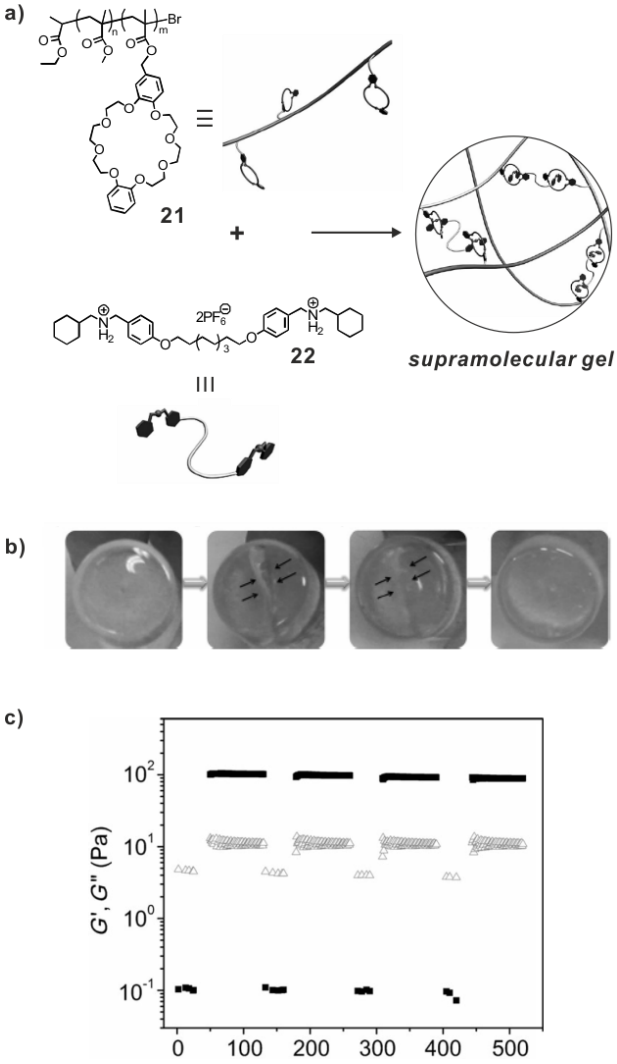

Figure 18. a) Chemical structures of crown ether functionalized polymer **21** and the cross-linker **22**.[177] The cartoon represents the formation of supramolecular gels. b) Photographs of the resulting supramolecular gel, after damage, after free standing for 10 min, and after free standing for 20 min (from left to right). Rheological characterization of gel in continuous step strain measurement showed the rapid healing property. Copyright © 2012 WILEY-VCH Verlag GmbH & Co. KGaA, Weinheim.

From supramolecular gels towards gels systems

Although recently, stimuli-responsive supramolecular gels and their applications to functional materials have progressed significantly, developing new intelligent gels that can sense and process environmental stimuli (sequence, amount, types and so on) and function in a spatio-temporal manner remains highly challenging. However, these features are commonly observed in the living organism and cellular metabolism which require that their biological machinery functions in a systematic manner. Therefore, the limit of reductionism becomes more pronounced. In 2005, the term "Systems Chemistry" appeared in a conference on Prebiotic Chemistry and Early Evolution which brought to light that the great importance of underlying networks which organize the individual components and single reactions working in a systematic manner. Over extended periods of time, such an idea was largely underestimated.[178-180] Afterwards, more and more results illustrated that a systems chemistry approach can be of high potential to develop novel functional materials with unique properties.[181] This is also true for gel chemistry. The incorporation of Belousov-Zhabotinski reaction into gels is one of prominent examples utilizing a systems approach to construct unique gel materials.[182-184] The autocatalyzed oscillations between two catalyst redox states can be used to alter the viscosity of gels and to achieve directional transport of macroscopic particles on the surface of gels. For the macrocycle containing supramolecular gels, the macrocycle moieties will continue to demonstrate advantages in elucidating systems chemistry, endowing the resulting gels with unprecedented properties.

Self-sorting gels: macroscopic molecular recognition

Self-sorting is one of central topics in the systems chemistry.[185] Controlling the order and spatial distribution of self-assembly in multicomponent supramolecular systems is the prequisite for the construction of complicated supramolecular structures. For a long time, the study of self-sorting in supramolecular systems was restricted to the microscopic scale in solution.[186-190] However, reports on sorting behavior in the macroscopic word (on the scale of millimeters to centimeters) are extremely rare, particularly for gel materials.[191-194] Recently, Harada and his group demonstrated that self-discriminating molecular-recognition events on the microscopic scale can be utilized to direct the

assembly of macroscopic objects (here hydrogels) into larger aggregated structures.[195] In their study, they synthesized two types of cyclodextrins-appended (*α*-CD and *β*-CD) acrylamide-based gels serving as two types of host-gels (*α*-CD-gel and *β*-CD-gel, respectively). Admantyl (Ad), *n*-butyl (*n*-Bu) and *t*-butyl (*t*-Bu) groups were selected as guest moieties which were also attached on the side chain of polyacrylamide polymers, as guest gels (Ad-gel, *n*-Bu-gel and *t*-Bu-gel respectively). Previous investigations in solution phase have shown that the Ad and *t*-Bu bind strongly to *β*-CD while *n*-Bu prefers to bind *α*-CD. Accordingly, they raised the question as to what would happen if the four pieces of gels (*α*-CD-gel, *β*-CD-gel, *n*-Bu-gel and *t*-Bu-gel) were simultaneously mixed in water and shaken (Figure 19a). Interestingly, a fascinating phenomenon occurred: Pieces of *α*-CD-gel selectively stuck to pieces of *n*-Bu-gel, and pieces of *β*-CD-gel exclusively stuck to pieces of *t*-Bu-gel producing two totally self-sorted 'gel islands' (Figure 19c). However, the rule actually is quite straight forward. The orthogonal binding preference in solution remains (Figure 19b), which indicates that the discovered selective recognition properties of macrocycles to their preferred guests can be applied to generate self-sorting behavior at the macroscopic level. Such macroscopic self-sorting molecular recognition can be further controlled by other factors like shape selectivity,[196] substitute position,[197] linkage,[198] temperature sensitivity[199] and photo-switchable conformation.[200] This work would be a great starting point to obtain even more complicated macroscopic assemblies.

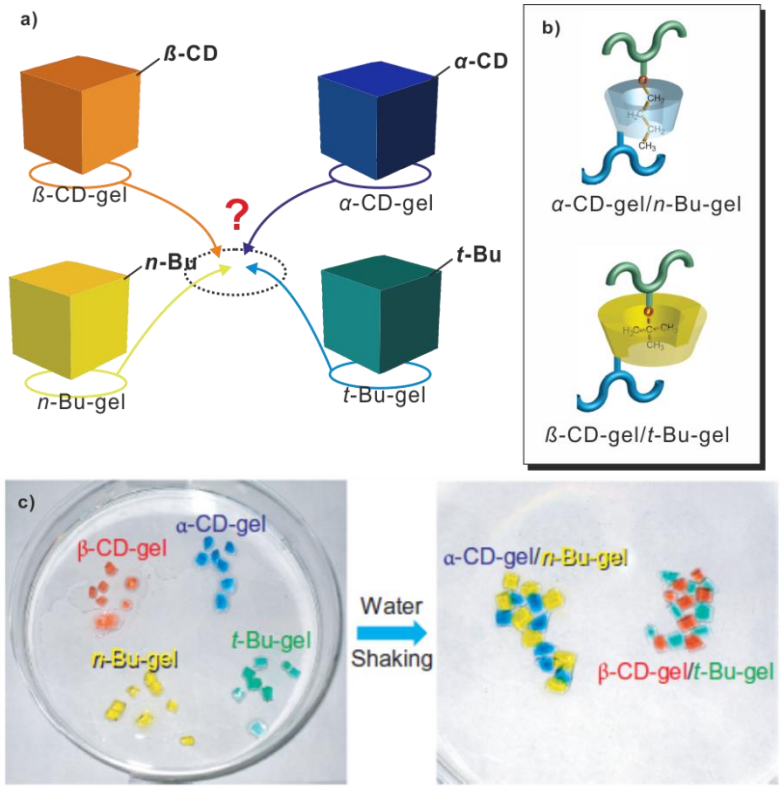

Figure 19. a) Cartoon illustration of the potential recognition problem in 'the party of gels'. b) The preferential host-guest complexation among four supramolecular building blocks. c) Photograph shows the macroscopic gel self-sorting phenomenon. Apparently, the preference of molecular recognition at the nano-level determines the macroscopic preferential behavior at the centimeter-level.[195] Copyright © 2010, Nature Publishing Group.

3.4 Mass spectrometry for the examination of non-covalent complexes

With the development of soft ionization techniques, electrospray ionization (ESI)[201-204] and matrix-assisted laser desorption/ionization (MALDI),[205-207] the survival of complexes without destroying the non-covalent bonds during the transfer from solution to gas-phase becomes simply achievable. Consequently, modern mass spectrometry plays a more and more important role in examining non-covalent complexes, not only for biomolecular species,[208-212] but also for synthetic supramolecular assemblies.[213-215] The high vacuum inside the mass spectrometer provides an unprecedented environment for studying the intrinsic properties of these complexes, which is hardly accessible in solution. In this section, we aim to utilize mass spectrometry to investigate the host-guest chemistry of dendrimers in the gas phase. Therefore, we will first briefly introduce the setup of Fourier transform ion cyclotron resonance mass spectrometry (FTICR-MS) which is coupled with an ESI ion source in our lab and the principle of how it works. Afterwards, some recent examples which have applied the mass spectrometry in regard to this topic have been summarized in the review paper 'host-guest chemistry of dendrimers in the gas phase'. A comprehensive introduction of the mass spectrometry and the gas-phase chemistry of non-covalent complexes can be found in the book edited by Schalley et al.[216]

ESI-FTICR Mass Spectrometry

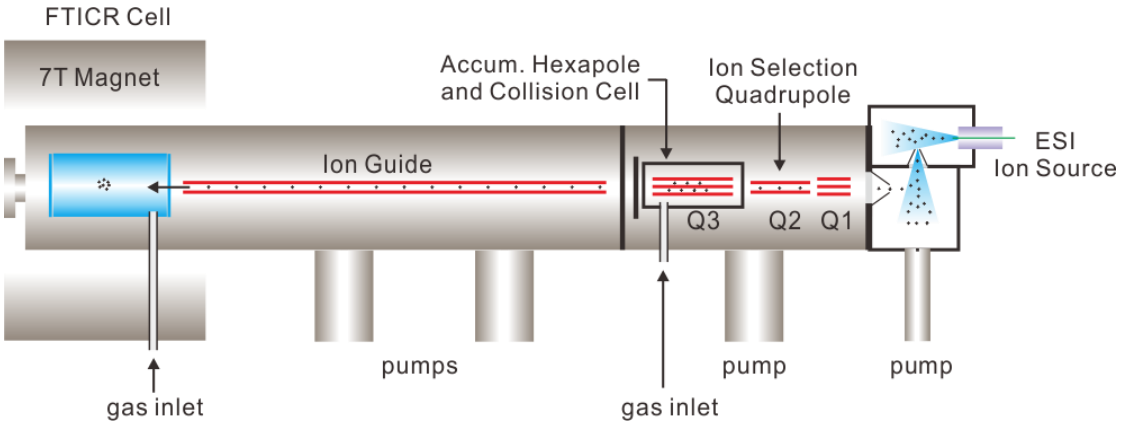

Figure 20. Schematic illustration of the ESI-FTICR mass spectrometer.

The key components of the ESI-FTICR-MS are shown in Figure 20. On the right side of the Figure is the ESI source. The ESI source allows a facile generation of the ions directly

from the solution of samples if the analyte carries proton(s), cation(s) or anion(s). If ions are produced, they will be transferred to the following regions composed by two hexaploes (Q1, Q3) and one quadrupole (Q2). In the Q2 and Q3 regions, one can select and accumulate the ions of interest through setting up proper instrumental parameters. Since Q3 is equipped with a pulsed gas inlet, some tandem-MS experiments like collision-induced dissociation (CID) and hydrogen/deuteron (H/D) exchange can be performed here. The resulting ions are further transported by an ion guide to the FTICR analyzer cell. There, the ions will be detected and analyzed, which eventually affords the observed mass spectrum.

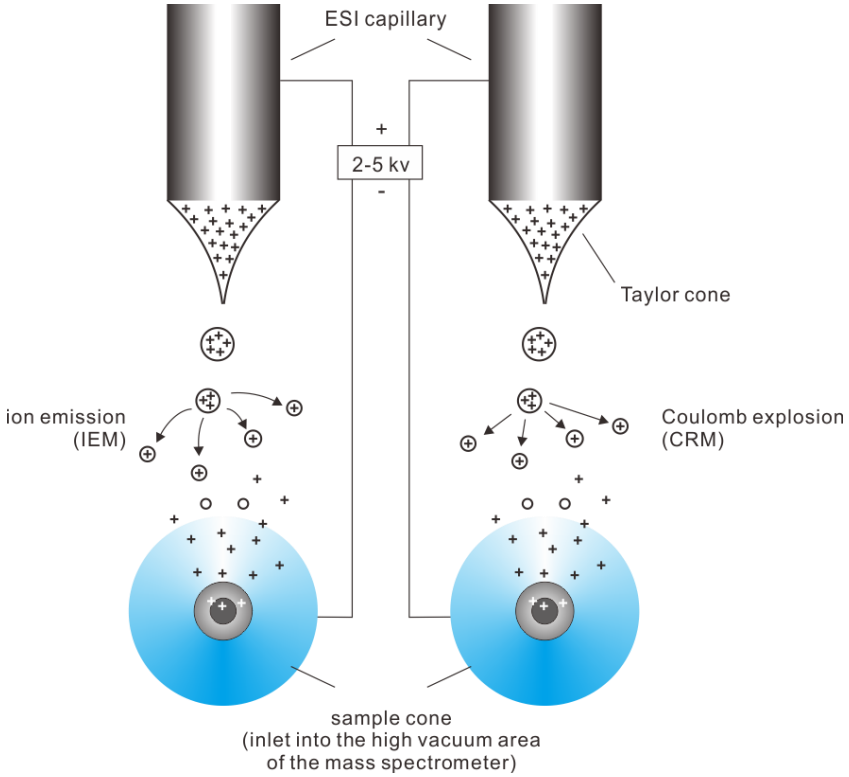

Figure 21. The principles of the ESI process. The two most important electrospray ionization models are shown: the ion-evaporation model (IEM, left) and the Coulomb-explosion model (CRM, right).[217]

ESI uses a narrow capillary operated at high voltage to ionize analytes dissolved in solution (Figure 21). As the liquid stream leaves the capillary, it is polarized by the electric field and forms the so-called Taylor cone. From the tip of the Taylor cone, a jet is formed, which is accompanied by the formation of micrometer-sized charged droplets.

Due to Coulomb repulsion, the droplets are repelled away from each other and the charge of the droplets depends on the electric field which is applied. Upon the evaporation of solvent, these droplets further shrink and the charged particles in one droplet get closer to each other. When the Coulomb repulsion in a droplet is too high, these droplets further divide into even smaller droplets, through Column explosions. The limiting diameter *d* of a charged droplet is directly related to its charge *q*, the permittivity ε_0 of the environment around the droplet and the surface tension γ of the liquid (Eq. 3.4.1, Eq. 3.4.2), termed Rayleigh limit. The whole process constantly generates a fine electronic spray.

$$q^2 = 8\pi^2\varepsilon_0\gamma d^3 \qquad \text{Eq. 3.4.1}$$

$$d = \sqrt[3]{\frac{q^2}{8\pi^2\varepsilon_0\gamma}} \qquad \text{Eq. 3.4.2}$$

Currently, two different models are widely used to describe the formation mechanisms of completely desolvated ions that enter the mass spectrometer: One is called ion evaporation model (IEM),[218-220] which proposes that a single ion can "evaporate" from the surface of a droplet when the Coulomb repulsion is too high (Figure 21, left side); the other is known as the charge residue model (CRM),[221, 222] which states that the splitting of the droplets goes on until the resulting droplets contain just single ions and some solvent molecules (Figure 21, right).

When the ions are injected into the mass spectrometer, they are collected and sent into the ICR cell (Figure 22) as ion packages. The principle of detection of *m/z* by ICR-MS is quite different from other mass spectrometry techniques. Whereas ions are detected in different places as with sector instruments or at different times as with time-of-flight instruments, ICR-MS detects the ions simultaneously during the detection interval. The ICR cells employ high magnetic fields of superconducting magnets to guide the ion to a small orbit within the analyzer cell. The moving ions imposed within a magnetic field are influenced by Lorentz force thus inducing into a circular movement and are preventing them from escaping the ICR cell in the *x/y* direction if the ion's kinetic energy is not too high.

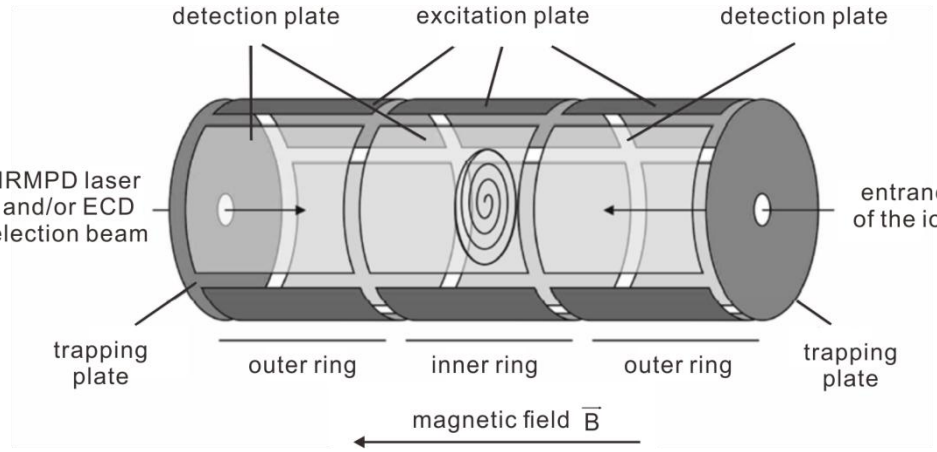

Figure 22. Schematic overview of an ICR cell and its three different opposing sets of electrode plates: trapping plates, excitation plates and detection plates.[223] [217]

Equation 1.3.3 depicts the radius *r* of the ion's orbits in which *B* is the magnetic field strength; *v* is the velocity of the ions in the circuit.

$$\gamma = \frac{mv}{qB} \qquad \text{Eq. 3.4.3}$$

Substitution of *v* by *rω* in equation 1.3.3 gives the angular frequency *ω*:

$$\omega = \frac{qB}{m} \qquad \text{Eq. 3.4.4}$$

From equation 3.4.4, we can clearly observe that the angular frequency *ω* is a function of the ion's mass, charge, and the magnetic field. Since the magnetic field *B* is constant, the *m/z* ratio only corresponds to one particular cyclotron frequency and is independent of the ions' orbital radii. Therefore, if a transverse high-frequency alternating electrical field is employed to the transmitter plates shown in Figure 22, the trapped ions in the ICR cell will be excited to acerbate its velocity and move in a larger radius. When the radius is large enough, the detection of ions become possible by measuring the frequency of the mirror current when the ion package fly along the detection or receiver plates. Since this frequency measurement can be done with extremely high precision as well as with the continuous induction of image currents, the ICR analyzer provides a very high resolution that can be used to determine masses with extremely high accuracy.

Moreover, if one properly selects the high-frequency pulse, all ions except the one of interest can be accelerated to a radius larger than the diameter of the ICR cell, and thus vanish due to the neutralization resulting from its collision with the cell walls. As a result, only the desired ions survive in the cell and can be used for various tandem MS experiments. For example, if the FTICR instrument is coupled with infrared lasers, one can conduct the fragmentation experiment through infrared multiphoton irradiation (IRMPD) with defined laser irradiation interval.[224, 225] The irradiation of the desired ions with an IR laser (10.6 μm) results in a significant increase of the internal energy of the selected ions to induce the fragmentation of ions. Other fragmentation reactions like electron-capture dissociation (ECD),[226-228] electron-transfer dissociation (ETD),[229, 230] and sustained off-resonance irradiation collision-induced decay (SORI-CID)[231] are all possible to perform in the FTICR instruments. Besides fragmentation reactions, bimolecular reactions like hydrogen-deuterium exchange (H/D exchange) can be carried out with the of our FTICR instrument, which is discussed in the following chapter.

The principle of H/D exchange

H/D exchange is a chemical reaction in which a covalently bound, but labile hydrogen atom is replaced by a deuterium atom, or vice versa. H/D-exchange is an effective method to detect the reactivity of the groups with liable hydrogens and is therefore capable of providing information about the solvent accessibility of various parts of the molecule and structural conformation. The H/D-exchange can be performed both in solution- and gas-phase. Monitoring the isotope exchange in solution-phase can be achieved by NMR spectroscopy or mass spectrometry. In comparison with NMR, mass spectrometry has several advantages: a) less sample material is required; b) the concentration of samples can be very low (as low as 0.1 μM); c) the size limit is much greater, even in the case of large biomolecules (proteins, peptides, and their complexes).[232] Therefore, H/D-exchange coupled with mass spectrometry has been extensively used to study protein folding processes and monitor conformational changes in proteins as they relate to protein function.[233, 234]

Recently, the gas-phase H/D-exchange was found to be particular useful for examining

hydrogen-bonded supramolecular complexes.[235] In solution, the building blocks in supramolecular complexes undergo in a highly dynamic intermolecular exchanges process. Therefore, the direct analysis of intramolecular process becomes extremely difficult. However, the intermolecular exchanges can be efficiently blocked in the gas-phase of mass spectrometer due to charge repulsion and high vacuum conditions. Since the hydrogen atoms involved in hydrogen-bonded interactions usually will behave differently in comparison with freely accessible ones, the isotope exchange experiments in the gas-phase offer a different view on the complexes' intrinsic reactivities.

As mentioned in the last chapter, the H/D-exchange can be conducted both in the ICR cell and hexapole Q3 in our FTIC-MS. The rate of H/D-exchange is sensitive to the pressure of exchange reagent.[236] The isotope exchange is executed more efficiently in the Q3 than in ICR cell (the pressure in Q3 is *ca.* 10^{-5} mbar, that in ICR cell is *ca.* 10^{-7} mbar). So far, ND_3, D_2O, CH_3OD, DCOOD and CH_3COOD are the most commonly used deuteration reagents which can be introduced into the reaction region for a defined reaction time. It should be noted that one should consider the nature of the deuteration site before choosing a specific reagent since the rate of H/D-exchange and the reaction mechanism is largely dependent on the type of exchange reagents.[235]

Normally, the HDX reaction consists of five steps: 1) the formation of an encounter complex of substrate and deuteration reagent, 2) a followed proton transfer, 3) isotope scrambling, 4) deuteron back-transfer and 5) dissociation of the product complex (Figure 23).[237, 238] The difference in proton affinities (*ΔPA*) of the analyte and the exchange reagent is one of most decisive parameter concerning the H/D-exchange rates of the two reaction partners. The larger *ΔPA*, the slower the exchange becomes.[239, 240] If the *ΔPA* is more than 85 kJ mol^{-1}, the exchange is usually prohibited.[237 238, 239] However, if there is a second functional group available in the substrate, the H/D-exchanges are postulated to proceed through a so-called 'onium mechanism' or 'relay mechanism,[241-245] and the reaction becomes significantly faster than expected even for objects whose *ΔPA* is as large as 200 kJ mol^{-1} (particularly for amino acids and peptides).[246] For basic donor reagents like ND_3 (small *ΔPA*), the 'onium mechanism' prevails (Figure 5, up). In this

case, the proton is directly transferred to the ammonia molecule, the carboxyl group only serves as an molecular anchor forming hydrogen bonding with one proton of reagent. The onium mechanism is only possible when the difference in proton affinities between the neutral substrate and exchange reagent is small enough. For less basic reagents like D_2O or MeOD, a direct proton transfer is not feasible, thus the relay mechanism is favorable (Figure 24, bottom). In this case, two protons involved in hydrogen bonding are transferred simultaneously without requiring a net proton transfer to the reagent.

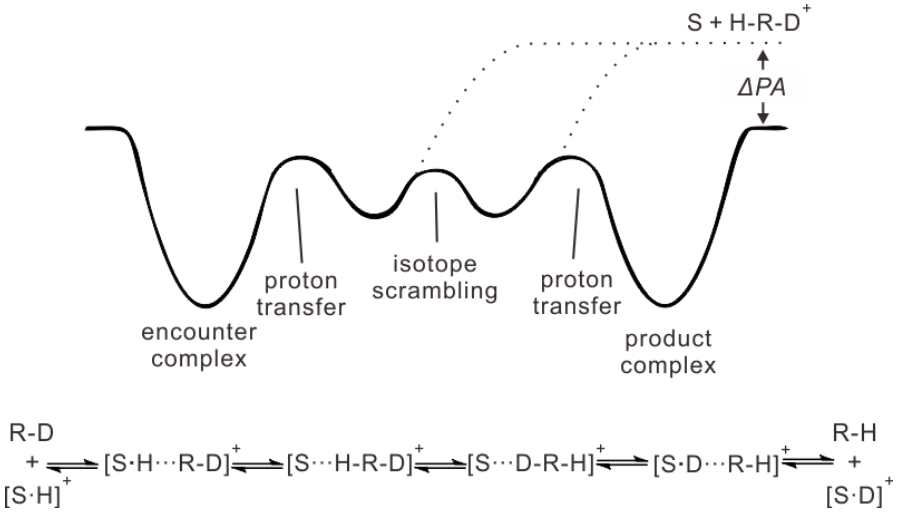

Figure 23. Reaction coordinate of an H/D exchange reaction between a substrate ion $[S \bullet H]^+$ and a neutral deuteration reagent R-D. Dotted lines indicate the dissociation of the proton-transfer complexes ion into its constituents.

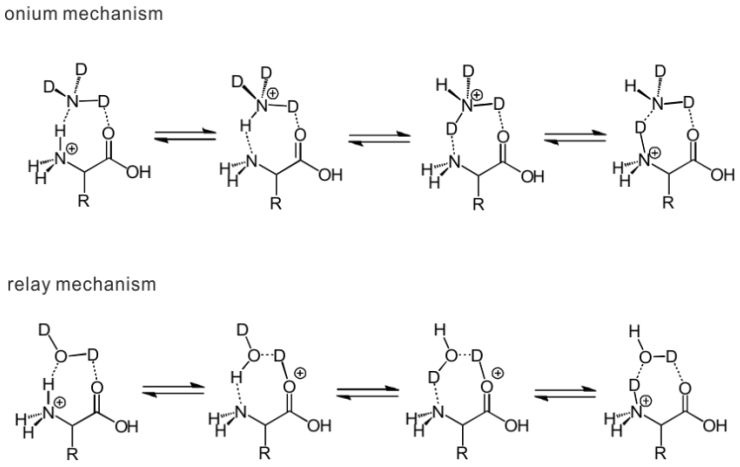

Figure 24. Two exchange mechanisms that operate in the H/D-exchange in amino acids and peptides.[216]

4. Review article: Host-guest chemistry of dendrimers in the gas phase

This chapter was published in the following journal:
Z. Qi, C. A. Schalley, *Supramol. Chem.* **2010**, *22*, 672-682.

http://dx.doi.org/10.1080/10610278.2010.486438

Declaration on the personal contribution in this work

The conception of the work as well as the full range of all references and writing the final manuscript happened in cooperation with C. A. Schalley.

Content and summary of the work

This work is a review article concerning developments in the field of host-guest chemistry of dendrimers in the gas-phase during recent years.

We first summarized the past development of dendrimers and its host-guest chemistry in the solution phase. Then we introduced the basic principles of mass spectrometry and how it has contributed to the host-guest chemistry as well as the characterization of dendrimers itself. Accordingly, we analyzed some problems which are hard to solve by conventional methods in solution phase and evaluated the potential advantage of mass spectrometry. Furthermore, how powerful tandem mass spectrometric experiments could benefit the host-guest chemistry of dendrimers was also discussed.

Some recent examples were selected to demonstrate how useful mass spectrometry and its gas phase chemistry are for the host-guest chemistry of dendrimers, including: 1) screening the specificity and stability of multivalent dendritic host–guest complexes depending on the nature of the guests, 2) revealing a dendritic effect during dendrimer–tweezer complex fragmentation, and 3) monitoring an highly dynamic intracomplex movement of crown ether(s) along the dendrimer periphery.

5. Systems chemistry: logic gates based on the stimuli-responsive gel-sol transition of a crown ether-functionalized bis(urea) gelator

This chapter was published in the following journal:
Z. Qi, P. Malo de Molina, W. Jiang, Q. Wang, K. Nowosinski, A. Schulz, M. Gradzielski, C. A. Schalley, *Chem. Sci.* **2012**, *3*, 2073-2082.
http://dx.doi.org/10.1039/C2SC01018F

Declaration on the personal contribution in this work

Z. Qi and W. Jiang proposed the idea and developed the conception of the work. Z. Qi, P. Malo de Molina, Q. Wang, K. Nowosinski and A. Schulz conducted the experiments. The full range of all references and writing the final manuscript were completed in cooperation with W. Jiang, A. Schulz. M. Gradzielski and C. A. Schalley.

Content and summary of the work

We reported a crown ether-functionalized bis(urea) organogelator equipped with two benzo[21]crown-7 moieties at both terminal ends. Its gel-sol transition can be controlled by several different molecular recognition events: K^+ binding to the crown ether, formation of *pseudo*rotaxane with secondary amine and the interaction of Cl^- anion with urea unit. The intriguing part of this research occurred through the rational design of the components (gelator alone or with one of these chemical stimuli), the inputs (the rational choice of the type and amount of these chemical stimuli), as well as the sequence of the addition of these inputs into the system, the macroscopic gel-sol transition was able to be operated in a logical way. Accordingly, the designed system can act as different chemical logic gates including OR, AND, XOR, NOT, NOR, XNOR and INHIBIT gates. The resultant supramolecular gels system shows great potential by simply choosing and arranging the known responsive properties to endow the gel materials with ‘smart thinking’.

6. Fibrous networks with incorporated macrocycles: a chiral stimuli-responsive supramolecular supergelator and its application to biocatalysis in organic media

This chapter was published in the following journal:
Z. Qi, C. Wu, P. Malo de Molina, H. Sun, A. Schulz, C. Griesinger, M. Gradzielski, R. Haag, M.B. Ansorge-Schumacher and C.A. Schalley, *Chem. Eur. J.*, **2013**, *19*, accepted (DOI: 10.1002/chem.201300193)
http://dx.doi.org/10.1002/chem.201300193

Declaration on the personal contribution in this work

Z. Qi and C. Wu proposed the idea and developed the conception of the work. Z. Qi. P. Malo de Molina, H. Sun, and A. Schulz conducted the experiments. The full range of all references and writing the final manuscript were completed in cooperation with C. Wu. R. Haag, M. Gradzielski and C.A. Schalley.

Content and summary of the work

We designed and synthesized a new and versatile crown ether-appended chiral gelator which shows impressive gelation ability in a variety of organic solvents, particularly in acetonitrile. Due to the crown ether, the resultant supramolecular gel is sensitive to multiple chemical stimuli and the sol-gel phase transitions can be reversibly triggered by host-guest interactions. Furthermore, we proposed a strategy to utilize the selective responsive supramolecular gel as an immobilization and recycling media for Pickering emulsion. We demonstrated that the 3D-network in the gel can entrap the enzyme (CalB, lipase B from *Candida antarctica*) and release it upon the addition of potassium ions. The obtained environmental responsive gel system was extended to be utilized as a novel matrix for Pickering emulsion as a proof of concept. The advantage of this gel matrix is it not only contributes to solving the phase problem that often exists when enzymes are to be used to catalyze organic reactions in unpolar organic media, but also realize the recycling of the entrapped enzyme on demand by chemical stimuli. The similarity of both CD spectra indicates almost no structural differences between the native enzyme and the one which was released from the emulsion microparticles.

7. Self-recovered macrocycle-equipped low-molecular-weight ionogels and their host-guest chemistry in pure ionic liquids

This chapter contains an unpublished manuscript:

Z. Qi, N.L. Löw, P. Malo de Molina, C. Schlaich, M. Gradzielski, C.A. Schalley, *Org. Bio. Chem.* (manuscript in preparation)

Declaration on the personal contribution in this work

Z. Qi developed the conception of the work. Z. Qi. N.L. Löw, P. Malo de Molina conducted the experiments. The full range of all references and writing the final manuscript were completed in cooperation with N.L. Löw. M. Gradzielski and C.A. Schalley.

Content and summary of the work

An unexpected finding in which the chiral gelator we developed can also form gels in ionic liquids, which were accordingly termed ionogels. The gelation of this gelator in different ionic liquids with varied structures was examined. The resultant ionogels showed remarkable thermostability. The temperatures of gel-sol transition (T_{gs}) of all ionogels were over 100 degree. We found that the host-guest complexation of crown ether and secondary ammonium still occurs in pure ionic liquids, which was proved by ITC experiments. Based on this observation, the gel-sol transition could be further stimulated by the addition of a suitable amount of guests which were able to form *pseudo*rotaxane structures with the appended crown units. The obtained ionogels exhibited impressive mechanical properties. The mechanical strength of the corresponding ionogels was considerably high and even comparable with cross-linked protein fibers. Furthermore, all ionogels displayed rare rheopexy (shear thickening) phenomena instead of thixotropy at low shear rates. Interestingly, the ionogels even possesses a rapid self-recovery property.

Organic & Biomolecular Chemistry

Dynamic Article Links ►

ARTICLE TYPE

Cite this: DOI: 10.1039/c0xx00000x

www.rsc.org/obc

Self-recovered macrocycle-equipped low-molecular-weight ionogels and their host-guest chemistry in pure ionic liquids

Zhenhui Qi,[a] Nora L. Löw,[a] Paula Malo de Molina,[a,b] Christoph Schlaich,[a] Michael Gradzielski,[b] and Christoph A. Schalley*[a]

Received (in XXX, XXX) Xth XXXXXXXXX 20XX, Accepted Xth XXXXXXXXX 20XX
DOI: 10.1039/b000000x

An unexpected finding concerned that the crown-ether-functionalized chiral bisurea gelator form ionogels was reported. The detailed gelation ability of this macrocycle-containing gelator in different ionic liquids was examined. The resulting ionogels showed remarkable high thermal stability. The temperatures of gel-sol transition (T_{gs}) of all ionogels reach over 100 degree. The employing of ionic liquids as solvents endows the ionogels with impressive mechanical properties. The mechanical strength of the corresponding ionogels was considerably high and was even comparable with that of cross-linked protein fibers. Furthermore, all ionogels displayed rare rheopexy (shear thickening) phenomena instead of thixotropy at low shear rates. Interestingly, the ionogels even possesses a rapid self-recovered property. Besides, the host-guest complexation of crown ether and secondary ammonium still occurs in pure ionic liquids, which was proved by isothermal titration calorimetry (ITC) experiments. Based on this observation, the gel-sol transition of ionogels could be further stimulated by the formation of *pseudo*rotaxane structures.

Introduction

Low-molecular-weight gelator (LMWG) is an interesting type of soft materials which have drawn considerable attention recently due to their unique reversibility.[1] Numerous functional LMWGs have been realized with selective environmental responsiveness, which can be further applied in drug/protein delivery, catalytic medium, self-healing materials and so on. However, designing new types of LWMGs and predicting their gelation behavior remain great challenging. Previous investigations were mostly based on serendipitous discovery or on structural optimization of discovered basic gelation elements. Less attention was paid to manipulation of solvents which may be also a facile way to improve gel's property.[2] Apart from most tested solvents (e.g. water, toluene and other conventional organic solvents), ionic liquid is one sort of solvents that has been developed in broad areas, while infrequently employed in gel chemistry. Ionic liquids have been widely recognized as a new generation of green solvents due to their unique physical properties, including negligible vapor pressure, thermal stability, non-flammability, and exceptional electrochemical properties.[3] These characteristics have endowed them with a broad range of applications in science, technology and industry, such as organic synthesis (e.g. solvents, catalysis), engineering (e.g. coatings, lubricants), electrochemical devices (e.g. electrolytes, solar cells) and biological use (e.g. active pharmaceutical ingredients).[4]

Ionogels are kind of gel formed in ionic liquids. They keep the main properties of ionic liquids except outflow, thus greatly expand their possibility for applications.[5] Currently, the study concerned LMWGs-based ionogels just began,[6] if in comparison with the tremendous effort made on the low-molecular-weight hydrogels/organogels.[7] These reported LMWGs-based ionogels have shown a great potential due to their combination of both the advantages of ionic liquids and supramolecular chemistry.[8] However, the environmental responsiveness of most reported ionogels merely restricts in thermal reversibility.[9] And the mechanical strength of the LMWG based ionogels are still far from that required for practical uses. For the point of material applications, it is still a challenge to integrate the processability, stimuli-responsiveness and mechanical properties into one single ionogel.

Previously, we designed and synthesized a new benzo[21]-crown-7-functionalized LMWG **1** based on bisurea structures, which shows impressive gelation ability in numbers of organic solvents, particularly in acetonitrile.[10] Herein, we report our lucky founding that this crown ether functionalized chiral bisurea compound is able to form ionogels in different ionic liquids (Scheme 1). To the best of our knowledge, no macrocycle functionalized compound has been applied in this context. The detail gelation behavior of this macrocycle-functionalizaed gelator in different ionic liquids was investigated. Surprisingly,

employing ionic liquids not only significantly increases the mechanical strength of the resulting gels, but also leads the ionogels with unforeseen rapid self-recovered property. expanding the useful lifespan of materials. Furthermore, the molecular recognition properties of the crown ether unit in the gelator still exist in pure ionic liuqids with its secondary ammonium guest. As a result, the formation of *pseudo*rotaxane becomes a new chemical stimulus for the gel-sol transition of ionogels.

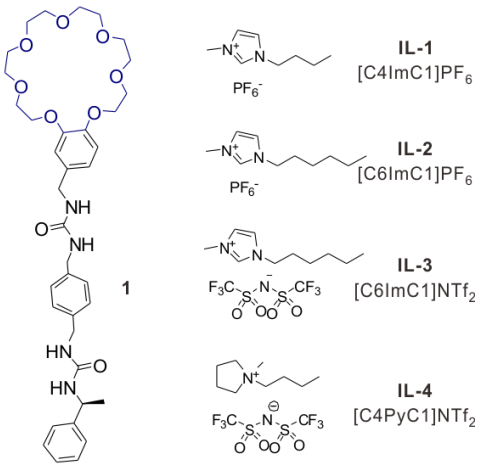

Scheme 1 The chemical structures of macrocycle-functionalized gelator **1** and ionic liquids tested.

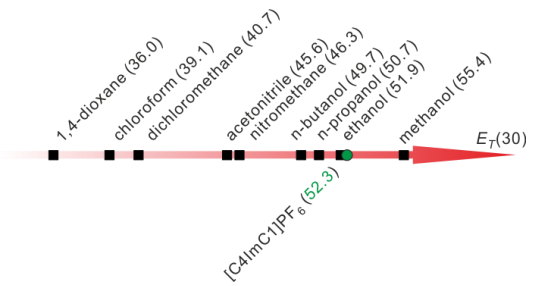

Fig. 1 The *ET* polarity scale of the organic solvents where **1** form gels, the green spot indicates the $E_T(30)$ value of ionic liquid [C4ImC1]PF_6 which falls in the rage of gelation.

Result and discussion

Gelation study

A few studies disclosed that the gelling power of a LMWG is closer relate to the polarity of solvents (*ET* polarity scale).[11] Scanning the polarity of all the previses tested gelated solvents for **1** (Figure 1), we found that their polarity value ($E_T(30)$) ranges from 36.0 to 55.4 kcal/mol,[12] which coincidentally covers that of ionic liquid, e.g. [C4ImC1]PF6 with $E_T(30)$ is 52.3 kcal/mol.[13] Therefore, we expected that this crown-equipped gelator may form gels in ionic liquids.

The gelation behavior of compound **1** was evaluated in four different kinds of ionic liquids with diverse structures. The detailed gelation results are displayed in Table 1. The critical gelation concentration (cgc) of **1** in [C4ImC1]PF_6, one of most widely used ionic liquids, is 1.14 wt.% (below the cgc, no stable gel forms). The elongation of the alkyl chain on the imidazolium or replacement of counterion does not affect the trend of gelation. Gelator **1** successfully formed stable ionogels in [C6ImC1]PF_6 and [C6ImC1]NTf_2, respectively. In [C6ImC1]PF_6, compound **1** showed particularly proficient gelation ability with very low cgc (0.47 wt.%). This value is even comparable with the most efficient polymeric gelating spices.[14] In the ionic liquid with pyrrolidinium cation, [C4PyC1]NTf_2, the gelator showed moderate gelation ability (cgc = 2.92 wt.%).

Table 1 Gelation ability of gelator 1 in selected ionic liquids

Entry	Ionic liquid	States	CGC
1	**IL-1**: [C4ImC1]PF_6	Gel	1.14 wt.% (23.0 mM)
2	**IL-2**: [C6mC1]PF_6	Gel	0.47 wt.% (15.3 mM)
3	**IL-3**: [C6ImC1]NTf_2	Gel	1.48 wt.% (31.2 mM)
4	**IL-4**: [C4PyC1]NTf_2	Gel	2.92 wt.% (60.6 mM)

Thermo stability

To probe the thermal properties of the ionogels, the effect of the concentration on the gel−sol phase transition temperatures (T_{gs}) upon heating were examined. As shown in Figure 2, all the ionogels display thermal reversible nature that they melted upon heating and turned into a gel when the temperature cooling, indicating the self-assembled aggregation of the LMWGs in ionic liquids. Interestingly, The T_{gs} of each type of ionogels was able to reach greater than 100 ℃ with the increased concentration of the gelators. The thermal stability above 100 ℃ suggests that these ionogels can be used as quasi-solid ionic materials under conditions that include relatively high temperatures.

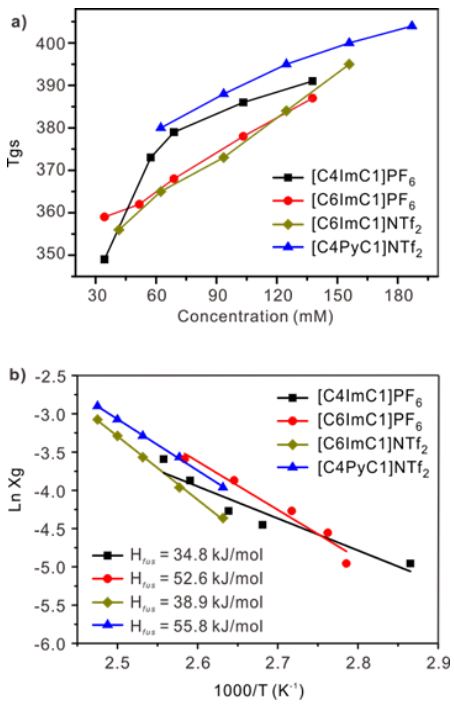

Fig. 2 a) Variation of the gel-to sol transition temperature T_{gs} with the gelator concentrations of representative ionogels; b) Semi-log plot of ionogels. The results are analyzed according to the following Schröder-van Laar equation.

This journal is © The Royal Society of Chemistry [year]

Table 2. FT-IR data for 1 in the gel state.[a]

Solvents	Absorptions / cm^{-1}		
	NH-stretch	Amide-I	Amide-II
$[C4ImC1]PF_6$	3316,0	1616,1	1582,1
$[C6ImC1]PF_6$	3326,6	1616,1	1560,1
$[C6ImC1]NTf_2$	3319,9	1617,0	1568,8
$[C4PyC1]NTf_2$	3329,5	1615,1	1571,7
CH_3CN	3325,5	1611,1	1568,6

[a]All spectra are recorded at room temperature, using the corresponding ionic liquid as background.

By applying Schröder-van-Laar equation to the observed results, the enthalpy change ΔH_{fus} in these phase transitions can be calculated (see the detail calculation in ESI).[15] The semi-log of the mole fraction of each gelator at each concentration was plotted against $1000/T_{gs}$, K^{-1} (Figure 2b). The calculated values of ΔH_{fus} clearly reflect the main cause for the high thermal stability of ionogels lie in the larger heat of fusion for disrupting strong cation-anion attractions in ionic liquids.[16]

FT-IR characterization

The urea functionality has been used widely in LMWGs because it provides a convenient 1D directionality and strong intermolecular hydrogen-bonding interactions. [17] Therefore, Fourier transform infrared (FT-IR) measurements were conducted to probe the hydrogen bonding in the resultant ionogels. As summarized in Table 2, all ionogels exhibit similar N-H stretch band ranged from 3316-3329 cm^{-1} and amide band around 1616 cm^{-1}, indicating the exist of strong intermolecular hydrogen bonding between urea groups in ionic medium.[18] Atomic force microscopy (AFM) investigation on gel of **1** in acetonitrile found the gel to be composed by numerous entangled fibers connecting by strong hydrogen bonding between intermolecular urea moieties. Due to the presence of analogous strong hydrogen bonding (Table 2, bottom line), we speculate such fibrous structures preserve in the resulting ionogels.

Rheological characterization

The mechanical properties of ionogels are one of the most important factors considered for their practical and sustainable applications. Therefore, all ionogels were examined with a Malvern (Bohlin) Gemini rheometer employing a plate - plate geometry at a constant temperature of 25 ℃. In order to determine the linear viscoelastic area, we performed strain amplitude sweeps on the gel samples. Shown in Figure 3a, all the ionogel gels showed elastic response, and the value of storage modulus G´decreased rapidly above the critical strain regions, indicating a strain induced collapse of the gel state. The critical strain of tested ionogels does not depend on the type of ionic liquid, although it varies slightly from one to another. With a fixed deformation of 0.5 %, the ionogels thereby were ascertained to work in the linear viscoelastic regime. The obtained storage moduli G′ and loss moduli G″ of all the gel samples are plotted against the angular frequency, and G′ was constantly greater than G″ for the entire range of frequencies, evidencing that all these gels are dominated by their elastic properties and show the typical behavior of a Bingham fluid,[19] which is usually observed for gel materials.[20]

Interestingly, employing ionic liquids as solvent, the mechanical strength of corresponding gels significantly increases in comparison to those using conventional organic solvents. Shown in Figure 4, the gel in acetonitrile exhibits moderate mechanical strength, whose storage modulus G´reaches 2000 Pa at concentration of 40 mM (3.6 wt.%).[10] However, the G´of ionogel in $[C4ImC1]PF_6$ at lower concentration (30 mM, 1.5 wt.%) have already reached 30 000Pa. The value of G´increased with an increase in the concentration of 1 and eventually reached 1.6×10^5 Pa at 60 mM (3 wt.%, Figure 4 and Figure S3) This value is exceptionally high and comparable with the G′ values of the hydrogel based on cross-linked protein fibers[21] as well as ionogels based on polymeric materials.[14] This significant increased mechanical strength indicates that the network formation in these ionic liquids is more effective than that in the acetonitrile. From the storage modulus one can estimate an effective number density ${}^1N$ of elastic network points based on the relation $G' \approx G^0 = {}^1N \bullet k \bullet T$. From the values given here, one arrives at approximately one network point per (2.9 - 4.7 nm)^3. This can be considered a rheological relevant structural size of the elastic network.

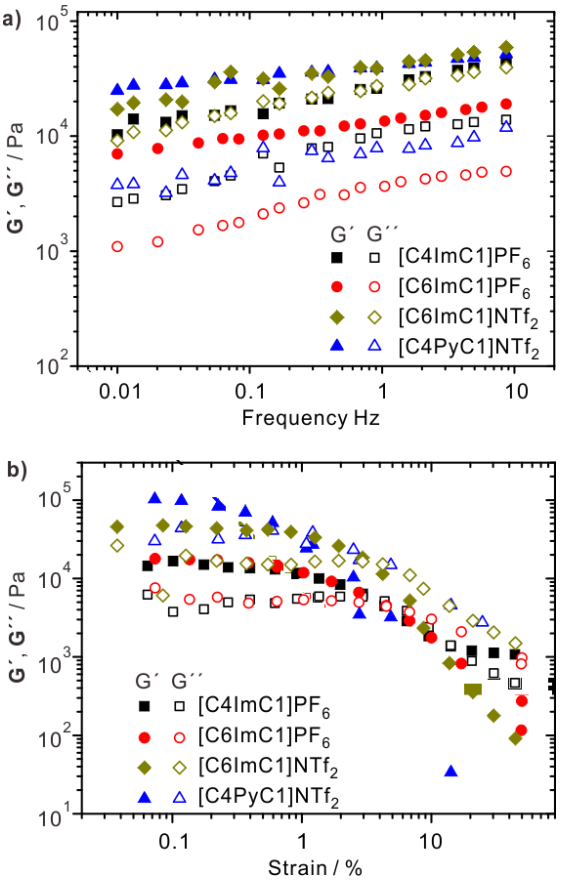

Fig. 3 Oscillatory rheological analysis of the ionogels: (a) Storage modulus and complex viscosity obtained from a strain-amplitude sweep performed at 10 Hz. (b) Storage and loss moduli obtained from a frequency sweep performed at 0.005 strain.

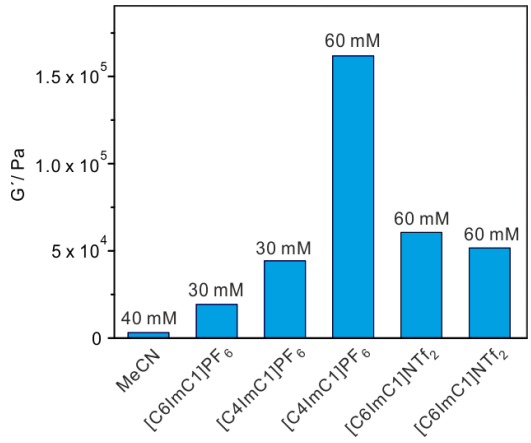

Fig. 4 Values of storage elastic modulus of gel 1 prepared in different solvents. The parallel comparison is operated under the same frequency (10 Hz) and stran (0.050%).

All the ionogels display rare rheopexy (shear thickening) phenomenon instead of thixotropy at low shear rates. Displayed in Figure 5, the time dependent shear viscosity of ionogel in $[C4ImC1]PF_6$ was measured at several shear rates (0.001, 0.01, 0.1, 1 and 10 s^{-1}) respectively. At shear rates lower than 1s^{-1}, the time dependent shear thickening is observed, indicating the ionogel solidify more quickly when subjected to shear. It is widely admitted that the shear thickening is caused by the building up of shear induced structures.[22] For the samples in other ionic liquids, an almost identical behavior was (Figure S1 in ESI). However, if the shear rate increases, the typical shear thinning phenomena for LMWGs still observed (Figure S2).[23] Shear-thinning behavior is a characteristic feature of self-assembled LMWGs. Indeed, intermolecular interactions can be disrupted if the shear rate is high enough.

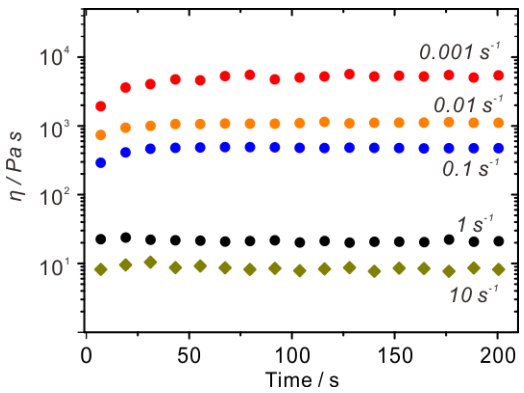

Fig. 5 Typical time dependent shear viscosity measured at several shear rates (0.001, 0.01, 0.1, 1 and 10 s^{-1}) for ionogel in $[C4ImC1]PF_6$.

Intriguingly, the ionogel consisting of **1** {$[C4ImC1]PF_6$ was demonstrated a rapid recovery in its mechanical strength after a breakdown at oscillations of shear rates (Figure 6). The recovery was fully reproducible for at least eight cycles. To the best of our knowledge, this is the first observation of a rapid recovery and rheopexy in an LMWG based ionogel, although a similarly rapid recovery has been previously reported in several polymer based systems.[24] We consider that the rapid recovery should be mainly caused by instinct high viscosity of ionic liquids. Since the electrostatic interaction between ionic pairs was a long-range force in comparison with the other ones such as hydrogen bond interaction between urea groups. Therefore, the local gel network was not disrupted under large strain, but only the interconnects between gel domains were broken, similar to the other rapid recovery gels. Consequently, ionic liquids effectively contribute a rapid reconstruction of the gel network. Until now, this is the first example which shows low-molecular weight ionogel with rapid self-recovery property.

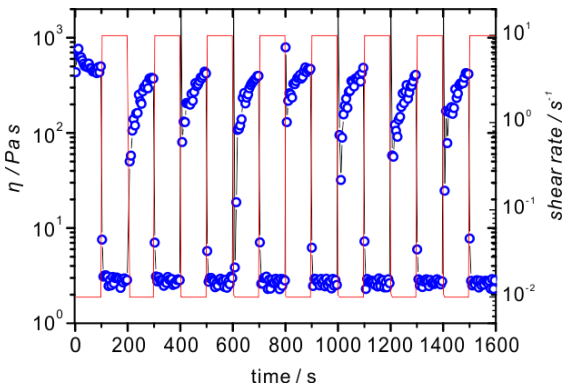

Fig. 6 Step shear rate measurement of ionogel in $[C4ImC1]PF_6$ displaying recovery of its structure with 8 cycles.

Molecular Recognition in Ionic Liquids for Gel-Sol Transition

Until now, most investigations on the host-guest recognition behavior invoving ionic liquid were conducted in mixed solvent systems.[25] Study which was carried out in pure ionic liquids is quite rare. Benzo-21-crown-7 (**BC7**) has been reported as smallest macrocycle to form *pseudo*rotaxane structures with secondary ammoinium ions (Scheme 2),[26] thus have been utilized to construct elaborated supramolecular architectures.[27] However, their formation of *pseudo*rotaxane structures in pure ionic liquids have never been investigated. Here, the gelator **1** naturally equipped with **BC7**, that promots us to probe the potential host-guest reconginition in pure ionic liquids.

Since secodary ammonium like guest **G1** was domonstrated to slip through the cavity of BC7, the gel-sol transition might be triggered by formation of *pseudo*rotaxane, thus was tested using monovalent guest **G1**. Depicted in Figure 7a, when guest **G1** was added into the ionogel **1** in [C4ImC1]PF6, the existence of three equivalent **G1** is enough to trigger the gel phase into solution phase, implying the ocuurence of complexation between BC7 unit with G1. The existen of G1 resuling the same gel-sol transition in other ionogels which prepared in other three kinds of ionic liuqids. Interestingly, the gel-sol transitions can be reversed by the addition of triethylamine (TEA) as a base. Upon addition of certain amount of TEA, the gel phase was regained. It's plausible that TEA deprotonates and unthreads **G1** from the crown ether, thus destroys the *pseudo*rotaxane structure. Such a reversible gel-sol transition was conductible in all the ionogels which prepared in different ionic liquids. When the same complexation experiments were carried out with

This journal is © The Royal Society of Chemistry [year]

Table 3. Thermodynamic data for host-guest binding of **BC7** and **G1** in different ionic liquids

entry	ionic liquid	K_a (M^{-1})	Δ G (kJ/mol)	Δ H (kJ/mol)	-TΔS (kJ/mol)
1	**IL-1**: $[C4ImC1]PF_6$	546	-15,6	-21,9	-6,3
2	**IL-2**: $[C6ImC1]PF_6$	350	-14,5	-21,6	-7,1
3	**IL-3**: $[C6ImC1]NTf_2$	969	-17.0	-18.4	-1.4
4	**IL-4**: $[C4PyC1]NTf_2$	5270	-21,2	-31,9	-10,7

dibenzylammonium hexafluorophosphate, no gel-sol transition was observed (Figure 7b. The dramatical difference in the same condition indicate the phenyl group is too large to penetrate the **BC7**'s cavity, expels all other possible interaction modes such as side-on coordination to the crown or hydrogen bond formation with the urea carbonyl oxygen atom, thus confirm that the formation of *pseudo*rotaxane in pure ionic liquid and mediates the gel-sol transition.

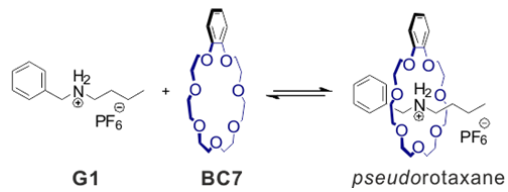

Scheme 2. The formation of *pseudo*rotaxane structure based on **BC7** and its secondary ammonium guest **G1**.

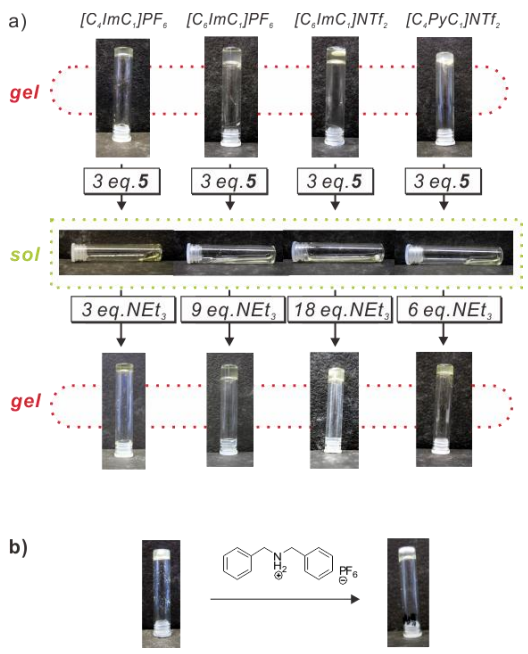

Fig. 7 Photographs of ionogels prepared from different ionic liquids. The stimuli-responsive behavior: Gel-sol transitions controlled by acid/base-controlled *pseudo*rotaxane with **G1**. Typical control experiments of ionogel **1** in [C4ImC1]PF6 and the mixture obtained after adding 3.0 eq. of dibenzyl ammonium hexafluorophosphate. Since the phenyl group is too large to penetrate the crown ether, no *pseudo*rotaxane forms and the gel persists.

Isothermal titration calorimetry (ITC) is a powerful physical technique for measuring thermodynamics and stoichiometry in solution.[28] Therefore, ITC measurement were perfomed on **BC7** and **G1** in pure ionic liquids, in order to obtain quantitative information of the binding strength of crown ether unit with secondary ammonium ion. The resulting isotherm fits extremely well to a 1:1 binding mode (Figure S8), which is consistence with the mode of *pseudo*rotaxane. The detailed ITC measurements results were summarized in Table 2. The binding bonstants K_a of **BC7** and **G1** in four tested ionic liquids range from 350 M^{-1} to 5270 M^{-1}. For the imidazolium cation based ionic liquids, all the K_a values in there are below 1000 M^{-1}, which are close to that in aceton (615 M^{-1}).[26a] While in pyrrolidinium cation based ionic liquid, $[C4PyC1]NTf_2$, the K_a value increases signifcantly to 5270 M^{-1}, indicating that the K_a is largely dependent on cation, anion only has minor effect on the formation of *pseudo*rotaxae. The big diffence can be assigned to the different competitive abilities of the cations of ionic liquids to form complex with crown ether. Previous studies on crown ethers and five-membered *N*-heteroaromatic cations showed that the imidazolium cation is able to weakly interact with benzo-crown-ether,[29] through H-bonding and cation−π interactions. While, the interaction between crown ether and pyrrolidinium is neglective due to the steric hinderance. Therefore, the competition binding between imidazolium cation resulting in the great reduce of binding constant of secondary ammonium with the crown's cavity. Therefore, one can conclude that the formation of a *pseudo*rotaxane is possible in pure ionic liquids, and can be further applied as new stimulus to trigger the macrocycle-containing ionogels.

Conclusions

In conclusion, for the first time, we developed crown-ether macrocycle-functionalized low molecular-weight ionogels. The crown ether-appended chiral gelator shows considerable gelation in ionic liquids. The resulting ionogels showed impressively a high thermal stability with T_{gs} over 100 degree. In comparison with conventional gels formed in organic solvents, ionic liquids significantly increase the mechanical strength of the corresponding gels. The storage modulus G´is impressively high and is even comparable with cross-linked protein fibers. Moreover, all ionogels displayed rare rheopexy (shear thickening) phenomenon instead of thixotropy at low shear rates. Intriguingly, the ionogel even possesses rapid self-recovery properties. Our investigation shows that the ionic liquids have a great potential to manipulate gels' properties. The molecular recognition in pure ionic liquid might bring new possibility to

construct novel supramolecular architectures combining the unique properties of ionic liquids.

Acknowledgements

We thank the Deutsche Forschungsgemeinschaft (SFB 765) and the Fonds der Chemischen Industrie for financial support. Z. Q. is grateful to the China Scholarship Council (CSC) for a Ph.D. fellowship.

Notes and references

[a] *Institut für Chemie und Biochemie, Freie Universität Berlin, Takustrasse 3, 14195 Berlin, Germany, Fax: +49 30-838-55817; Tel: +49 30-838-52639; E-mail: christoph@schalley-lab.de*

[b] *Institut für Chemie, Sekretariat TC7, Technische Universität Berlin, Strasse des 17. Juni 124, 10623 Berlin*

[c] *Present Address: The Skaggs Institute for Chemical Biology, The Scripps Research Institute, 10550 N. Torrey Pines Road, La Jolla, California 92037, USA*

† Electronic Supplementary Information (ESI) available: Synthetic procedures and characterization data for new compounds; COSY NMR spectra supporting the NMR signal assignment; additional experiments for the characterization of the gels; ^{1}H NMR experiments supporting the stimuli-responsive behavior. See DOI: 10.1039/b000000x/

1 a) P. Terech and R. G. Weiss, *Chem. Rev.*, 1997, **97**, 3133; (b) L. A. Estroff and A. D. Hamilton, *Chem. Rev.*, 2004, **104**, 1201; (c) N. M. Sangeetha and U. Maitra, *Chem. Soc. Rev.*, 2005, **34**, 821; (d) A. R. Hirst, B. Escuder, J. F. Miravet and D. K. Smith, *Ange. Chem. Int. Ed.*, 2008, **47**, 8002; (e) S. Banerjee, R. K. Das and U. Maitra, *J. Mater. Chem.*, 2009, **19**, 6649; (f) E. A. Appel, J. del Barrio, X. J. Loh and O. A. Scherman, *Chem. Soc. Rev.*, 2012, **41**, 6195; (g) L. E. Buerkle and S. J. Rowan, *Chem. Soc. Rev.*, 2012, **41**, 6089; (e) A. Noro, M. Hayashi and Y. Matsushita, *Soft Matter*, 2012, **8**, 6416; Z. Qi, P. Malo de Molina, W. Jiang, Q. Wang, K. Nowosinski, A. Schulz, M. Gradzielski and C. A. Schalley, *Chem. Sci.*, 2012, **3**, 2073.

2 (a) P. Dastidar, *Chem. Soc. Rev.*, 2008, **37**, 2699; (b) J. H. van Esch, *Langmuir*, 2009, **25**, 8392.

3 (a) R. D. Rogers and K. R. Seddon, *Science*, 2003, **302**, 792; (b) M. Armand, F. Endres, D. R. MacFarlane, H. Ohno and B. Scrosati, *Nat. Mater.*, 2009, **8**, 621; (c) J. Dupont, *Acc. Chem. Res.*, 2011, **44**, 1223-1231.

4 (a) T. Welton, *Chem. Rev.*, 1999, **99**, 2071; (b) N. V. Plechkova and K. R. Seddon, *Chem. Soc. Rev.*, 2008, **37**, 123; (c) J. W. Lee, J. Y. Shin, Y. S. Chun, H. B. Jang, C. E. Song and S.-g. Lee, *Acc. Chem. Res.*, 2010, **43**, 985; (d) T. Torimoto, T. Tsuda, K.-i. Okazaki and S. Kuwabata, *Adv. Mater.*, 2010, **22**, 1196; (d) A. Kavanagh, R. Byrne, D. Diamond and K. J. Fraser, *Membranes*, 2012, **2**, 16; (e) C. Maton, N. De Vos and C. V. Stevens, *Chem. Soc. Rev.*, 2013. Advance Article.

5 J. Le Bideau, L. Viau and A. Vioux, *Chem. Soc. Rev.*, 2011, **40**, 907.

6 (a) N. Mohmeyer, D. Kuang, P. Wang, H.-W. Schmidt, S. M. Zakeeruddin and M. Gratzel, *J. Mater. Chem.*, 2006, **16**, 2978; (b) G. Feng, Y. Xiong, H. Wang and Y. Yang, *Electrochim. Acta*, 2008, **53**, 8253; (c) T. Tu, X. Bao, W. Assenmacher, H. Peterlik, J. Daniels and K. H. Dötz, *Chem. Eur. J.*, 2009, **15**, 1853; (d) S. Dutta, D. Das, A. Dasgupta and P. K. Das, *Chem. Eur. J.*, 2010, **16**, 1493; (e) A. K. Gupta, M. P. Singh, R. K. Singh and S. Chandra, *Dalton Trans.*, 2012, **41**, 6263; (f) S. K. Mandal, T. Kar, D. Das and P. K. Das, *Chem. Commun.*, 2012, **48**, 1814; (g)N. Minakuchi, K. Hoe, D. Yamaki, S. Ten-no, K. Nakashima, M. Goto, M. Mizuhata and T. Maruyama, *Langmuir*, 2012, **28**, 9259; (h) S. S. Moganty, S. Srivastava, Y. Lu, J. L. Schaefer, S. A. Rizvi and L. A. Archer, *Chem. Mater.*, 2012, **24**, 1386; (i) J. C. Ribot, C. Guerrero-Sanchez, T. L. Greaves, D. F. Kennedy, R. Hoogenboom and U. S. Schubert, *Soft Matter*, 2012, **8**, 1025; (j) J. Yan, J. Liu, P. Jing, C. Xu, J. Wu, D. Gao and Y. Fang, *Soft Matter*, 2012, **8**, 11697.

7 J. H. v. Esch and B. L. Feringa, Gels in *Encyclopedia of Supramolecular Chemistry*, Taylor & Francis, 2007, pp. 586.

8 (a) K. Hanabusa, H. Fukui, M. Suzuki and H. Shirai, *Langmuir* 2005, **21**,10383; (b) W. Kubo, S. Kambe, S. Nakade, T. Kitamura, K. Hanabusa, Y. Wada and S. Yanagida, *J. Phys. Chem. B* 2003, **107**, 4374; (c) A. Ikeda, K. Sonoda, M. Ayabe, S. Tamaru, T. Nakashima, N. Kimizuka and S. Shinkai, *Chem. Lett.* 2001, 1154; (d) N. Kimizuka, T. Nakashima, *Langmuir* 2001, **17**, 6759; (e) M. Amaike, H. Kobayashi and S. Shinkai, *Bull. Chem. Soc. Jpn.* 2000, **73**, 2553; f) K. Hanabusa, K. Hiratsuka, M. Kimura and H. Shirai, *Chem. Mater.* 1999, **11**, 649.

9 K. Hanabusa, H. Fukui, M. Suzuki and H. Shirai, *Langmuir*, 2005, **21**, 10383-10390.

10 Z. Qi, C. Wu, P. M. d. Molina, H. Sun, A. Schulz, C. Griesinger, M. Gradzielski, R. Haag, M. B. Ansorge-Schumacher and C. A. Schalley, *Eur. Chem. J.*, 2013, **19**, DOI: 10.1002/chem.201300193.

11 A. R. Hirst and D. K. Smith, *Langmuir*, 2004, **20**, 10851.

12 C. Reichardt, *Chem. Rev.*, 1994, **94**, 2319.

13 S. Zhang, N. Sun, X. He, X. Lu and X. Zhang, *J. Phys. Chem. Ref. Data*, 2006, **35**, 1475.

14 J. i. 14, H. Matsumoto and M. Yoshida, *ACS Macro Lett.*, 2012, **1**, 1108.

15 J. Weiss, M. Koepf and J. A. Wytko, Self-Assembly of Supramolecular Wires in *Supramolecular Chemistry: From Molecules to Nanomaterials*, ed. P. P. G. a. P. J. Steed, John Wiley & Sons, Ltd, 2012.

16 H. Sato, T. Yajima and A. Yamagishi, *Chem. Commun.* , 2011, **47**, 3736.

17 J. W. Steed, *Chem. Soc. Rev.*, 2010, **39**, 3686.

18 R. M. Versteegen, R. P. Sijbesma and E. W. Meijer, *Macromolecules*, 2005, **38**, 3176.

19 (a) E. C. Bingham, *Fluidity and Plasticity*, McGraw-Hill, New York, 1922; (b) J. D. Ferry, *Viscoelastic Properties of Polymers*, Wiley, New York, 1980.

20 (a) P. L. Luisi, R. Scartazzini, G. Haering and P. Schurtenberger, *Colloid Polym. Sci.*, 1990, **268**, 356; (b) C. M. Garner, P. Terech, J.-J. Allegraud, B. Mistrot, P. Nguyen, A. de Geyer and D. Rivera, *J. Chem. Soc., Faraday Trans.*, 1998, **94**, 2173; (c) P. Terech, D. Pasquier, V. Bordas and C. Rossat, *Langmuir*, 2000, **16**, 4485; (d) M. Burkhardt, S. Kinzel and M. Gradzielski, *J. Colloid Interface Sci.*, 2009, **331**, 514.

21 A. A. Martens, J. van der Gucht, G. Eggink, F. A. de Wolf and M. A. Cohen Stuart, *Soft Matter*, 2009, **5**, 4191.

22 (a) H. Rehage and H. Hoffmann, *Rheol. Acta*, 1982, **21**, 561; (b) N. J. Balmforth and R. V. Craster, Geophysical Aspects of Non-Newtonian Fluid Mechanics in *Geomorphological Fluid Mechanics*, eds. N. J. Balmforth and A. Provenzale, Springer Berlin Heidelberg, 2001, vol. 582, pp. 34.

23 C. Chassenieux and L. Bouteiller, Rheology in *Supramolecular Chemistry: From Molecules to Nanomaterials*, eds. P. Gale and J. Steed, John Wiley & Sons, Ltd, 2012.

24 E. A. Appel, X. J. Loh, S. T. Jones, F. Biedermann, C. A. Dreiss and O. A. Scherman, *J. Am. Chem. Soc.*, 2012, **134**, 11767.

25 X. H. Shen, Q. D. Chen, J. J. Zhang and P. Fu, Supramolecular Structures in the Presence of Ionic Liquids in *Ionic Liquids: Theory, Properties, New Approaches*, ed. A. Kokorin, 2011.

26 (a) C. Zhang, S. Li, J. Zhang, K. Zhu, N. Li and F. Huang, *Org. Lett.*, 2007, **9**, 5553; (b) C. Zhang, K. Zhu, S. Li, J. Zhang, F. Wang, M. Liu, N. Li and F. Huang, *Tetrahedron Lett.*, 2008, **49**, 6917; (c) X. Yan, M. Zhou, J. Chen, X. Chi, S. Dong, M. Zhang, X. Ding, Y. Yu, S. Shao and F. Huang, *Chem. Commun.*, 2011, **47**, 7086–7088.

This journal is © The Royal Society of Chemistry [year]

27 (a)W. Jiang, H. D. F. Winkler and C. A. Schalley, *J. Am. Chem. Soc.*, 2008, **130**, 13852; (b) W. Jiang and C. A. Schalley, *Proc. Natl. Acad. Sci. U. S. A.*, 2009, **106**, 10425; (c) W. Jiang, A. Schäfer, P. C. Mohr and C. A. Schalley, *J. Am. Chem. Soc.*, 2010, **132**, 2309; (d) W. Jiang, D. Sattler, K. Rissanen and C. A. Schalley, *Org. Lett.*, 2011, **13**, 4502.

28 (a) W. Jiang, K. Nowosinski, N. L. Löw, E. V. Dzyuba, F. Klautzsch, A. Schäfer, J. Huuskonen, K. Rissanen and C. A. Schalley, *J. Am. Chem. Soc.*, 2012, **134**, 1860; (b) N. L. Löw, E. V. Dzyuba, B. Brusilowskij, L. Kaufmann, E. Franzmann, W. Maison, E. Brandt, D. Aicher, A. Wiehe and C. A. Schalley, *Beilstein J. Org. Chem.*, 2012, **8**, 234; (c) L. Kaufmann, E. V. Dzyuba, F. Malberg, N. L. Low, M. Groschke, B. Brusilowskij, J. Huuskonen, K. Rissanen, B. Kirchner and C. A. Schalley, *Org. Biomol. Chem.*, 2012, **10**, 5954.

29 S. Kiviniemi, M. Nissinen, M. T. Lamsa, J. Jalonen, K. Rissanen and J. Pursiainen, *New J. Chem.*, 2000, **24**, 47.

Electronic Supplementary Material (ESI) for Organic & Biomolecular Chemistry
This journal is © The Royal Society of Chemistry 2012

Support Information

Self-Recovered Macrocycle-Equipped Low-Molecular-Weight Ionogels and Their Host-Guest Chemistry in Pure Ionic Liquids

Zhenhui Qi,[a] Nora L. Löw,[a] Paula Malo de Molina,[b,c] Christoph Schlaich,[a] Michael Gradzielski,[b] and Christoph A. Schalley*[a]

[a] *Institut für Chemie und Biochemie, Freie Universität Berlin, Takustraße 3, 14195 Berlin, Germany,*

[b] *Institut für Chemie, Sekretariat TC7, Technische Universität Berlin, Straße des 17. Juni 124, 10623 Berlin, Germany*

[c] *Department of Chemical Engineering, University of California Santa Barbara, 3357 Engineering II, Santa Barbara, USA*

Email: christoph@schalley-lab.de

Table of Contents

1. General methods

All reagents were commercially available and used as supplied without further purification if not mentioned otherwise. The compounds **1**, **BC7**, and **G1** were synthesized by previous methods.[1] Four ionic liquids, which are 1-Butyl-3-methylimidazolium hexafluorophosphate ([C4ImC1]PF_6), 1-Hexyl-3-methylimidazolium bis(trifluormethylsulfonyl)imide ([C6ImC1]NTf_2), 1-Hexyl-3-methylimidazolium hexafluorophosphate ([C6ImC1]PF_6), 1-Butyl-1-methylpyrrolidinium bis(trifluoromethylsulfonyl)imide ([C4PyC1]NTf_2) were purchased from Sigma-Aldrich, and used without further purification. FT-IR spectra recorded on the Nicolet Avatar 320 FT-IR spectrometer.

Preparation of gelator in Ionic Liquids The gelator and solvents (dichloromethane and ionic liquid) were put into a capped test-tube sonicated for 15 min to aid the dissolution process. Afterwards, the dichloromethane in the mixture was removed under vacuum at room temperature. The sample vial was left for 12 h at ambient condition. The state was evaluated by the "stable to inversion of a test tube" method. In the gel-sol transition test, the sample vial was left for 15 min before inversion test. The critical gelation concentration (cgc) was defined as the lowest concentration of the gelator which leads to a stable gel.

Gel-sol transition temperature measurements: T_{gs} was determined by a 'dropping-ball method'.[2] A small ball (166 mg) was placed on top of the gel in a test tube (inner diameter 1.0 cm), which was slowly heated in a oil bath at a rate of 1 K min^{-1}. T_{gs} is defined as the temperature when the ball had reached the bottom of the test tube. Dropping-ball experiments were carried out at least in duplicate, and the T_{gs} obtained were reproducible to within $\pm$ 2 ^{o}C.

The obtained Tg was plotted with the concentration of agelator (Cg) for 1: a) Tg versus Cg (Figure 2a); b) lnXg (Xg = the molar ratio of a gelator) versus 1/Tg (Figure 2b). The results are analyzed according to the following Schröder-van Laar equation:

$$\ln Xg = \frac{\Delta H_{fus}}{RT_g} + \frac{\Delta H_{fus}}{RT_{fus}}$$ eq 1

in which ΔH_{fus} and T_{fus} are the enthalpy of sol-gel transition and the melting temperature of a gelator, respectively. The obtained thermodynamic parameters are listed in Figure 2b in the maintext.

Guest-induced stimuli-responsive behavior: The guest compound was added to the test tube containing the already prepared gel. Subsequently, the capped test tube was heated until the guest molecule was dissolved in ionic liquid. The sample vial was left standing for 12 h at ambient conditions. The state was evaluated by the "stable to inversion of a test tube" method.

Rheological characterization of the gels: Rheology measurements were performed with a Malvern (Bohlin) Gemini 150 rheometer employing a plate-plate geometry (40 mm diameter; steel) with a gap of 400 micrometer and a constant temperature of 25 ℃. Oscillatory measurements were performed at a fixed deformation of 0.005 was employed and being in the linear viscoelastic regime was ascertained by confirming the sinusoidal shape of the response function during the measurements. The measurement range was from 0.01 - 10 Hz taking 50 measurement points spaced logarithmically.

2. Rheological characterization of ionogels

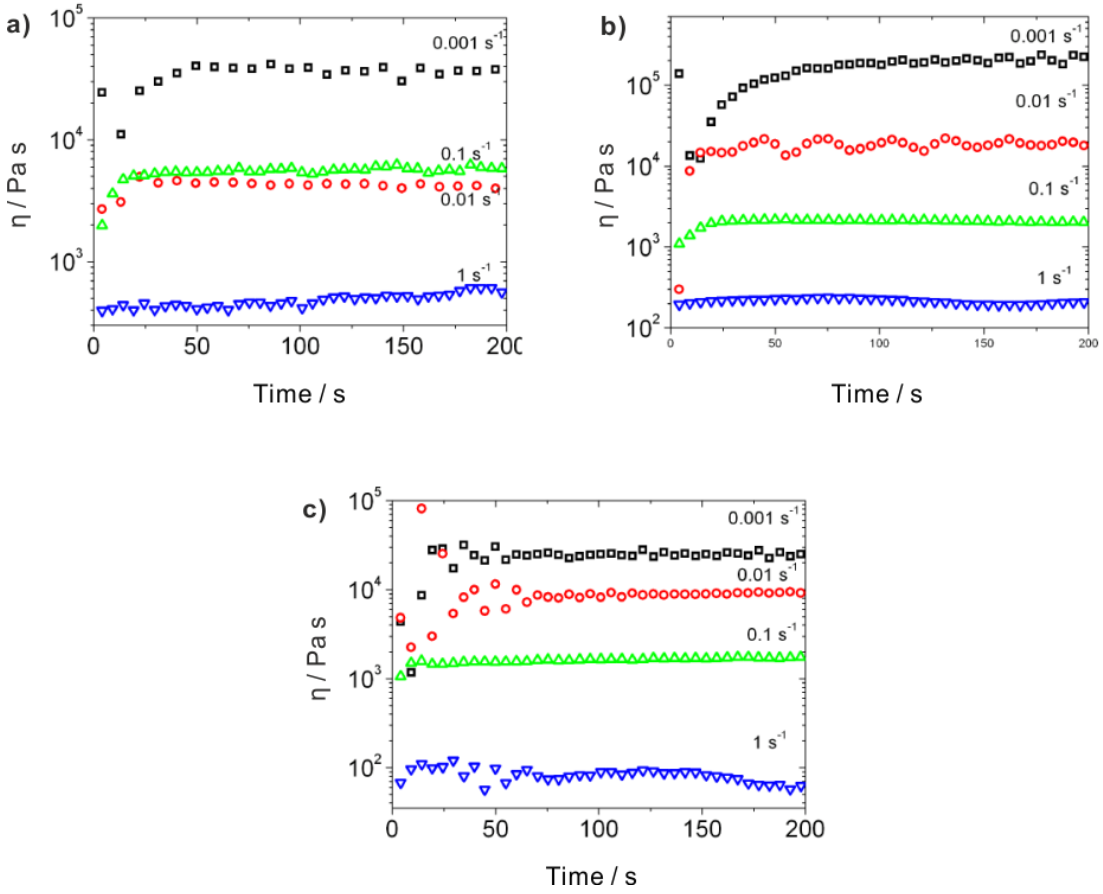

Figure S1. Time dependant shear viscosity measuread at several shear rates (0.001, 0.01, 0.1, and 1 s^{-1}) for ionogels in a) [C6ImC1]PF_6 (30 mM), b) [C4PyC1]NTf_2 (60 mM), c) [C6ImC1]PF_6 (60 mM).

At shear rates lower than 1 s^{-1}, a time dependent shear thickening behavior is observed in all the tested ionic liquids, indicating the rheopexy property is a general property when ionic liquids are used.

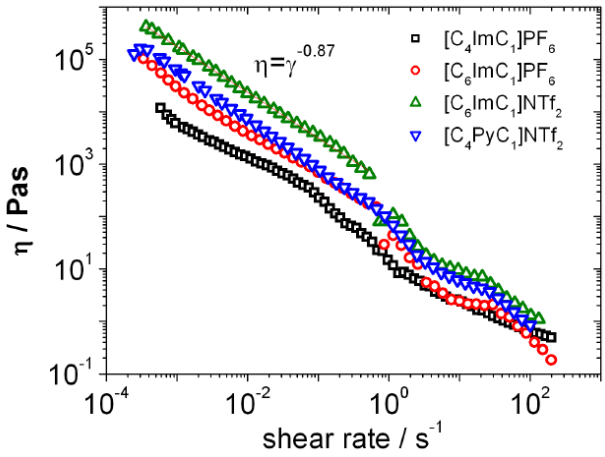

Figure S2. Viscosity as a function of the shear rate for gelator **1** in different ionic liquids. Each point was measured after 150 seconds shearing.

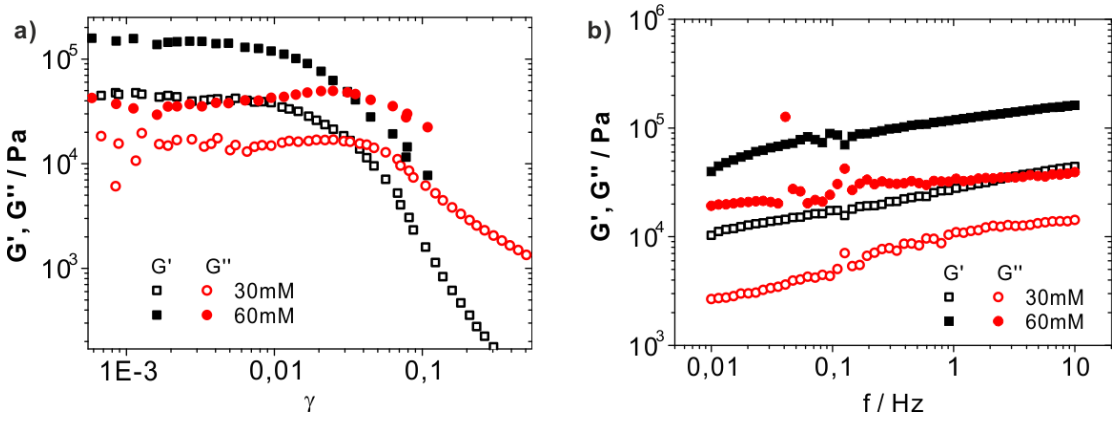

Figure S3. Concentration dependent oscillatory measurements of ionogel **1** in [C4ImC1]PF_6: Storage and loss moduli obtained from a) a strain-amplitude sweep performed at 10Hz; b) a frequency sweep performed at 0.005 strain.

3. Rheological characterization of ionogels recovered from gel-sol transition

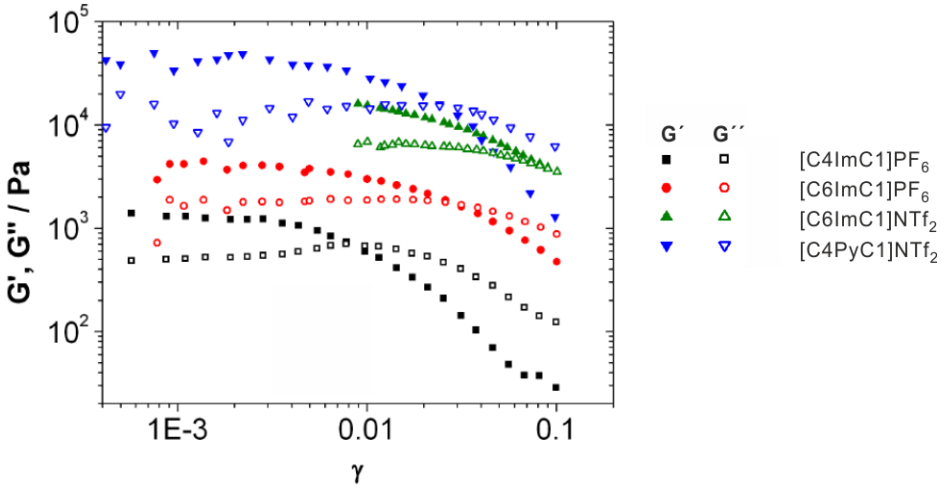

Figure S4. Storage and loss moduli obtained from a strain-amplitude sweep performed at 10Hz of regained ionogels after gel-sol transition.

A constant value of the moduli is observed up to a deformation of 0.01. For deformations higher than 0.01, a significant weakening of gel properties is observed, indicating the network inside the ionogel is broken up.

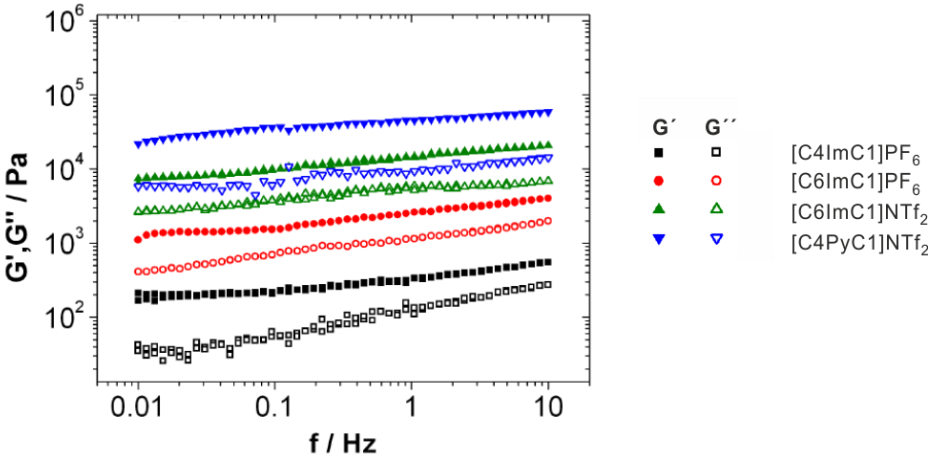

Figure S5. Storage and loss moduli obtained from a frequency sweep performed at 0.005 strain of regained ionogels after gel-sol transition.

The data shows that the storage moduli G´is still constantly greater than loss moduli G´´for the entire range of freqence, suggesting the regained ionogels showed typical gel-like

behavior. The G´of regained ionogels after gel-sol transition is still very high, indicating the high mechanism strength is not changed significantly after reversible gel-sol transition.

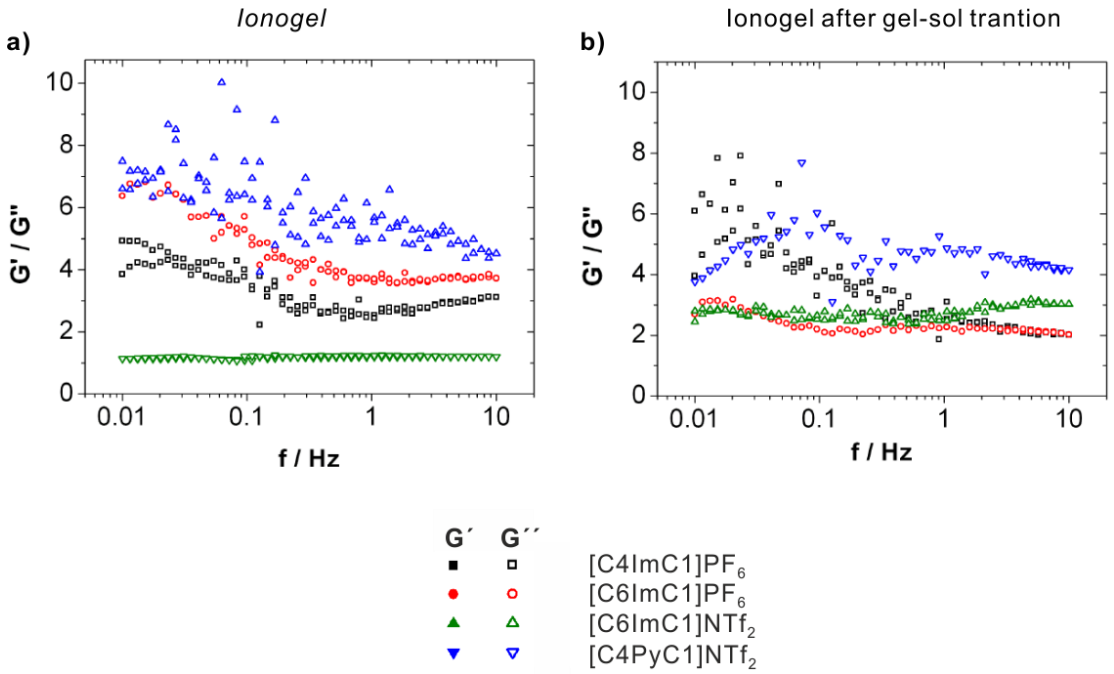

Figure S6. Ratio between the elastic and viscous modulus G'/G" of ionogels before and after gel-sol transition.

The ratio G´/G´´ is a measure of the relative elasticity of the gel compared to its viscous properties. It is clear that relatively similar value for all the ionogels before and after gel-sol transition, indicating the elasticity is not significantly changed after the reversible gel-sol transition.

4. Control experiments on other ionogels demonstrating formation of pseudorotaxane as the trigger for the gel-sol transition

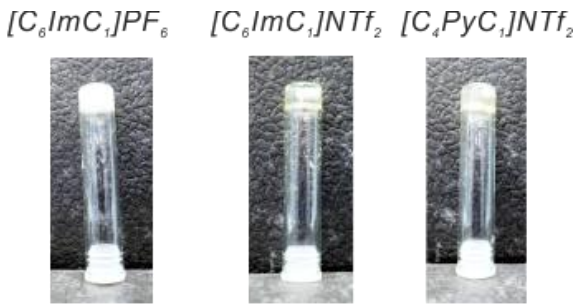

Figure S7. Photographs of the control experiments of addition of 3.0 eq. dibenzylammonium hexafluorophosphate into ionogels (30 mM for ionogel in [C6ImC1Pf6, 60 mM for ionogels in [C6ImC1]NTf_2 and [C4PyC1]NTf_2) prepared from other three tested ionic liquids. Since the phenyl group is too large to penetrate the crown ether, no pseudorotaxane forms and the gel persists.

5. Data obtained from ITC experiments.

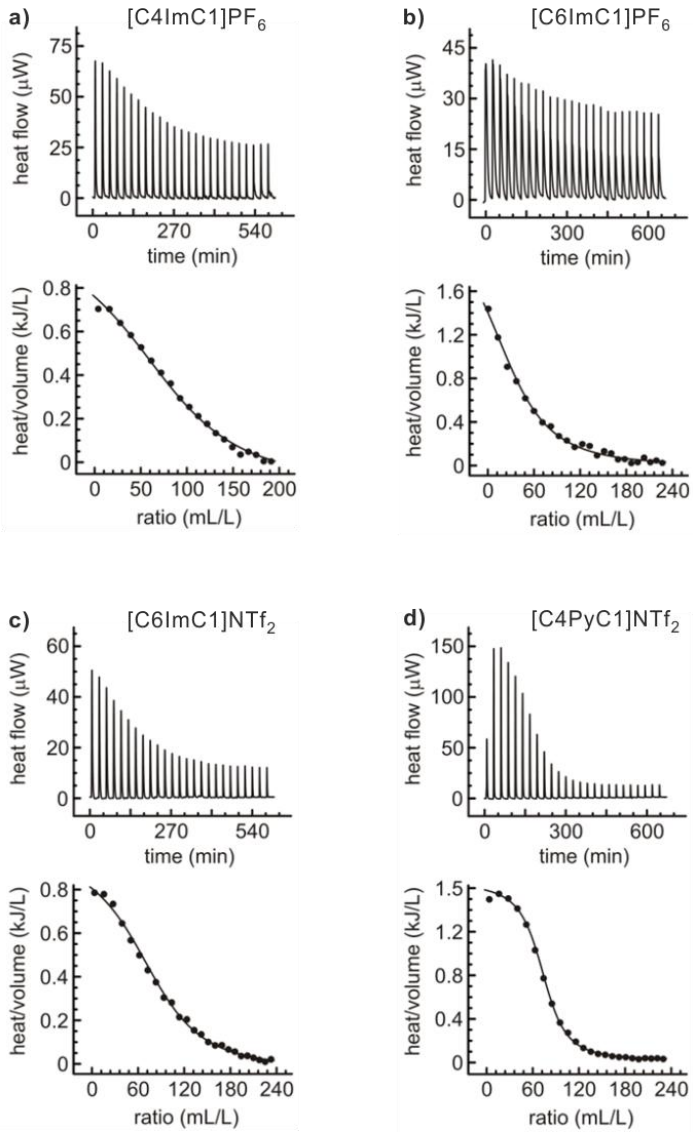

Figure S8. Data obtained from ITC experiments of BC7 and guests G1 in different ionic liquids.

6. References

1. Z. Qi, P. Malo de Molina, W. Jiang, Q. Wang, K. Nowosinski, A. Schulz, M. Gradzielski and C. A. Schalley, *Chem. Sci.*, 2012, **3**, 2073-2082.
2. P. Terech, C. Rossat and F. Volino, *J. Colloid Interface Sci.*, 2000, **227**, 363-370.

8. Gas-phase multivalency: H/D-exchange reactions unravel the dynamic “rock ‘n roll” motion in dendrimer-dendrimer complexes

This chapter was submitted to the following journal:
Z. Qi, C. Schlaich, C.A. Schalley, *Chem. Sci.* (submitted)

Declaration on the personal contribution in this work

Z. Qi and C.A. Schalley developed the conception of the work. C. Schlaich contributed to the synthesis of crown-functionalized dendrimer, Z. Qi did all other experiments. Full range of all references and writing the final manuscript were completed in cooperation with C.A. Schalley.

Content and summary of the work

Herein, we designed novel dendrimer-dendrimer complexes and investigated their dynamic motion through H/D-exchange in the gas phase. The system is represented here as new multivalent model system in which the binding event happened in both scaffolds with multiple binding sites on each component. This complexation behavior is quite similar to the multivalent phenomena in natural systems. Several conclusions can be drawn from the results we described in the manuscript: 1) Benzo[21]crown-7 has similar non-covalent protective group capabilities as [18]crown-6, which was examined earlier. 2) Benzo[21]crown-7 was able to conduct a similar ‘spacewalk’ like [18]crown-6, in which the crown ethers can migrate from one side-chain of a POPAM dendrimer to another. 3) Dendrimer-dendrimer complexes undergo the so called “rock ‘n roll” motion in the gas phase. 4) The surprising isotope exchange behavior of the urea groups has resulted in an important extension of the relay mechanism concept. For the first time, we were able to demonstrate the participation of two auxiliary functional groups that make the exchange efficient only when they cooperate.

Chemical Science

Dynamic Article Links ►

Cite this: DOI: 10.1039/c0xx00000x

www.rsc.org/xxxxxx

EDGE ARTICLE

Multivalency in the gas phase: H/D-exchange reactions unravel the dynamic "rock 'n roll" motion in dendrimer-dendrimer complexes

Zhenhui Qi,[a] Christoph Schlaich,[a] and Christoph A Schalley*[a]

Received (in XXX, XXX) Xth XXXXXXXXX 20XX, Accepted Xth XXXXXXXXX 20XX

DOI: 10.1039/b000000x

Non-covalent dendrimer-dendrimer complexes were successfully ionized by electrospray ionization (ESI) of partly protonated amino-terminated polypropylene amin (POPAM) and POPAM dendrimers fully functionalized with benzo[21]crown-7 on all branches. Hydrogen/deuterium exchange (HDX) experiments conducted on dendrimer-dendrimer complexes in the high vacuum of a mass spectrometer give rise to a complete exchange of all labile N-H hydrogen atoms. As crown ethers represent non-covalent protective groups against HDX reactions on the ammonium group they coordinate to, this result provides evidence for a very dynamic binding situation: Each crown is mobile enough to move from one ammonium binding site to another one. Schematically, one might compare this motion with two rock 'n roll dancers that swirl around each other without completely losing all contact at any time. Although the multivalent attachment certainly increases the overall affinity, the "microdynamics" of individual site binding and dissociation remains fast.

Introduction

Since the discovery of molecular motion by Ingenhousz and Brown,[1] the thermal movement of molecules continues to be a fascinating topic. In particular, when one considers molecules not only to be hard spheres that simply collide, thermal processes can become highly complex. Water may serve as an example. Despite of the many studies devoted to the dynamic processes continuously proceeding in liquid water, the details of water structure are still under debate:[2] Water molecules form a large number of different clusters through hydrogen bonding that associate and dissociate, arrange and rearrange on short timescales.[3] Simple Brownian motion and with it molecular mobility thus becomes a rather complex yet highly intriguing process, when non-covalent interactions between the molecules affect their mutual collisions.

Multivalency[4] is a concept closely related to the well-known chelate effect. The term is usually used in the context of large supramolecular complexes, biomolecules or even whole virus particles that dock to the corresponding receptors on the cell surface. The dimensions are thus orders of magnitude larger than those of the classical chelate complexes of for example transition metal ions. On this size scale, multivalency offers enhanced binding through a velcro-like effect. While each individual binding site may be rather weak, they form very strong bonds together. Beyond binding strength enhancement, multivalency is also offering a means of geometry control on the nano-scale, for example, when a virus induces endocytosis through deformation of the cell's membrane upon multivalent binding.[5] Quite often, the enhanced thermodynamic stability of multivalent complexes is rationalized through the so-called rebinding effect.[6] When many binding sites cooperate simultaneously, dissociating a single one will not have a significant effect neither on the binding strength nor on the overall geometric arrangement of receptor or ligand. The corresponding ligand binding site will remain in the vicinity of its complement on the receptor as it is restricted by the other surrounding binding sites that are still connected. Due to the high local concentration, it thus easily rebinds rather than continuing to a complete dissociation of the multivalent complex. One could therefore conclude that even very stable multivalent complexes are expected to exhibit complicated "microdynamics" for its individual binding sites.

Here, we make use of dendrimer-dendrimer complexes as synthetic models for such multivalent complexes. Figure 1 shows the dynamic processes which can in principle occur within such a (quite flexible) structure: Receptor sites displayed on the red dendrimer can associate with the ligand sites of the blue partner. They can also dissociate at another position or they can open and rebind at the same position. Potentially, crown ethers can even

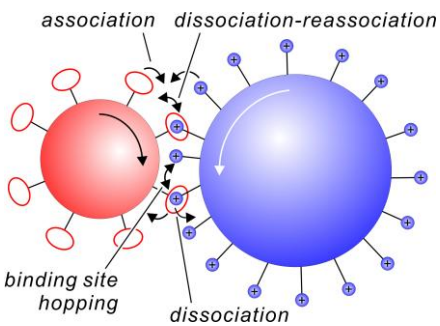

Fig. 1 Schematic representation of different dynamic reactions that can occur in a complex generated from a crown ether-functionalized dendrimer (red) and a (partially) protonated POPAM dendrimer (blue).

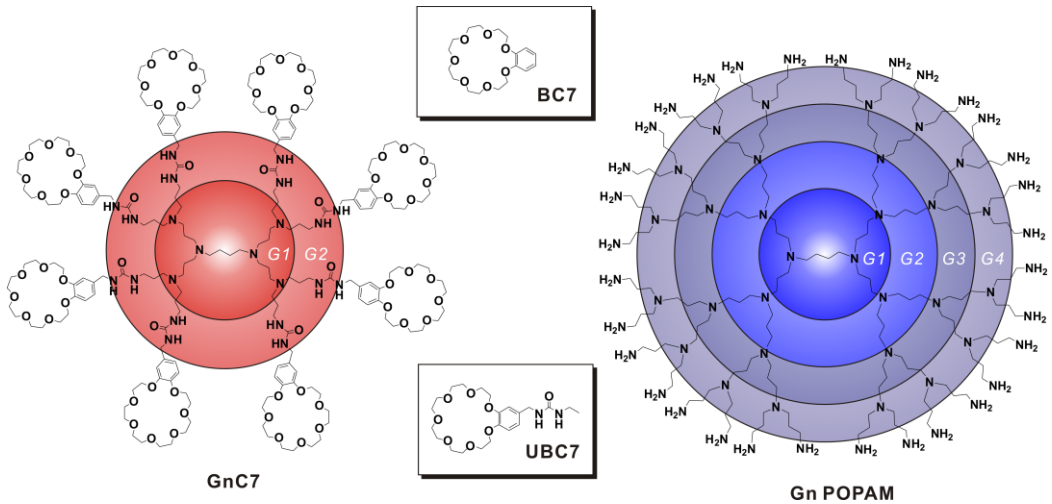

Fig. 2 Chemical structures of benzo[21]crown-7-functionalized dendrimer **GnC7** (n = 1, 2) and POPAM dendrimers **Gn** (n = 1 – 4). The insets show the structures of two control compounds **BC7** and **UBC7**, which both represent key structural elements in **GnC7**.

directly move from one side chain to another one as implied by earlier studies with monovalent crown ethers.[7] Thermally driven, all these processes together result in what we wish to coin "rock 'n roll" motion here: The dancing pair remains connected at all times, but individual arms and legs are released in between and find back together to finally allow the couple to swirl around each other in a complex overall movement consisting of a large number of individual steps.

Each dendrimer-dendrimer complex under study here is composed of one polypropylene amine (POPAM) dendrimer **Gn** (Figure 2) that bears some protonated amino groups in its periphery, and of a POPAM dendrimer **GnC7** that is fully functionalized with benzo[21]crown-7 ethers. Both dendrimers interact through crown-ammonium hydrogen bonding as a reliable non-covalent binding motif. We decided to use the [21]crown-7 termini as this would not only allow us investigating the interaction with multivalent ammonium guests, but also the formation of multivalent pseudorotaxanes with secondary ammonium axles[8] in future.

To detect the dynamic nature within such a complex in condensed phase is certainly not a trivial task. First of all, the dendrimers may form larger aggregates that precipitate and thus evade the typical spectroscopic methods. Second, each binding site resides in a slightly different environment. Superimposed with the expected dynamic reactions as detailed in Figure 1, this will lead for example to broadened signals in NMR spectra. To avoid these difficulties, we decided to examine dendrimer-dendrimer complexes in the gas phase by tandem mass spectrometric experiments, [9] i.e. here in particular H/D-exchange (HDX) reactions [10] in the high vacuum of the mass spectrometer to provide evidence for the dynamic nature of the multivalent interaction between the two dendrimers in the complex.[7,11] On one hand, the dendrimer-dendrimer complex ions are isolated in the gas phase and thus do neither associate with other dendrimers nor do they undergo dynamic exchange reactions between each other. On the other hand, dissociation – if it occurs at all – will immediately be detected by the corresponding mass shift.

As the intracomplex movement of the dendrimers does neither alter the elemental composition nor the charge state, the ions' mass-to-charge ratios will not change during the dynamic processes proceeding within the complex. A gas-phase probe reaction is thus needed which (i) has an activation barrier below the dissociation limit of the complex, (ii) leads to an easy-to-detect change in *m/z*, and (iii) is connected to the dynamic processes in the dendrimer-dendrimer complexes. HDX reactions are such a probe reaction.[7,11] Crown ethers are known to act as non-covalent protective groups for ammonium ions and thus to suppress the HDX of the ammonium NH hydrogen atoms in the gas phase.[7,12] If the crown ethers in our dendrimer-dendrimer complexes were thus positionally fixed without dynamic processes interconverting different structures, an incomplete HDX would be expected leaving those NH hydrogen atoms unexchanged that are involved in the binding event. If this scenario holds, the HDX reaction should provide a measure of how many interactions are formed. In contrast, dynamic crown-ammonium binding sites should result in a complete exchange of all NH hydrogen atoms on these scaffolds. This result would thus provide insight into the "microdynamics" of the multivalent interaction.

Results and discussion

Conceptual considerations, synthesis, ion generation

Conceptually, a simple HDX reaction in the gas phase proceeds mechanistically by (i) the formation of an encounter complex, followed by (ii) a proton shift from the ion under study to the exchange reagent, (iii) isotope scrambling, (iv) the reverse deuteron shift and finally (v) the dissociation of the exchange reagent from the complex. The rate of such a simple HDX reaction therefore depends on the proton affinity differences between the sample molecule and the exchange reagent. The choice of the reagent is therefore important here. The larger the difference in proton affinities, the slower the reaction, because the initial proton shift become energetically more demanding. If, however, other functional groups can contribute by stabilizing intermediates, so-called relay machanisms[12, 13] can help circumvent problems related to larger proton affinity differences. This is certainly the case in crown ether-dendrimer complexes.[7a]

This journal is © The Royal Society of Chemistry [year]

In such cases, the proton affinity differences are usually less important and a broader range of exchange reagents can therefore be used. Methanol-OD has proven to be a suitable and practical choice in earlier studies[7] and is therefore used here as well.

The crown-ether substituted POPAM dendrimers were synthesized following known literature procedures.[14] Detailed procedures and analytical data are provided in the ESI.[†] With the isocyanate-functionalized POPAM dendrimer as the precursor of crown attachment, the reaction can be driven to completion. This reduces or even avoids potential difficulties arising from incompletely substituted defect dendrimers.

Crown ethers including **BC7** are well known to bind to primary ammonium ions in solution[15] as well as in the gas phase.[16] The generation of 1:1 dendrimer-dendrimer complexes **GnC7•Gn** is quite straightforward. Mixing the two dendrimers at 50 µM concentration in methanol containing 1% formic acid for protonation and sonicating the mixture for five minutes provides a sample solution, which can directly be used for electrospray ionization (ESI). In contrast to expectation, no severe difficulties with the formation of precipitates were encountered at these concentrations. As a consequence, however, the intensities of dendrimer-dendrimer complex signals in the mass spectra are not very intense compared to those of the individual protonated dendrimers (see overview spectra shown in the ESI[†]). Increasing the concentration of the dendrimers in the sample solution increases the complex ion intensities, but on the other hand also leads to more frequent blockage of the ion source capillary due to the formation of precipitates.

Is BC7 a sufficiently capable protective group against H/D-exchange?

As most of the HDX studies on crown/ammonium complexes were devoted to [18]crown-6 so far,[7,12] we started the present study with a series of control experiments. In particular, it is necessary to test whether **BC7** has the required ability to protect the ammonium NH hydrogen atoms against H/D-exchange. Monovalent **BC7** was therefore first mixed with ethylenediamine (**EDA**) in slightly acidic methanol and subjected to electrospray ionization (Figure 3). Free, singly protonated ethylenediamine is known to undergo a very rapid exchange of all five N-centered hydrogen atoms (almost complete after about 50 ms under the conditions used in the present study) through the relay mechanism[12] shown in Figure 3a. In marked contrast, its singly protonated 1:1 **BC7** complex [**BC7•EDA**+H]$^+$ at *m/z* 417 does not show any exchange over a reaction delay of 20 s (Figure 3b). The crown even blocks the exchange of all five labile hydrogen atoms, because the ammonium group is involved in crown binding and therefore not available for the relay mechanism.

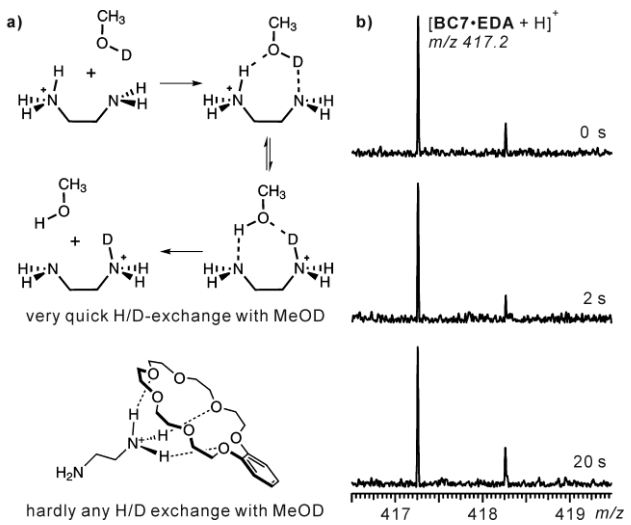

Fig. 3 a) Relay mechanism for the H/D-exchange on singly protonated ethylene diamine (**EDA**). b) ESI-FTICR mass spectra obtained after 0, 2 and 20 s reaction time of [**BC7•EDA**+H]$^+$ with CH_3OD.

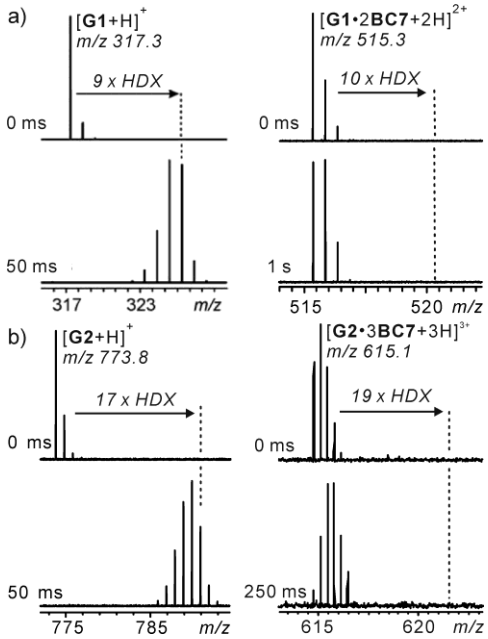

Fig. 4 a) Left: HDX of singly protonated [**G1**+H]$^+$. Fast exchange of all nine labile NH hydrogens is observed. Right: Only a very slow HDX is observed for the 2:1 [**G1**•2**BC7**+2H]$^{2+}$ complex. b) Left: HDX of [**G2**+H]$^+$. Fast exchange of all 17 NH protons is observed. Right: A very slow HDX is observed for the 3:1 [**G2**•3**BC7**+3H]$^{3+}$ complex.

Similar results are also obtained, when **BC7** is coordinating to larger scaffolds as for example POPAM dendrimers **G1** (Figure 4a) and **G2** (Figure 4b), respectively. For dendrimer ions without any crown ether attached, the relay mechanism is feasible and the exchange is fast. In Figure 4, this is exemplified for the two singly protonated dendrimer ions [**G1**+H]$^+$ and [**G2**+H]$^+$. After 50 ms, almost all of the labile NH hydrogens are exchanged. When all ammonium groups are occupied by **BC7** instead, the resulting H/D-exchanges become significantly slower in both cases as shown in Figure 4 for the doubly and triply charged ions [**G1**•2**BC7**+2H]$^{2+}$ and [**G2**•3**BC7**+3H]$^{3+}$. Even after significantly longer reaction times, only the first or first few exchange steps have occurred and the exchange is far from being complete. This behavior is observed for all complexes in which the number of crown ethers meets the number of ammonium sites. As they are all protected by crown ethers, no relay mechanism can operate slowing down the exchange. In conclusion, these substantial HDX rate differences demonstrate **BC7** to effectively protect the ammonium group from H/D-exchange – not only for small ammonium ions, but also for the POPAM dendrimers.

The urea NH protons also belong to the labile protons that potentially may exchange. Consequently, the control experiments

were extended to the urea-substituted crown ether **UBC7** in order to evaluate, whether the urea protons can be exchanged (see ESI†). The result was closely analogous to that obtained for **BC7**: The crown protects the ammonium NH hydrogen atoms efficiently. Furthermore, no HDX of the urea hydrogen atoms is observed in the **UBC7** complexes.

Does monovalent BC7 "walk" along the periphery of POPAM dendrimers from one side-chain to another?

In an earlier study[7b] on monovalent crown ether-POPAM complexes, H/D-exchange reactions were used to demonstrate [18]crown-6 to directly migrate together with a proton from an ammonium to an amine side chain. The next step in the present work is thus to evaluate whether **BC7** behaves analogously. In order to examine this, ions must be selected, which carry more charged ammonium sites than crown ethers. This ensures that the relay mechanism can efficiently operate due to the presence of unoccupied ammonium groups. If the crown ether moves, again a fast exchange of all labile hydrogen atoms is expected to occur. If the crown ether does not migrate, it should protect the three ammonium hydrogens of this side chain against the H/D-exchange. Figure 5 illustrates schematically the crown movement and provides the experimental results for the [**G2•BC7**+2H]$^{2+}$ ion at *m/z* 565.5 as a representative example. Indeed, the H/D-exchange proceeds quickly and after 50 ms, the isotope pattern has already shifted to beyond the position at which it were to stop in case of a non-migrating crown ether (red arrow). In line with the previous experiences on [18]crown-6, **BC7** thus is also capable of walking on the dendrimer periphery by migrating from one side chain to the other without intermediate dissociation.

H/D exchange on the crown-functionalized dendrimer alone

Although no exchange was observed on the urea groups in the **UBC7** complexes (see above), it is important to determine, how the urea hydrogens behave in the HDX experiments in the dendrimers **G1C7** and **G2C7**. In principle, the presence of more

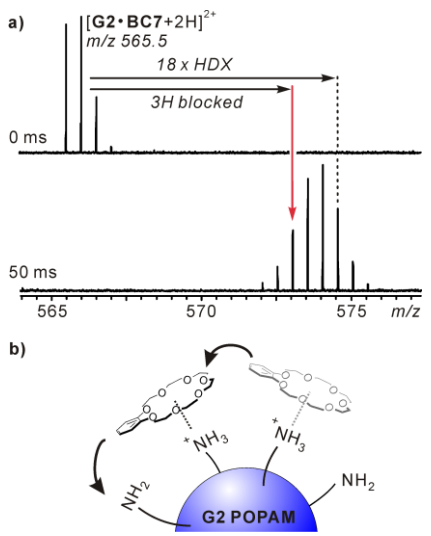

Fig. 5 a) HDX experiment with [**G2•BC7**+2H]$^{2+}$ complex ions (0 and 50 ms reaction time). The red arrow indicates the signal position at which the exchange reaction should terminate for a positionally fixed crown ether. The dotted line marks the position at which full exchange is achieved. b) Illustration of **BC7** moving along the periphery of POPAM dendrimer **G2**.

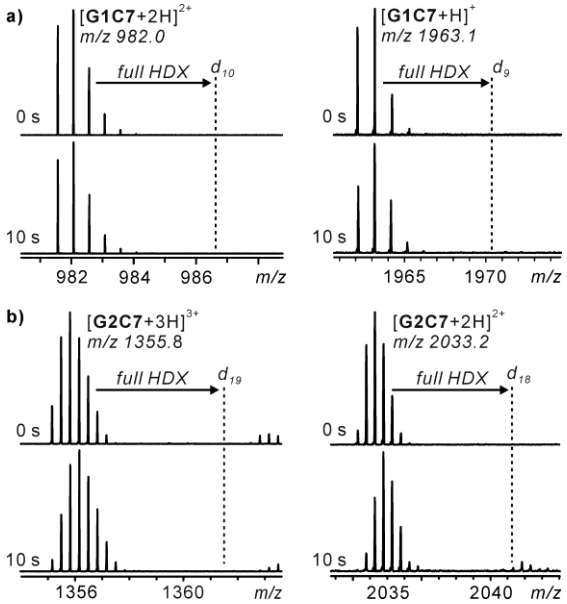

Fig. 6 a) H/D exchange experiment crown ether functionalized dendrimer **G1C7** and **G2C7** respectively. Obviously, the H/D exchange proceeds quite slowly, even after 10 s, no significant swift of the signals can be observed, regardless the charge states as well as generation of the crown-dendrimers. This result also indicates that the crown-dendrimer itself cannot catalyze the H/D exchange on the NH group of urea bonding.

than one urea group might enable new exchange mechanisms analogous to the relay mechanism which are not possible for a single urea group. Therefore, the two crown-functionalized dendrimers **G1C7** and **G2C7** were submitted to electrospray ionization and examined in HDX experiments (Figure 6). Irrespective of the charge states (+1 or +2 for **G1C7** and +2 or +3 for **G2C7**) only a very slow exchange of the urea hydrogen atoms is observed in line with the experiments conducted with **UBC7** described above (ESI†) as well as with HDX experiments conducted earlier on urea-containing macrocycles.[17]

Gas-phase H/D-exchange reactions of dendrimer-dendrimer complexes

For simplicity, we will begin the discussion of the H/D-exchange reactions performed with a smaller dendrimer-dendrimer complex ions, i.e. triply protonated [**G1C7•G2**+3H]$^{3+}$. In this complex, three amino groups are protonated so that three binding sites are available on the POPAM dendrimer **G2**, which can complex to crown ethers. The counterpart **G2C7** offers in total four crown ethers thus one more than ammonium groups present. Consequently, at any given time, the dendrimer-dendrimer complex may have one, two or three non-covalent connections between the two dendrimers. According to the results discussed above, a thorough, non-dynamic threefold connection would occupy all ammonium groups and thus suppress the relay mechanism. This situation should lead to either no exchange at all or a very slow exchange of all but the nine ammonium hydrogens involved in binding. If only one or two connections exist in a complex in which the crowns are positionally fixed on the timescale of the experiment, one would expect to see three or six hydrogen exchanges, respectively, less than the full exchange. The experimental result is shown in Figure 7. Within about 10

This journal is © The Royal Society of Chemistry [year]

seconds exchange reaction time, the exchange of 27 labile hydrogen atoms is observed. This result is surprising in view of the overall number of labile hydrogen atoms involved in the HDX reaction. **G2** offers 16 amine hydrogen atoms to which the three protons providing the charges need to be added. Consequently, a maxmimum number of 19 exchangeable hydrogen atoms is to be expected based on the control experiments discussed above. The additional eight H atoms can thus only be those incorporated in the urea groups in **G1C7** and become exchangeable in the dendrimer-dendrimer complex.

From these findings, three conclusions can be drawn: (i) All labile hydrogen atoms are exchangeable and thus none of the crowns is positionally fixed. (ii) Also, on time average, there must be free ammonium groups which permit the relay mechanism to operate. Otherwise , the HDX would be expected to proceed much slower. (iii) In contrast to the control experiments with ions containing urea groups discussed above, an exchange of the urea hydrogen atoms is possible within the dendrimer-dendrimer complex and the question arises, how this reaction proceeds, which does not occur in the absence of the POPAM dendrimer, i.e. on **G1C7** alone.

Before we come back to this question, let us first discuss the higher generation dendrimer-dendrimer complexes. Figure 8 shows the HDX reactions performed with [**G2C7•G2**+3H]$^{3+}$ and [**G2C7•G3**+3H]$^{3+}$ as representative examples. The first ion, [**G2C7•G2**+3H]$^{3+}$, bears 16 amine hydrogens, 16 urea hydrogens and three protons that provide the three charges. In total, this ion thus contains 35 labile hydrogen atoms. The [**G2C7•G3**+3H]$^{3+}$ ion contains 32 amine, 16 urea hydrogen atoms and three protons, thus overall 51 exchangeable hydrogen atoms. In both cases, the situation is analogous to that discussed for [**G1C7•G2**+3H]$^{3+}$. All labile hydrogen atoms can indeed be exchanged. This again includes the urea protons in contrast to the protonated **G2C7** dendrimer ions in any charge state. The same result is also obtained for the [**G2C7•G4**+5H]$^{5+}$ (ESI†). For this ion, the signal-to-noise ratio is somewhat lower because of the defects in the dendrimer structure of **G4** which lack one, two or three terminal branches. Consequently, the available intensity is distributed over more different ions each of which appears with lower signal intensity. Nevertheless, this experiment also clearly illustrates different charge states to behave similarly. For all the dendrimer-dendrimer complexes under study here, the conclusions are thus the same as those for [**G1C7•G2**+3H]$^{3+}$: Not all possible non-covalent connections between the two dendrimers are present at all times as this would shut down the relay mechanism and thus slow down the exchange rate significantly. Furthermore, multivalent binding undergoes dynamic exchange processes as none of the labile hydrogen atoms is protected against the HDX reaction. A particularly interesting observation is that the exchange of the urea hydrogen atoms becomes only possible in the presence of the amino/ammonium-terminated POPAM dendrimers **Gn**.

The dendrimer-dendrimer complexes contain two different types of labile hydrogen atoms. As the protons providing the charges are mobile within the complexes and quickly move between the amino groups, all amine and ammonium hydrogens represent one category. The urea hydrogen atoms represent the second category. In order not to overcomplicate a quantitative analysis,

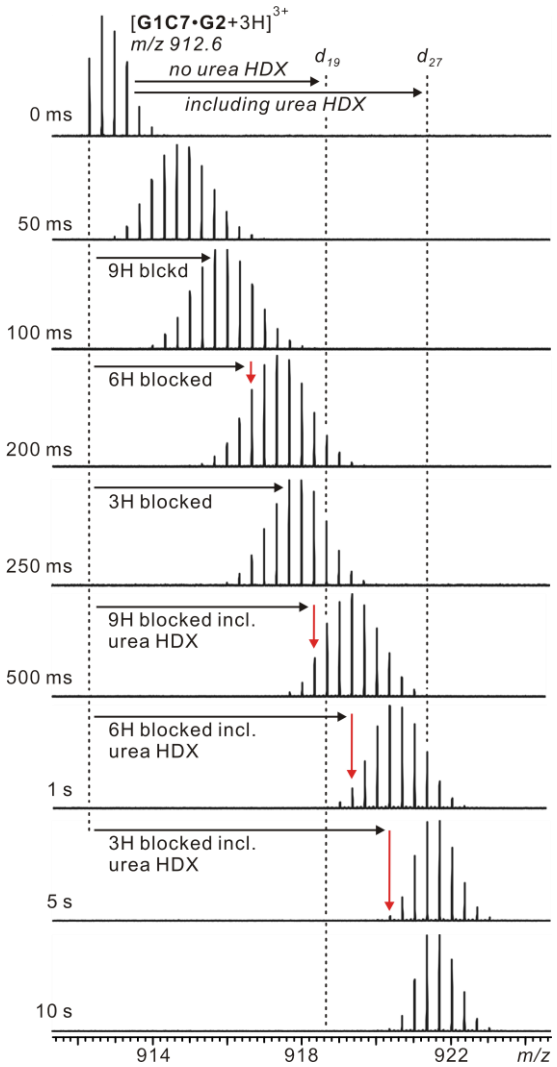

Fig. 7 HDX experiment with triply protonated dendrimer-dendrimer complex ions [**G1C7•G2**+3H]$^{3+}$. The dotted line at the position labeled "d_{19}" represents full exchange, when the urea H atoms do not participate. The "d_{27}" position represents full exchange including the urea H atoms. Arrows indicate the positions, at which the HDX is expected to terminate for six different scenarios: In this complex, one, two or three crown ethers can bind simultaneously to the three available ammonium sites. Depending on the exchange behavior of the urea NH hydrogens, two different thresholds are expected in each of these cases.

the intensity-weighted average *m/z* was calculated of each isotope pattern after defined reaction intervals (for details, see ESI†). These average values were then plotted over the reaction time and the data were fitted to monoexponential and biexponential fitting functions. While the fit with the monoexponential function did not result in good fits, the biexponential function (eq. 1) gives rise to very good fitting curves as shown in Figure 9.

$$I_t - I_\infty = c_{fast} e^{-t/\tau_{fast}} + c_{slow} e^{-t/\tau_{slow}} \quad \text{eq. 1}$$

Equation 1 contains one term for a faster and one term for a slower exchange reaction reflecting the two types of hydrogen atoms incorporated in the dendrimer-dendrimer complexes. We attribute the amine/ammonium H atom exchange to the faster and the urea NH exchange to the slower process. As the methanol-OD

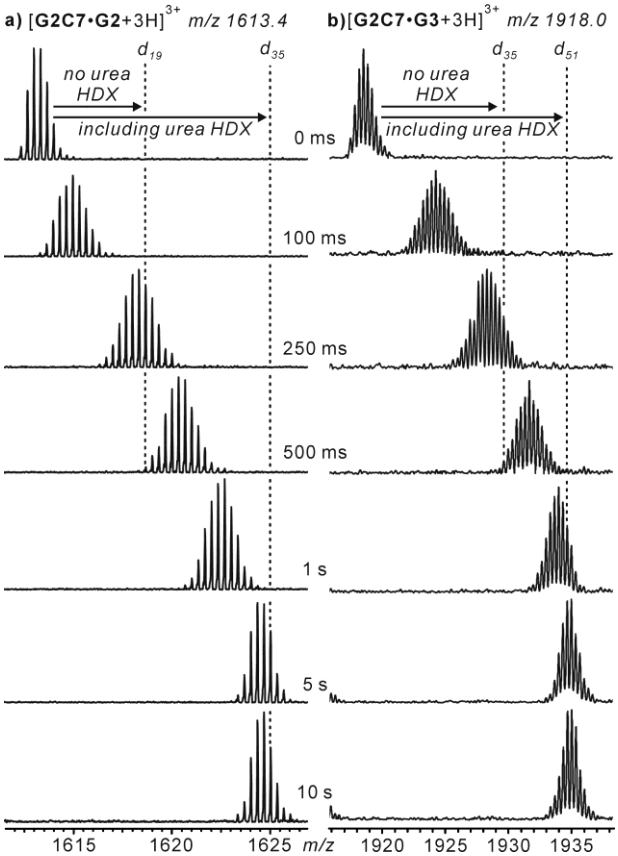

Fig. 8 H/D-exchange experiment with triply protonated dendrimer-dendrimer complexes a) [**G2C7•G2**+3H]$^{3+}$ and b) [**G2C7•G3**+3H]$^{3+}$. Dotted lines indicate where the HDX is expected to terminate, when either only the amine/ammonium hydrogen atoms are exchanged or when in addition the urea NH atoms exchange as well.

pressure in the hexapole of the instrument is not exactly known, the determination of absolute rate constants is not straightforward, but the two processes can be compared to each other as they always proceed under identical conditions. According to the fitting parameters (ESI†), the amine and ammonium NH exchange proceeds about three to five times faster than the urea NH exchange, when the two time constants are normalized to the number of hydrogen atoms in the two categories.

Conclusions drawn from H/D-exchange rate differences

Basically, the ions examined here can be divided into three categories: The first category comprises all those ions that undergo no or only very slow exchanges. To this category those ions belong, which either do not carry any primary ammonium site (i.e. [**G1C7**+*n*H]$^{n+}$ or [**G2C7**+*n*H]$^{n+}$) or in which all ammonium sites are occupied by crown ethers, e.g [**BC7•EDA**+H]$^{+}$ (Figure 3), [**G1•2BC7**+2H]$^{2+}$ or [**G2•3BC7**+3H]$^{3+}$ (Figure 4). For these ions, the HDX is very slow and proceeds on at least a many-minute timescale, if one extrapolates the results discussed above. The reason is the absence of free, primary ammonium groups that could mediate the HDX reaction through a relay mechanism.

The second category contains all those ions which undergo very fast exchanges, e.g. [**EDA**+H]$^{+}$, [**G***n*+H]$^{+}$ (Figure 4), [**G2•BC7**+2H]$^{2+}$ (Figure 5). In these ions, a permanently free primary ammonium group ensures the efficient operation of a relay mechanism. The HDX reaction is close to completion on a timescale of less than 100 ms. Although an exact quantification of the absolute HDX rates is not straightforward, the picture is clear-cut: An efficient HDX reaction requires the presence of a free primary ammonium group.

Finally, the third category comprises the dendrimer-dendrimer complexes under study (e.g. [**G1C7•G2**+3H]$^{3+}$, [**G2C7•G2**+3H]$^{3+}$ and [**G2C7•G3**+3H]$^{3+}$ in Figures 7 and 8). For these ions, the H/D-exchange occurs on an intermediate second timescale and is thus significantly slower than that observed for ions of category 2 and much faster than that found for ions of category 1. We interpret these findings as follows: All dendrimer-

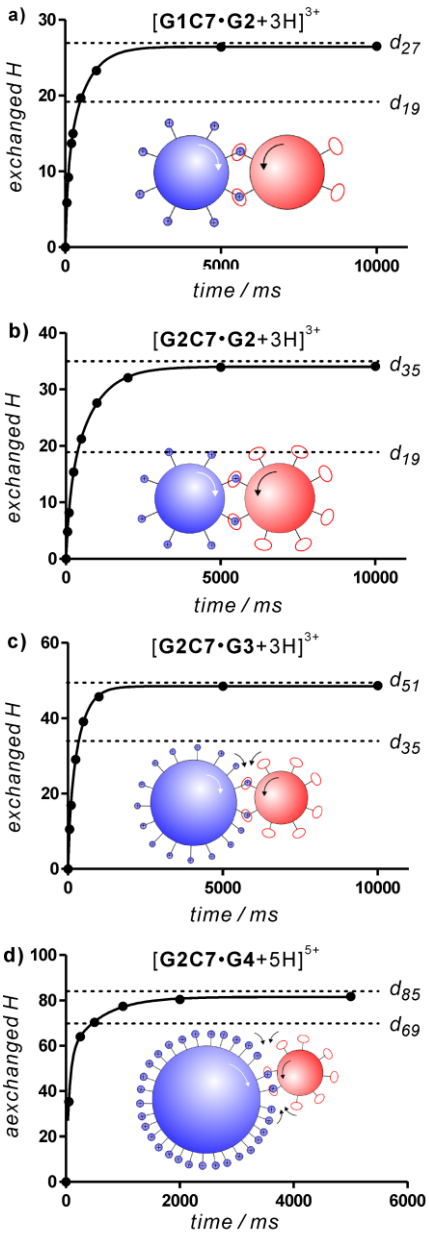

Fig. 9 HDX reactions fitted to a double-exponential rate law reflecting the amine/ammonium H atoms to exchange at a higher rate than the urea NH hydrogens.

This journal is © The Royal Society of Chemistry [year]

dendrimer complex ions bear fewer charges than crown ethers. Consequently, all ammonium ions could in principle be blocked. However, as the exchange is not completely shut down, some free, primary ammonium ion must exist at least for certain time intervals. On the other hand, a permanently uncomplexed ammonium group would result in an HDX reaction that is expected to proceed with similar rates as found for category 2 ions. This is neither the case and consequently, there must be time intervals in which all charged sites are indeed blocked.

One might argue that the H/D-exchange might be slowed down in complex ions with, for example, one permanently uncomplexed ammonium group, because the larger crown ether-substituted dendrimer blocks access of the exchange solvent to the labile hydrogens more efficiently than in the control complexes discussed above. However, this scenario can be ruled out: Either such a complex is still dynamic in nature so that the blocking crowned dendrimer moves. This would not be in contradiction to the interpretation that the binding situation is dynamic. Or the dendrimer-dendrimer complex exhibits slow microdynamics so that the POPAM dendirmer has one accessible and one non-accessible site. In this case, one would expect to see an initial fast HDX of part of the labile hydrogen atoms followed by a more slowly exchanging population that originates from the blocked site. As the biexponential fits in Figure 9 show, this is not observed experimentally and can be excluded.

The conclusion from these arguments is that multivalent binding is highly dynamic and individual binding sites undergo the processes that are depicted in Figure 1 while the overall binding between the two partners is ensured by other binding interactions at all times.

Mechanism of the accelerated H/D exchange on the urea groups in the presence of POPAM dendrimers

Finally, let us discuss the mechanistic features of the urea HDX reaction. Four experimental results are instructive here and need to be reflected in the mechanism: (i) Protonated $[\mathbf{GnC7}+n\mathrm{H}]^{n+}$ ions undergo only extremely slow HDX reactions at the urea groups irrespective of the charge state (Figure 6). Consequently, neither a tertiary amine, nor a tertiary ammonium groups nor any combination of two of them (amine/amine, amine/ammonium or ammonium/ammonium) is increasing the rate of the urea NH H/D-exchange. (ii) The $[2\mathbf{UBC7{\bullet}DAD}+2\mathrm{H}]^{2+}$ ion (ESI†) neither undergoes any significant isotope exchange. Consequently, cooperative action of two urea groups in proximity to each other does not accelerate the urea H/D-exchange. (iii) The $[\mathbf{UBC7{\bullet}DAD}+\mathrm{H}]^{+}$ ion does hardly exhibit any urea NH exchange (ESI†, Figure S8). Consequently, the presence of only an additional primary amine is not sufficient either for an efficient exchange of the urea NH hydrogen atoms. (iv) When, instead, a POPAM dendrimer is present that bears primary ammonium ions as well as primary amines, the exchange reaction becomes efficient. For the urea NH exchange, the cooperative action of three functional groups is thus required: one primary amine, one primary ammonium and the urea group.

In principle, there are two possibilities now: The methanol-OD also participates directly in the urea NH HDX reaction. This would make this process a four component reaction with all the entropic disadvantages that are expected to be related to such a reaction. Besides these entropic penalties, other reasons rule out mechanisms with direct participation of methanol-OD. A selection is discussed in greater detail in the ESI†. Alternatively, the urea exchange does not directly involve the presence of the exchange reagent, but is rather a hydrogen/ deuterium exchange between the urea group and an amine or ammonium that has already undergone the HDX. This would require only three functional groups to line up in a suitable structure.

Figure 10 shows such a mechanism. If the urea group forms one strong, ionic proton bridge between the carbonyl oxygen atom and an adjacent ammonium group and a somewhat weaker, non-ionic hydrogen bond between the urea NH and an adjacent primary ND_2 group, a mechanism similar to the relay mechanism discussed above becomes feasible. Proton transfers followed by isotope scrambling through rotation of an intermediate ammonium group and finally the back-transfer of proton and deuterium would account for all observations made. In particular, this mechanism rationalizes, why neither tertiary amines nor tertiary ammonium groups can mediate the exchange reaction: They simply are unable to undergo the isotope scrambling step (Figure 10, top inset). Furthermore, this mechanism is also in line with the observation that all three functional groups must be present for efficient exchange (Figure 10, bottom inset). If one follows for example the same mechanism without support from the ammonium group, an unfavorable charge separation step is required which renders the HDX reaction energy-demanding and thus makes it inefficient. Mechanisms without involvement of the amino group include unfavorable tautomerization steps similar to those shown in the ESI†. They can thus also be ruled out.

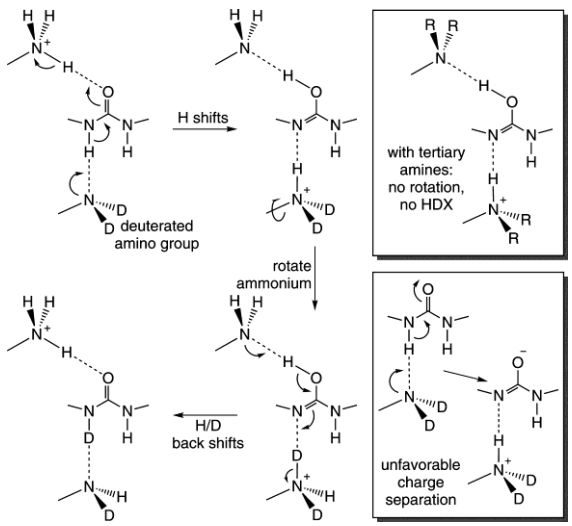

Fig. 10 Mechanism rationalizing the accelerated H/D-exchange of the urea NH hydrogen atoms through the simultaneous participation of one amine and one ammonium group. Insets: Other potential mechanisms that are unfavorable or not feasible and thus can be ruled out.

Conclusions

Several conclusions can be drawn from the results reported here: (i) Benzo[21]crown-7 has similar non-covalent protective group capabilities as [18]crown-6, which was examined earlier.[7] (ii) Also, both crown ethers behave similarly in that they can migrate from one side-chain of a POPAM dendrimer to another one.[7] (iii) In a multivalent binding situation, the individual binding sites

remain highly dynamic. Single binding sites can detach and re-attach. The efficient rebinding is favored by the increase in local concentration in such multivalent complexes. (iv) Overall, the dendrimer-dendrimer complexes thus undergo what we coined "rock 'n roll" motion. Several processes as depicted in Figure 1 contribute and allow the two dendrimers incorporated in the complex not only to undergo binding site de- and reattachment but also to move relative to each other. (v) The surprising isotope exchange behavior of the urea groups has resulted in an important extension of the relay mechanism concept. For the first time, we were able to demonstrate the participation of two auxiliary functional groups that make the exchange on a third group efficient only when all three cooperate.

Our study thus not only provides insight into the otherwise difficult to investigate microdynamics within multivalent complexes, but also a more profound understanding of the mechanistic implications of H/D-exchange reactions in the gas phase. Even though the results obtained are indirect, careful interpretation including all pieces of evidence provide quite a clear-cut mechanistic scenario finally.

Acknowledgements

We thank Prof. Dr. Bert Meijer (TU Eindhoven) and Dr. Henk M. Janssen (SyMO-Chem B.V., Eindhoven) for providing us with some of the dendrimer samples used in this study. We appreciate Dr. Andreas Springer (FU Berlin) for helping with the optimization of the MS experiments. Funding by the Deutsche Forschungsgemeinschaft (SCHA 893/5 and SFB 765) is acknowledged. Z. Q. is grateful to the China Scholarship Council (CSC) for a Ph.D. fellowship.

Notes and references

[a] *Institut für Chemie und Biochemie, Freie Universität Berlin, Takustrasse 3, 14195 Berlin, Germany, Tel: +49 30-838-52639; E-mail: christoph@schalley-lab.de*

† Electronic Supplementary Information (ESI) available: Overview mass spectra, control experiments done with **UBC7**, data fitting, synthetic procedures and characterization data for new compounds

References

1 (*a*) J. Ingenhousz, *Nouvelles expériences et observations sur divers objets de physique*, Barrois, Paris 1784, 2nd vol., pp. 122-126; (*b*) R. Brown, *Phil. Mag.*, 1828, **4**, 161-173.

2 For a recent example of such a debate, see: (*a*) P. Wernet, D. Nordlund, U. Bergmann, M. Cavalleri, M. Odelius, H. Ogasawara, L. Å. Näslund, T. K. Hirsch, L. Ojamäe, P. Glatzel, L. G. M. Pettersson and A. Nilsson, *Science*, 2004, **304**, 995-999; (*b*) C. Huang, K. T. Wikfeldt, T. Tokushima, D. Nordlund, Y. Harada, U. Bergmann, M. Niebuhr, T. M. Weiss, Y. Horikawa, M. Leetmaa, M. P. Ljungberg, O. Takahashi, A. Lenz, L. Ojamäe, A. P. Lyubartsev, S. Shin, L. G. M. Pettersson and A. Nilsson, *Proc. Natl. Acad. Sci. U.S.A.*, 2009, **106**, 15214-15218; (*c*) G. N. I. Clark, C. D. Cappa, J. D. Smith, R. J. Saykally and T. Head-Gordon, *Mol. Phys.*, 2010, **108**, 1415-1433; (*d*) T. D. Kühne and R. Z. Khaliullin, *Nat. Commun.*, 2012, **4**, 1450.

3 (*a*) R. Ludwig, *Angew. Chem. Int. Ed.*, 2001, **40**, 1808-1827; (*b*) J. D. Smith, C. D. Cappa, K. R. Wilson, R. C. Cohen, P. L. Geissler and R. J. Saykally, *Proc. Natl. Acad. Sci. U.S.A.*, 2005, **102**, 14171-14174.

4 (*a*) M. Mammen, S.-K. Choi and G. M. Whitesides, *Angew. Chem. Int. Ed.*, 1998, **37**, 2754-2794; (*b*) A. Mulder, J. Huskens and D. N. Reinhoudt, *Org. Biomol. Chem.*, 2004, **2**, 3409-3424; (*c*) J. D. Badjic, A. Nelson, S. J. Cantrill, W. B. Turnbull and J. F. Stoddart, *Acc. Chem. Res.* 2005, **38**, 723-732; (*d*) C. Fasting, C. A. Schalley, M. Weber, O. Seitz, S. Hecht, B. Koksch, J. Dernedde, C. Graf, E.-W. Knapp and R. Haag, *Angew. Chem. Int. Ed.*, **2012**, *51*, 10472-10498.

5 Selected reviews on virus docking and endocytosis: (*a*) J. T. Huiskonen, S. J. Butcher, *Curr. Opin. Struct. Biol.* **2007**, *17*, 229-236; (*b*) J. M. White, S. E. Delos, M. Brecher, K. Schornberg, *Crit. Rev. Biochem. Mol. Biol.* **2008**, *43*, 189-219; (*c*) J. Mercer, M. Schelhaas, A. Helenius, *Annu. Rev. Biochem.*, **2010**, *79*, 803-833.

6 For selected examples, see: (*a*) A. N. Gifford, J. Gatley and N. D. Volkov, *Synapse*, 1998, **28**, 167-175; (*b*) S. S. Andrews, *Phys. Biol.*, 2005, **2**, 111-122; (*c*) G. Vauquelin, *Expert Opin Drug Discov.* 2010, **5**, 927-941; (*d*) M. Weber, A. Bujotzek and R. Haag, *J. Chem. Phys.*, 2012, **137**, 054111.

7 (*a*) D. P. Weimann, H. D. F. Winkler, J. A. Falenski, B. Koksch and C. A. Schalley, *Nat. Chem.*, 2009, **1**, 573-577; (*b*) H. D. F. Winkler, D. P. Weimann, A. Springer and C. A. Schalley, *Angew. Chem. Int. Ed.*, 2009, **48**, 7246-7250; (*c*) H. D. F. Winkler, E. V. Dzyuba, A. Springer, L. Losensky and C. A. Schalley, *Chem. Sci.* 2012, **3**, 1111-1120.

8 Reviews: (*a*) T. J. Hubin and D. H. Busch, *Coord. Chem. Rev.*, 2000, **200-202**, 5-52; (*b*) B. Zheng, F. Wang, S. Dong and F. Huang, *Chem. Soc. Rev.*, 2012, **41**, 1621-1636. For examples of (pseudo)rotaxanes involving a secondary ammonium-benzo[21]crown-7 motif, some of which are multivalent in nature, see: (*c*) C. Zhang, S. Li, J. Zhang, K. Zhu, N. Li and F. Huang, *Org. Lett.*, 2007, **9**, 5553-5556; (*d*) C. Zhang, K. Zhu, S. Li, J. Zhang, F. Wang, M. Liu, N. Li and F. Huang, *Tetrahedron Lett.*, 2008, **49**, 6917-6920; (*e*) W. Jiang, H. D. F. Winkler and C. A. Schalley, *J. Am.* Chem. *Soc.*, 2008, **130**, 13852-13853; (*f*) W. Jiang and C. A. Schalley, *Proc. Natl. Acad. Sci. USA*, 2009, **106**, 10425-10429; (*g*) W. Jiang, A. Schäfer, P. C. Mohr and C. A. Schalley, *J. Am. Chem. Soc.*, 2010, **132**, 2309-2320; (*h*) W. Jiang, D. Sattler, K. Rissanen and C.A. Schalley, *Org. Lett.* 2011, **13**, 4502-4505; (*i*) X. Yan, M. Zhou, J. Chen, X. Chi, S. Dong, M. Zhang, X. Ding, Y. Yu, S. Shao and F. Huang, *Chem. Commun.*, 2011, **47**, 7086-7088; (*j*) W. Jiang, K. Nowosinski, N. L. Löw, E. V. Dzyuba, F. Klautzsch, A. Schäfer, J. Huuskonen, K. Rissanen, and C. A. Schalley, *J. Am. Chem. Soc.*, 2012, **134**, 1860-1868.

9 Reviews on the application of tandem mass spectrometry to the supramolecular chemistry of dendrimers: (*a*) B. Baytekin, N. Werner, F. Luppertz, M. Engeser, J. Brüggemann, S. Bitter, R. Henkel, T. Felder and C. A. Schalley, *Int. J. Mass Spectrom.*, 2006, **249**, 138-148; (*b*) C. A. Schalley, B. Baytekin, H. T. Baytekin, M. Engeser, T. Felder, A. Rang, *J. Phys. Org. Chem.*, 2006, **19**, 479-490; (*c*) C. A. Schalley and A. Springer, *Mass Spectrometry and Gas-Phase Chemistry of Non-Covalent Complexes*, Wiley, Hoboken/NJ **2009**; (*d*) Z. Qi and C. A. Schalley, *Supramol. Chem.*, 2010, **22**, 672-682. Also, see: (*e*) J. C. Hummelen, J. L. J. van Dongen and E. W. Meijer, *Chem. Eur. J.*, 1997, ***3***, 1489-1493; (*f*) J.-W. Weener, J. L. J. van Dongen and E. W. Meijer, *J. Am. Chem. Soc.*, 1999, *121*, 10346-10355; (*g*) M. A. C. Broeren, J. L. J. van Dongen, M. Pittelkow, J. B. Christensen, M. H. P. van Genderen and E. W. Meijer, *Angew. Chem. Int. Ed.*, 2004, **43**, 3557-3562; (*h*) T. Felder, C. A. Schalley, H. Fakhrnabavi and O. Lukin, *Chem. Eur. J.*, 2005, **11**, 5625-5636; (*i*) C. A. Schalley, C. Verhaelen, F.-G. Klärner, U. Hahn, F. Vögtle, *Angew. Chem. Int. Ed.*, 2005, **44**, 477-480; (*j*) H. T. Baytekin, M. Sahre, A. Rang, M. Engeser, A. Schulz and C. A. Schalley, *Small*, 2008, **4**, 1823-1834; (*k*) B. Baytekin, H. T. Baytekin, U. Hahn, W. Reckien, B. Kirchner and C. A. Schalley, *Chem. Eur. J.*, 2009, **15**, 7139-7149.

10 C. Lifshitz, *Int. J. Mass Spectrom.*, 2004, **234**, 63-70.

11 For a review on the use of gas-phase HDX reactions in supramolecular chemistry, see: H. D. F. Winkler, E. V. Dzyuba and C. A. Schalley, *New J. Chem.*, 2011, **35**, 529-541. Also, see: (*a*) E. Ventola, K. Rissanen and P. Vainiotalo, *Chem. Eur. J.*, 2004, **10**, 6152-6162; (*b*) E. Ventola, A. Hyyryläinen and P. Vainiotalo, *Rapid Commun. Mass Spectrom.*, 2006, **20**, 1218-1224; (*c*) E. Kalenius, D. Moiani, E. Dalcanale and P. Vainiotalo, *Chem. Commun.*, 2007, 3865-3867; (*d*) H. D. F. Winkler, E. V. Dzyuba, J. A. W. Sklorz, N. K. Beyeh, K. Rissanen and C. A. Schalley, *Chem. Sci.*, 2011, **2**, 615-624.

12 S.-W. Lee, H.-N. Lee, H. S. Kim and J. L. Beauchamp, *J. Am. Chem. Soc.*, 1998, **120**, 5800-5805.

This journal is © The Royal Society of Chemistry [year]

13 (*a*) S. G. Lias, *J. Phys. Chem.* **1984**, *88*, 4401-4407; (*b*) T. Wyttenbach, M. T. Bowers, *J. Am. Soc. Mass Spectrom.* **1999**, *10*, 9-14.
14 a) J. W. Jones, W. S. Bryant, A. W. Bosman, R. A. J. Janssen, E. W. Meijer and H. W. Gibson, *J. Org. Chem.*, 2003, **68**, 2385-2389; b) Z. Qi, P. Malo de Molina, W. Jiang, Q. Wang, K. Nowosinski, A. Schulz, M. Gradzielski and C. A. Schalley, *Chem. Sci.*, 2012, **3**, 2073-2082.
15 (*a*) D. J. Cram and J. M. Cram, *Acc. Chem. Res.*, 1978, **11**, 8-14; (*b*) V. Rüdiger, H. J. Schneider, V. P. Solov'ev, V. P. Kazachenko and O. A. Raevsky, *Eur. J. Org. Chem.*, 1999, 1847-1856.
16 (*a*) S. Maleknia and J. Brodbelt, *J. Am. Chem. Soc.*, 1993, **115**, 2837-2843; (*b*) D. V. Dearden, Y. Liang, J. B. Nicoll and K. A. Kellersberger, *J. Mass Spectrom.*, 2001, **36**, 989-997; (*c*) D. V. Dearden, C. Dejsupa, Y. J. Liang, J. S. Bradshaw and R. M. Izatt, *J. Am. Chem. Soc.*, 1997, **119**, 353-359; (*d*) H.-F. Wu and J. S. Brodbelt, *J. Am. Soc. Mass Spectrom.*, 1993, **4**, 718-722; (*e*) C. C. Liou and J. S. Brodbelt, *J. Am. Chem. Soc.*, 1992, **114**, 6761-6764; (*f*) D. V. Dearden and I. H. Chu, *J. Incl. Phenomena Mol. Recogn.*, 1997, **29**, 269-282.
17 T. Becherer, D. Meshcheryakov, A. Springer, V. Böhmer and C. A. Schalley, *J. Mass Spectrom.*, 2009, **44**, 1338-1347.

Supplementary Material (ESI) for Chemical Science

This journal is (c) The Royal Society of Chemistry 2011

Electronic Supplementary Information

Multivalency in the gas phase: H/D-exchange reactions unravel the dynamic "rock 'n roll" motion in dendrimer-dendrimer complexes

Zhenhui Qi,[a] Christoph Schlaich[a], and Christoph A. Schalley*[a]

[a] *Institut für Chemie und Biochemie, Freie Universität Berlin,*

Takustrasse 3, 14195 Berlin, Germany,

Email: christoph@schalley-lab.de

Table of contents

1. Description of the gas-phase experiments

All gas-phase experiments described herein were conducted with an Ionspec QFT-7 FTICR mass spectrometer (Agilent), equipped with a 7 T superconducting magnet and a Micromass Z-spray electrospray ionization (ESI) source (Waters). The sample solutions of dendrimer-dendrimer complexes (50 µM crown-functionalized dendrimer and 50 µM POPAM dendrimer; methanol, 1% formic acid) were sonicated for 5 min before being introduced into the ion source. Other sample solutions were prepared similarly (50 µM in the two components; methanol, 1% formic acid) without sonication. All the sample solutions were injected into the ion source at flow rates of 2 – 4 µL. The parameters for sample cone and extractor cone voltages were optimized for maximum abundances of the desired complex ions. Parameters like source temperature and temperature of desolvation gas were kept constant at 40 °C. No nebulizer gas was used for the experiments.

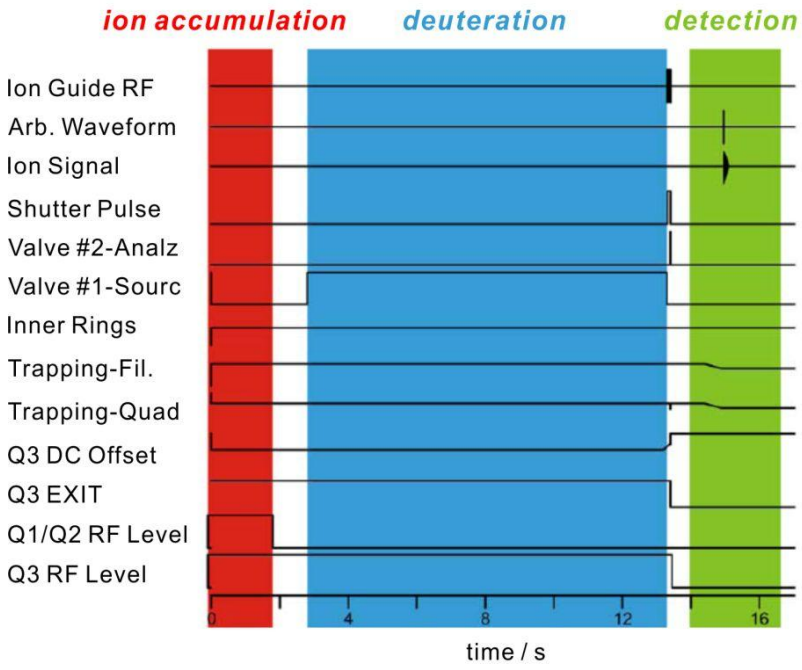

Figure S1. Pulse program for the H/D-exchange experiment in the instrument's hexapole collision cell.

For the gas-phase H/D-exchange experiments, we used the hexapole ion accumulation/collision cell of our instrument as an ion trap and reaction chamber. This approach allows higher pressures of the

exchange reagent to be used than those achievable in the FTICR cell.[1] Consequently, the exchange is more efficient and proceeds faster. In detail, the HDX reactions were performed as follows: After accumulation of a suitable number of ions in the hexapole, the entrance of new ions into the hexapole was blocked by switching off the radio frequency of the quadrupole in front of the hexapole ("Q1/Q2 RF level" in Figure S1). To conduct the isotopic exchange, CH_3OD was then introduced into the collision cell. The reaction time was controlled with the help of a solenoid pulse valve ("Valve #1-Sourc" in Figure S1) which can be controlled with high temporal precision (steps of down to ca. 25 μs caused reproducible changes in the exchange behavior in the early stages of the H/D-exchange). It should be noted that the time required for the methanol-OD to be transferred from the valve into the hexapole is in the order of ca. 1.3 ms. This time appears as an induction period in which the exchange proceeds very slowly. Afterwards, the methanol pressure remains constant as the amount of delivered methanol and that pumped away by the turbomolecular pumps reaches a steady-state. The reaction time is controlled by the valve#1 opening delay. After completion of the H/D-exchange reaction, the product ions were transferred into the instrument's analyzer cell through a quadrupole ion guide and detected by a standard excitation and detection sequence with high mass accuracy in the low ppm range.

2. Mass spectra of dendrimer-dendrimer complexes

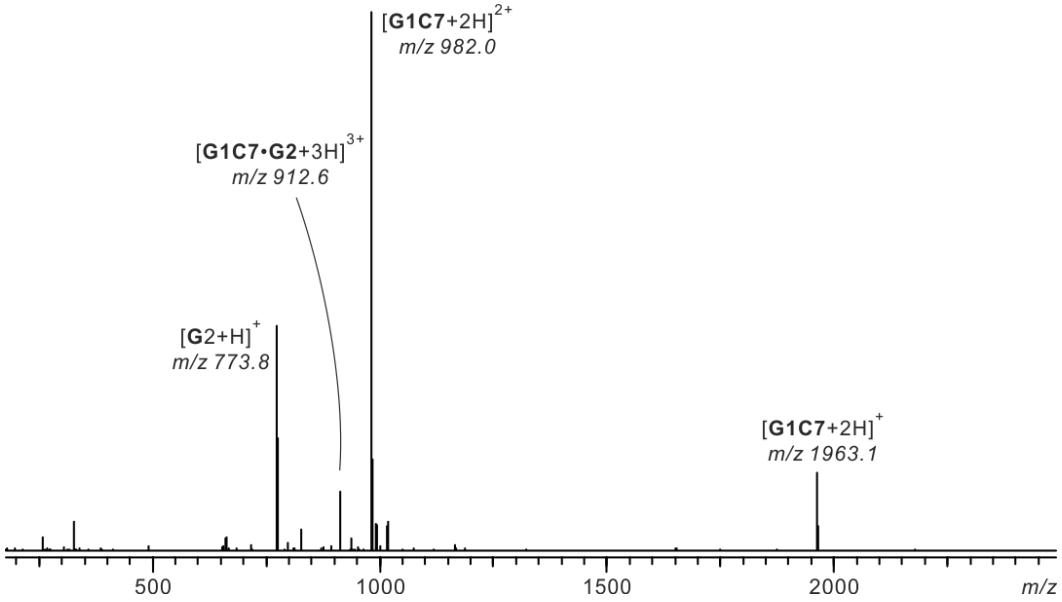

Figure S2. Mass spectrum of the **G1C7**/**G2** complex.

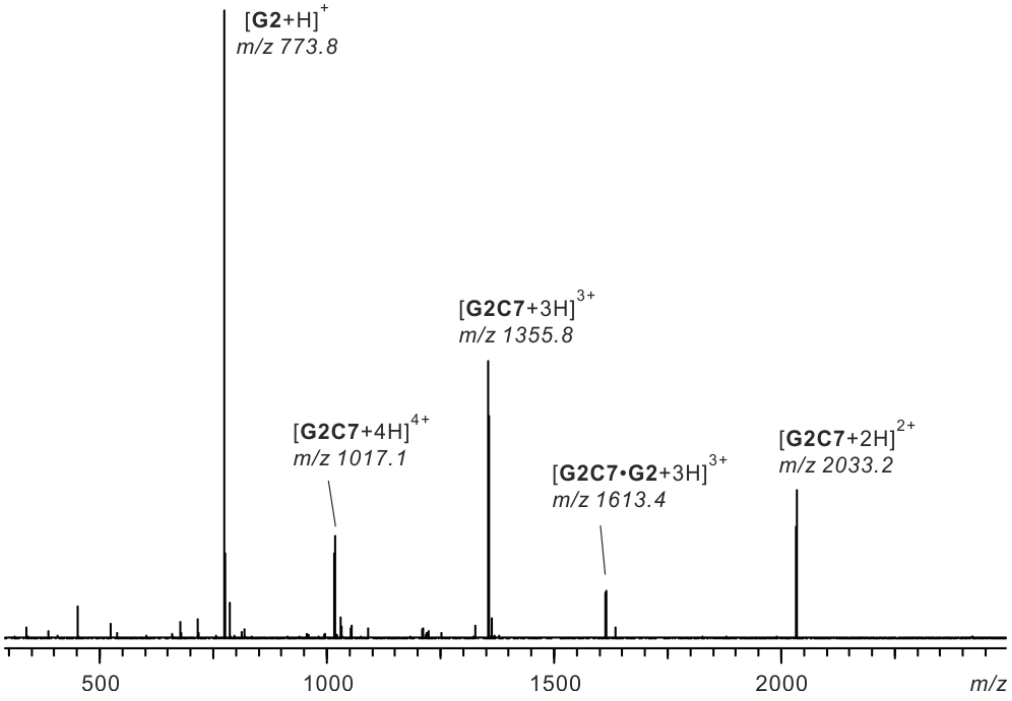

Figure S3. Mass spectrum of the **G2C7**/**G2** complex.

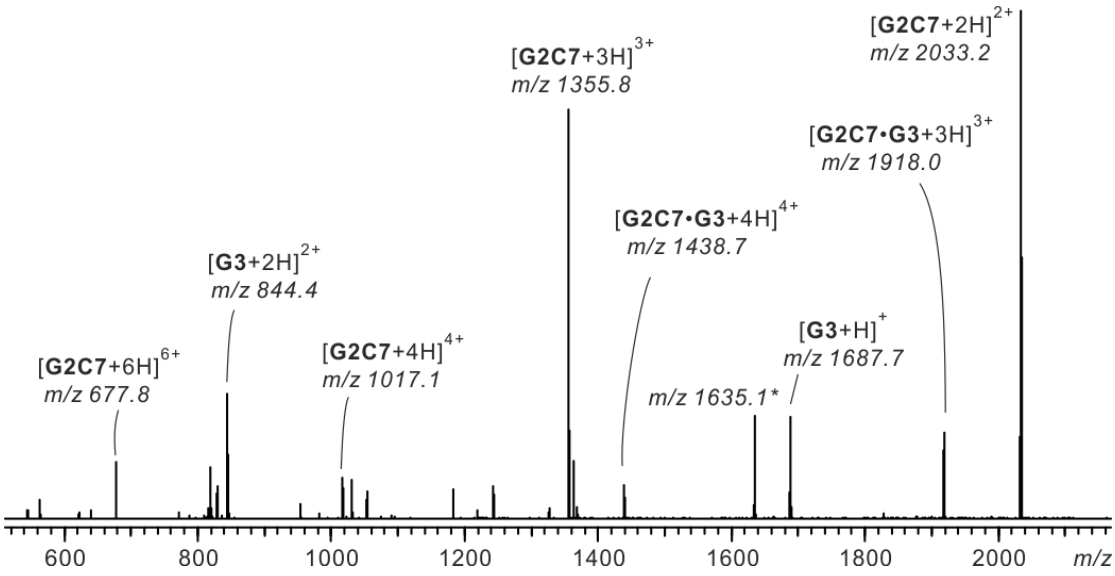

Figure S4. Mass spectrum of the **G2C7**/**G3** complex. The asterisk marks a signal for a defect dendrimer.

Figures S2-S4 show the mass spectra of sample solutions from which the dendrimer-dendrimer complexes were generated. The most intense signals correspond to the free dendrimers in different charge states, while the signals for the complexes are rather low in intensity. This can be ascribed to the rather low sample concentration. At higher concentrations, the abundance of complex ion signals increases, but also the propensity to form precipitates that block the ESI capillary and thus cause interruptions in the experiments.

3. H/D-exchange on the complex of G2C7 and G4

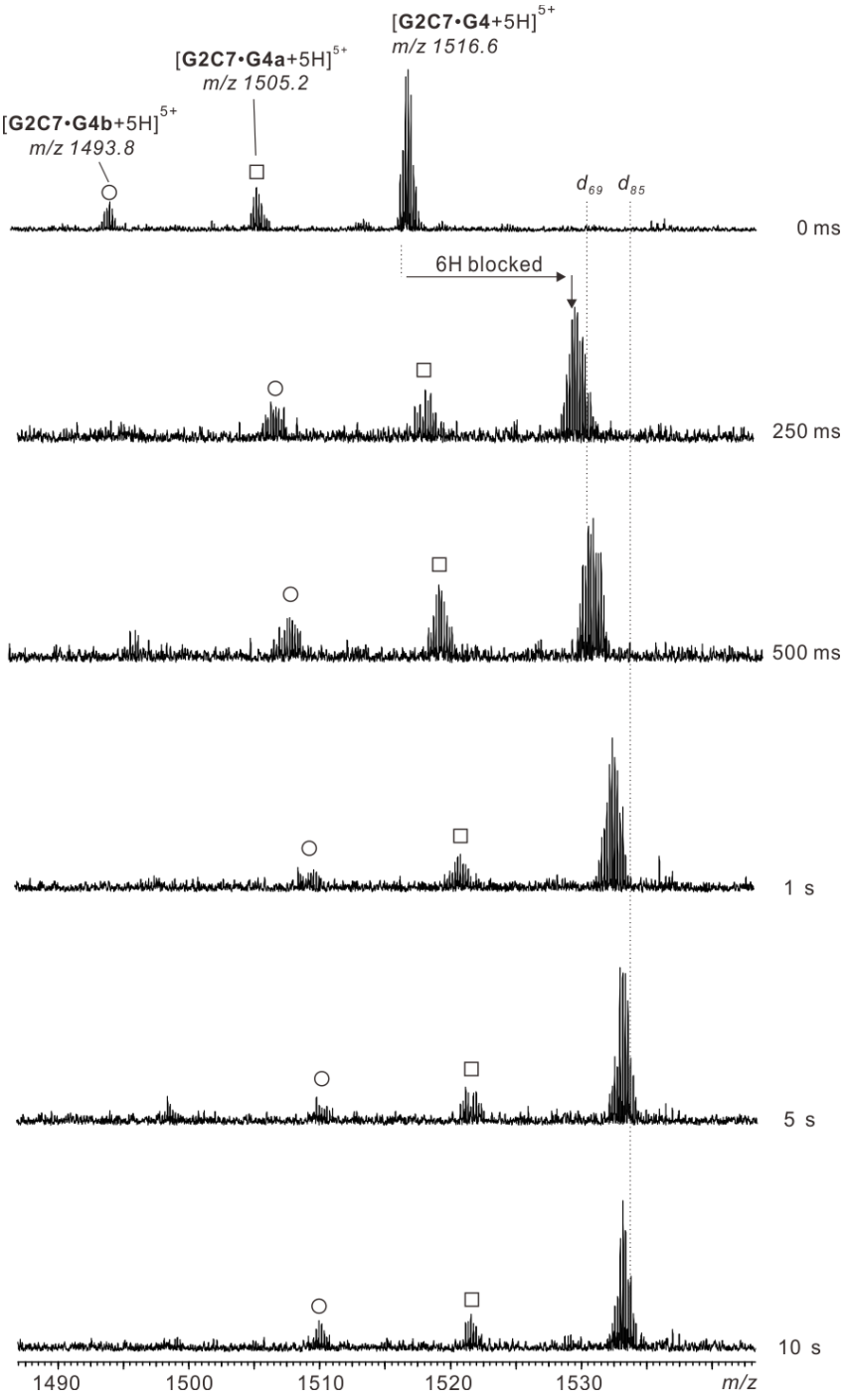

Figure S5. H/D-exchange reaction on **G2C7**/**G4** complex. Circles and squares indicate signals for defect structures with one and two missing terminal branches (see the defected structures in Figure S6). Although the defects reduced the available abundance of intact ions and hence cause lower signal-to-noise ratios, it is clearly visible that all arguments developed in the main text remain valid also for the larger generation complexes.

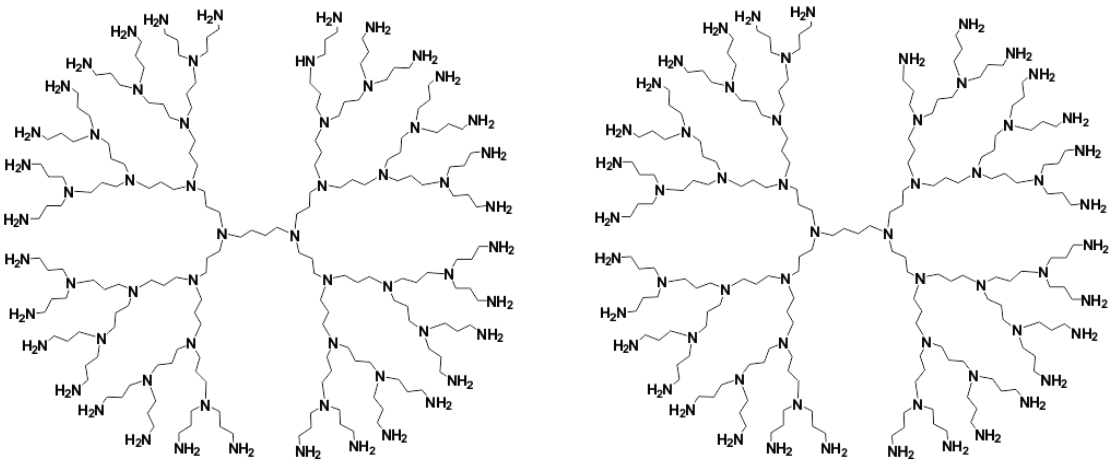

G4a **G4b**

Figure S6. Chemical structures of defected **G4** POPAM dendrimers missing one and two arms, which were observed in the H/D exchange on the **G2C7**/**G4** complex. Of course there are a number of different isomers of **G4b** besides the one shown here exemplarily.

4. H/D-exchange experiments with UBC7

In order to evaluate the protective group capabilities of the urea functionalized crown ether, we conducted the H/D-exchange reaction on the 1:1 complex of **UBC7** with protonated propylamine (Figure S7). For this complex ([**UBC7**•propylamine+H]$^+$ at *m/z* 516.3), only an extremely slow H/D-exchange is observed by the somewhat increased intensity of the second peak in the isotope pattern becoming visible after 50 s reaction time. The urea group therefore does not alter the protection efficiency of **BC7**.

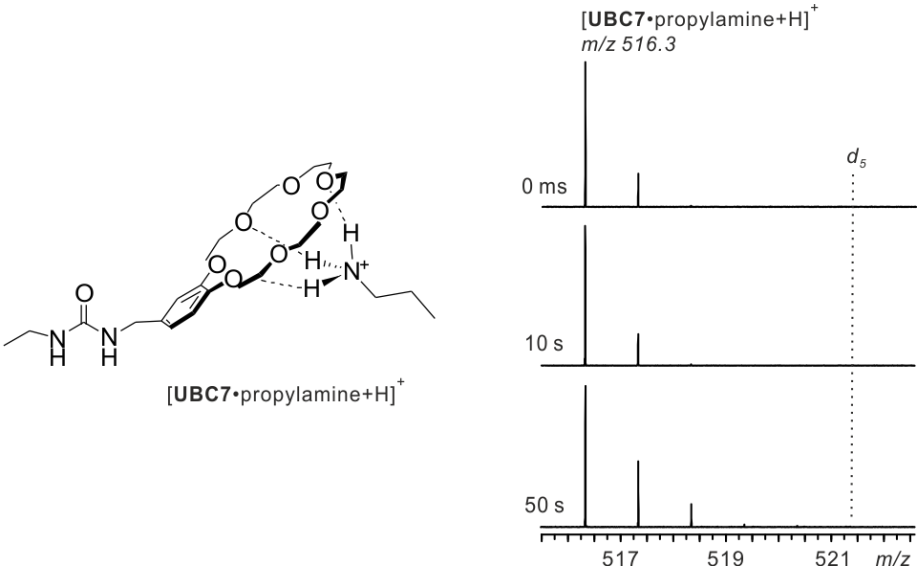

Figure S7. H/D-exchange conducted on **UBC7** complex with monoprotonated propylamine. The dotted line (d_5) indicates the place where the signal should terminate if all the hydrogens are exchanged.

Furthermore, the singly charged 1:1 and the doubly charged 2:1 complexes of **UBC7** and 1,12-diaminododecane, i.e. [**UBC7**·**DAD**+H]$^+$ at *m/z* 657.5 and [**UBC7**$_2$·**DAD**+2H]$^{2+}$ at *m/z* 557.3 were examined. While the singly charged 1:1 complex (Figure S8) showed a slow exchange due to the absence of a free ammonium group mediating the relay mechanism, the 2:1 complex did not show any significant HDX reaction within the same reaction time as both functional groups are protected by the crown ethers (Figure S9).

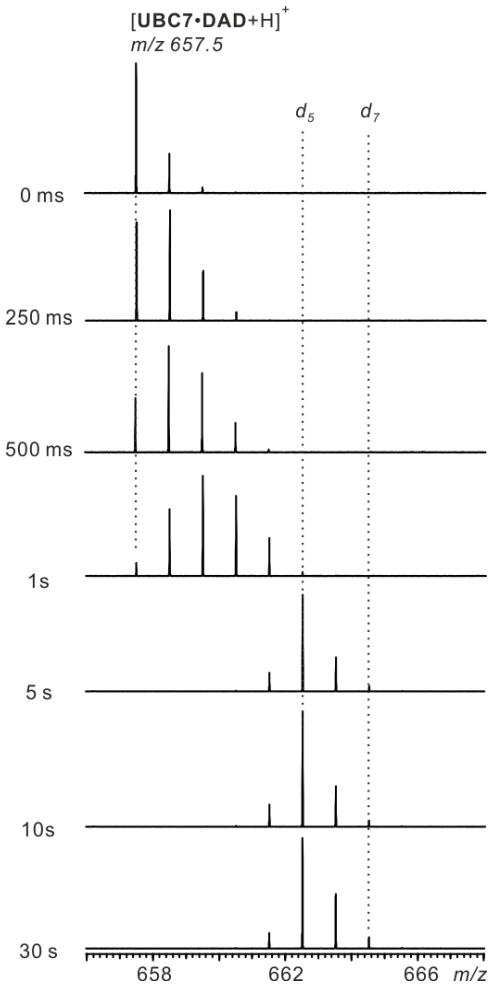

Figure S8. H/D exchange experiment with singly protonated [**UBC7**·**DAD**+H]$^+$. The exchange of the amine and ammonium hydrogen atoms is clearly visible, although it is slowed down by the protection of the ammonium group and is much slower than on dendrimer ions that carry a free ammonium group. The two urea protons, instead, undergo hardly any exchange even at prolonged exchange reaction intervals of 30 s.

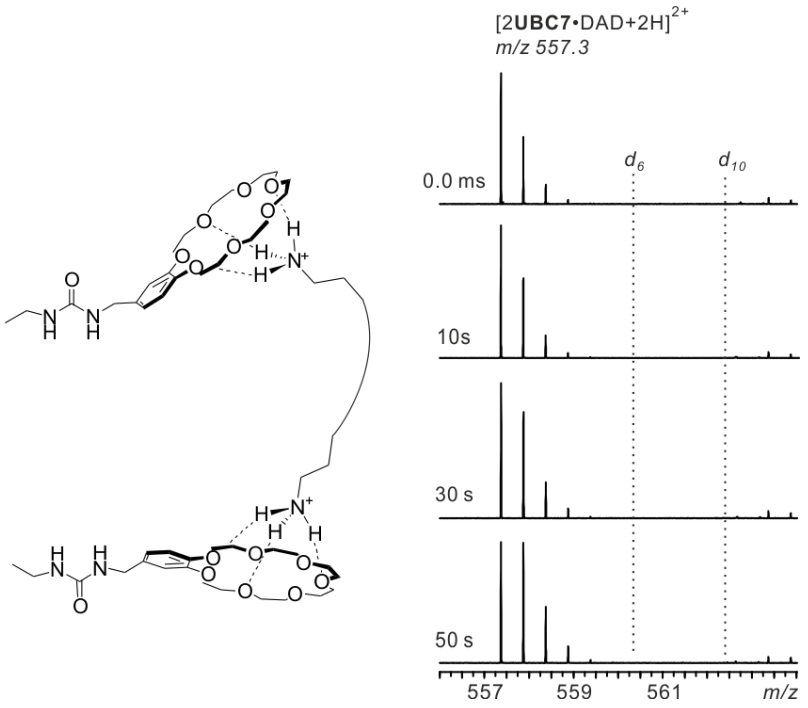

Figure S9. H/D exchange on **UBC7**/**DAD** complex, in which both ammonium groups are protected by **UBC7**. The dashed line indicates the fully exchange of the H atoms on the ammonium (d_6) plus those on urea groups (d_{10}) respectively.

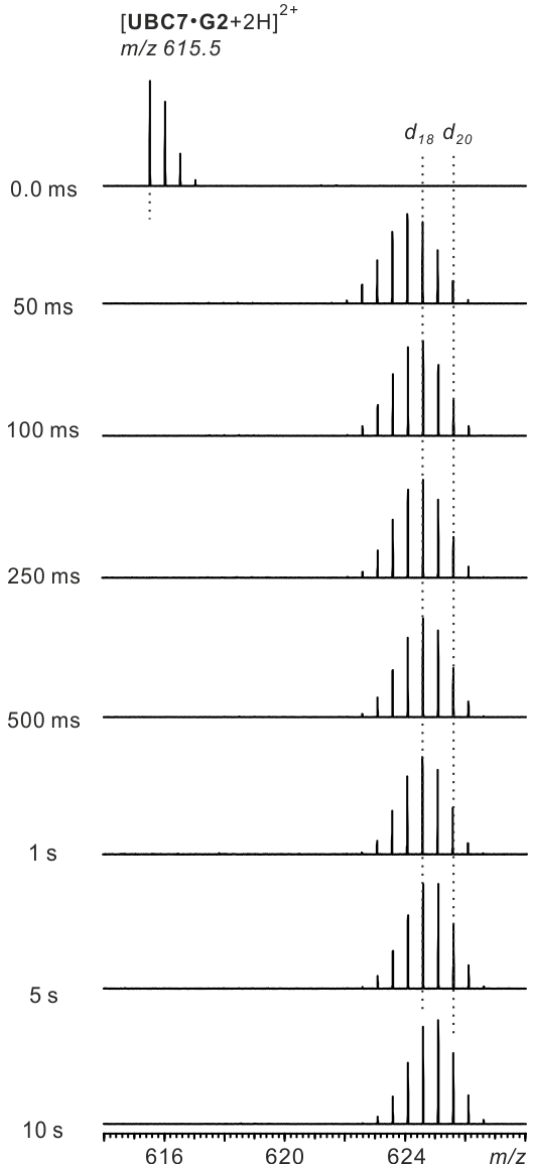

Figure S10. H/D-exchange experiment with doubly protonated dendrimer-dendrimer complexes composed of **UBC7** and **G2**. Within a very short time (50 ms), the H/D-exchange on the amino and ammonium groups of **G2** has is close to completion. This is easy to understand in view of the free ammonium group, which significantly speeds up the HDX by mediating the exchange in terms of the relay mechanism discussed in the main text. This reaction is followed by a very slow exchange of the two urea hydrogen atoms.

5. Data fitting of the time plots of H/D-exchange on the dendritic complexes

If we plot the average number of exchanged H atoms against reaction time, the exchange time plots described in the main text (Figure 9) can best be fitted to a double exponential function (eq. 1):

$$I_t - I_\infty = c_{fast}e^{-t/\tau_{fast}} + c_{slow}e^{-t/\tau_{slow}} \qquad \text{eq. 1}$$

in which c_{fast} and c_{slow} are normalized abundances (c_{fast} = 1 - c_{slow}), and τ_{fast} and τ_{slow} are the characteristic relaxation times of the fast and slow stages, respectively. The fact that two sets of τ value are required for a good data fit agrees well with the two different types of labile hydrogen atoms (amine/ammonium and urea). The detailed procedure of evaluating the average number of exchanged H atoms at a certain reaction time is shown in Figure S15.

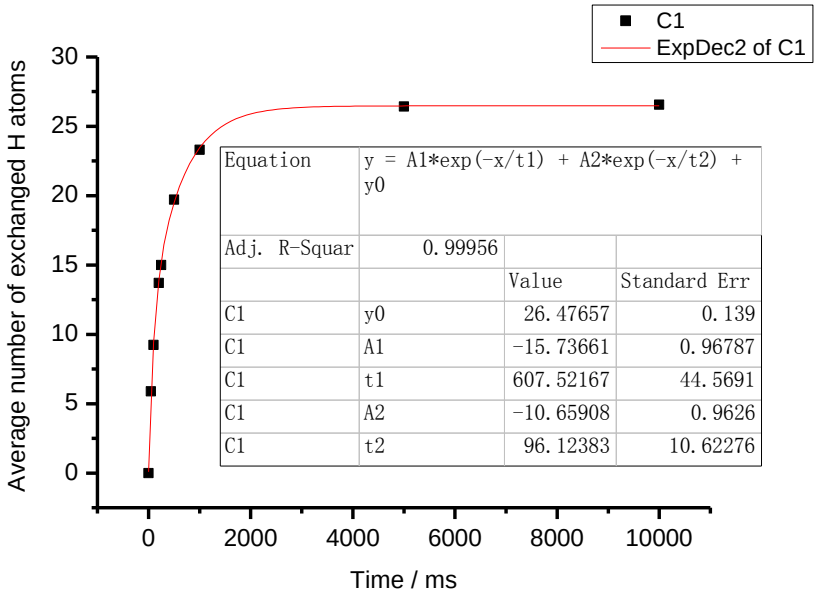

Equation	y = A1*exp(-x/t1) + A2*exp(-x/t2) + y0		
Adj. R-Squar	0.99956		
		Value	Standard Err
C1	y0	26.47657	0.139
C1	A1	-15.73661	0.96787
C1	t1	607.52167	44.5691
C1	A2	-10.65908	0.9626
C1	t2	96.12383	10.62276

Figure S11. Time plot of the average number of exchanged H atoms against time (ms) for dendritic complex [**G1C7 • G2**+3H]$^{3+}$ at *m/z* 912.6. The inset provides the detailed parameters for the fitting function (eq.1).

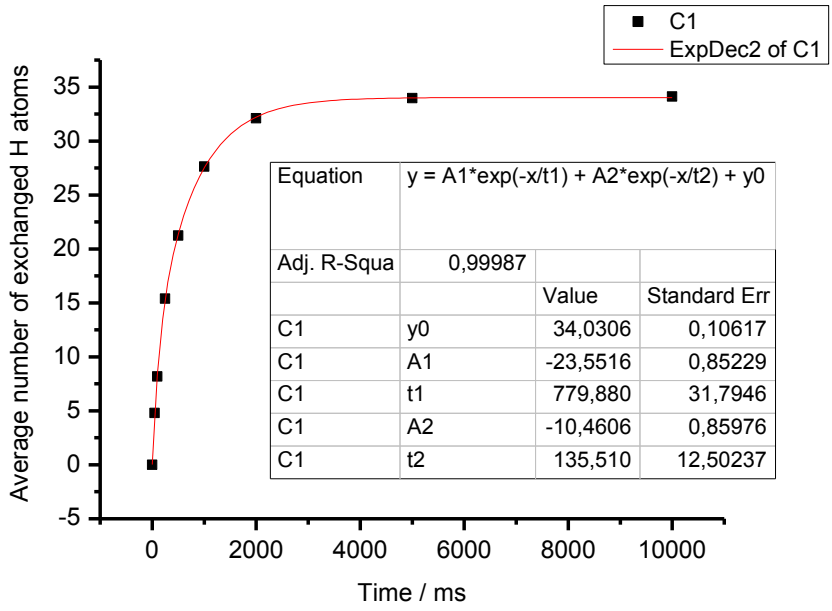

Figure S12. Time plot of the average number of exchanged H atoms against time (ms) for dendritic complex [**G2C7 • G2**+3H]$^{3+}$ at *m/z* 1613.4. The inset provides the detailed parameters for the fitting function (eq.1).

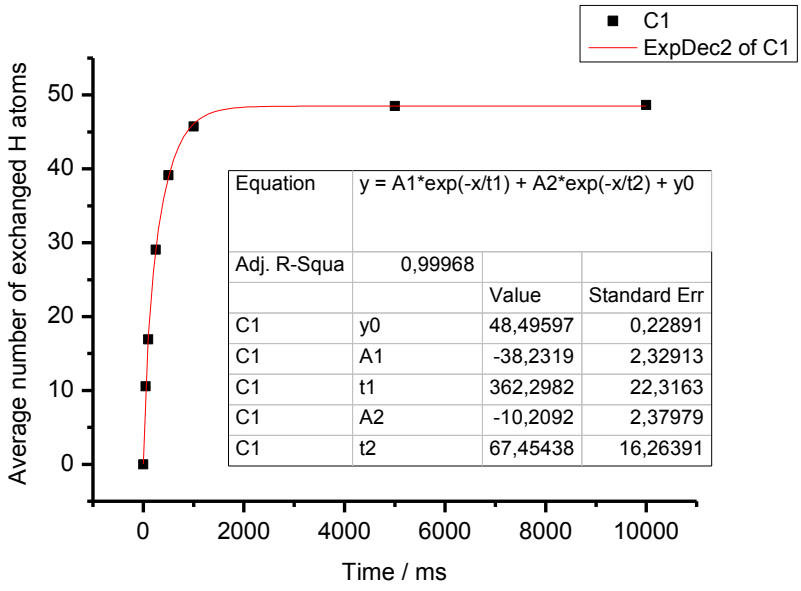

Figure S13. Time plot of the average number of exchanged H atoms against time (ms) for dendritic complex [**G2C7 • G3**+3H]$^{3+}$ at *m/z* 1918.0. The inset provides the detailed parameters for the fitting function (eq.1).

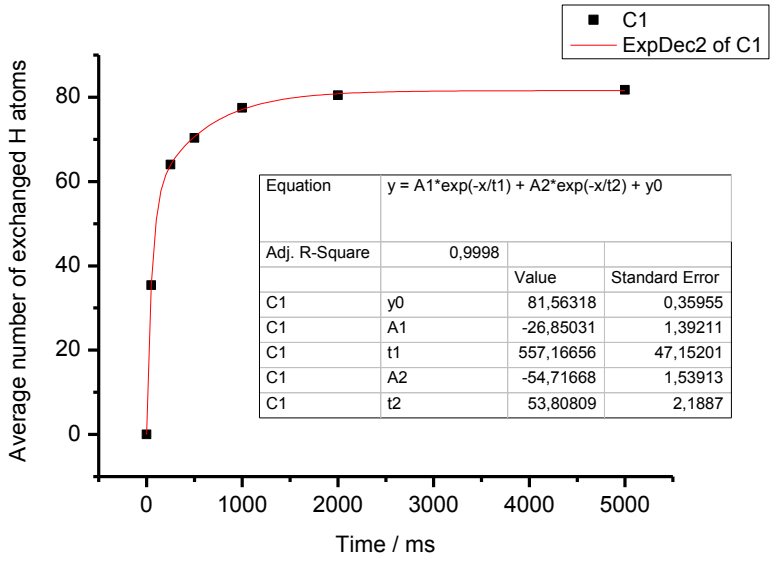

Figure S14. Time plot of the average number of exchanged H atoms against time (ms) for dendritic complex [**G2C7 • G4**+5H]$^{5+}$ at *m/z* 1516.5. The inset provides the detailed parameters for the fitting function (eq.1).

To determine the average number of exchanged hydrogen atoms, we followed this procedure: For both isotope patterns before and after the H/D-exchange, the weighted average is calculated (coined the "mass center" in the screenshots in Figure S15). The difference between the two values is then used as the average number of exchanged hydrogen atoms. For the example shown, the procedure is then:

Step 1 (Figure S15a): Start with the list of the initial undeuterated species. *m/z* values and the corresponding peak intensities are pasted from the Omega software controlling the mass spectrometer to the spreadsheet, which calculates the weighted average of the pattern.

Step 2 (Figure S15b): The same procedure is done with the isotope pattern after H/D-exchange (250 ms in the example)

Step 3: The difference of both values needs to be multiplied with the charge state, in this case +3, in order to calculate the average number of exchanged hydrogen atoms.

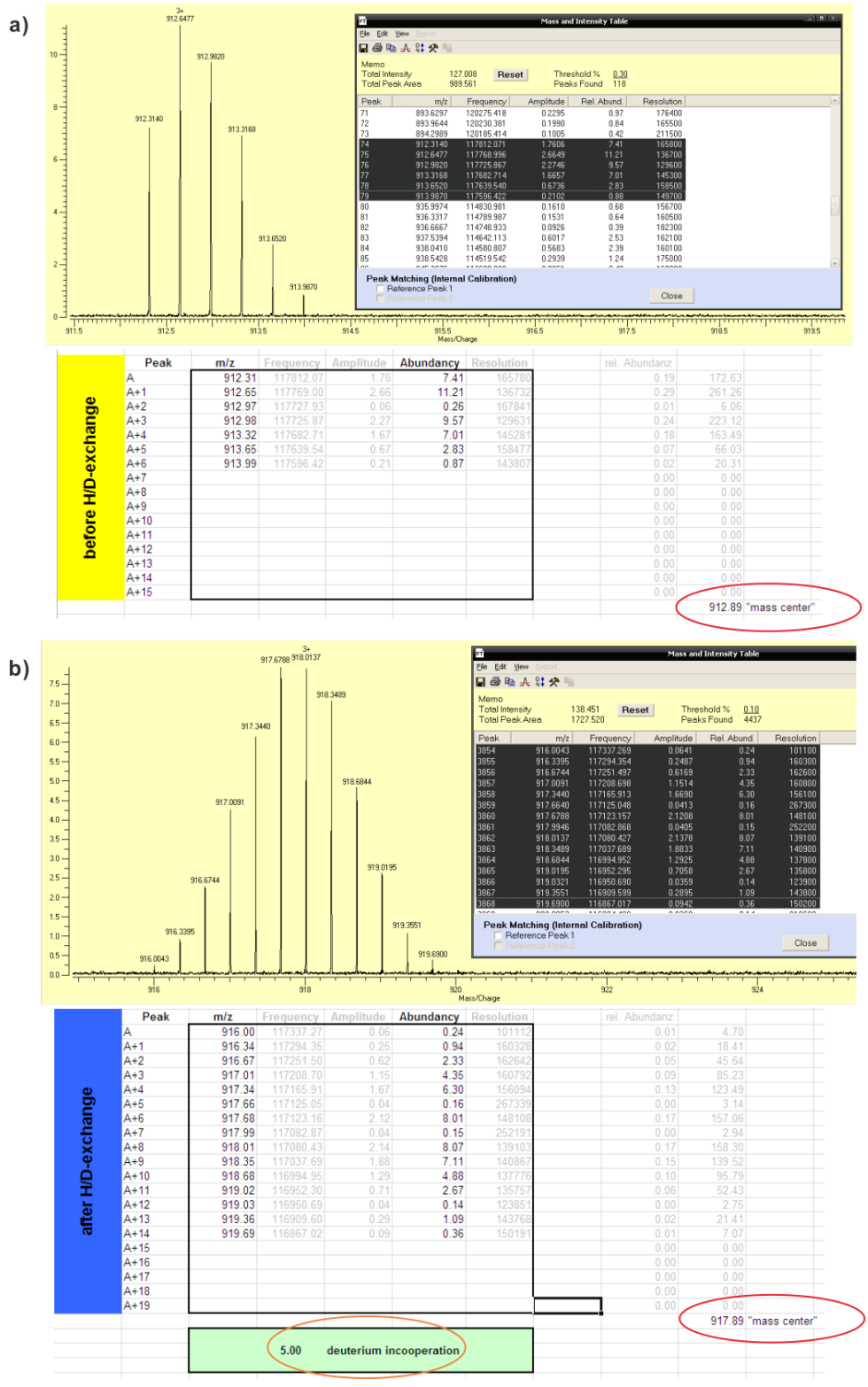

Figure S15. Screenshots of the evaluation process of the average number of exchanged H atoms after a specific reaction time (the dendrimer-dendrimer complex ion [**G1C7**·**G2**+3H]$^{3+}$ at *m/z* 912.6 was used for illustration).

6. Mechanistic considerations on the urea NH exchange reaction

As detailed in the main text, an efficient exchange of the urea NH hydrogen atoms requires the participation of a primary amine and a primary ammonium. The lack of one of these groups or the presence of tertiary amines and ammonium groups is not sufficient. In this section, several selected mechanistic alternatives to that favored in the main text are displayed and briefly discussed. In contrast to the mechanism in the main text, we assume a direct participation of MeOD in the mechanisms shown here.

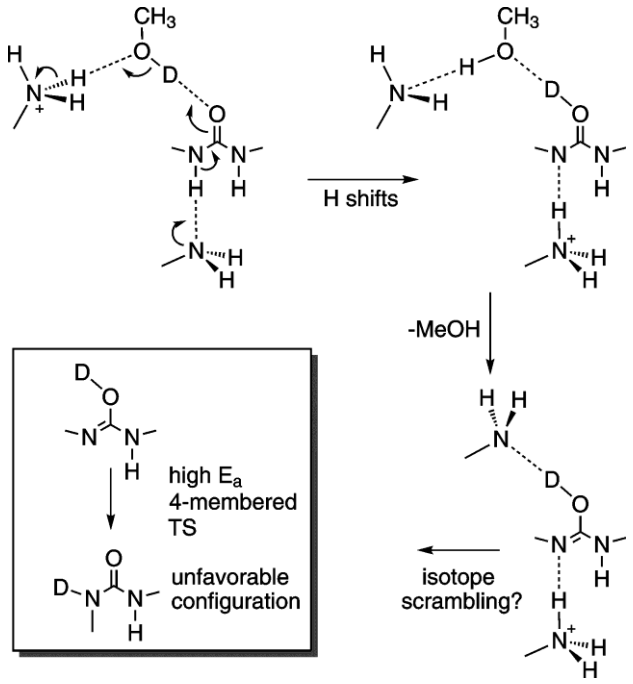

Figure S16. Insertion of a MeOD molecule between the urea carbonyl oxygen and the ammonium ion would enable the mechanism shown. However, it is not clear how the isotope scrambling step would proceed.

For the isotope scrambling step in Figure S16, several options may exist: (i) As shown in the inset a simple tautomerization within the urea group would be the simplest possibility. However, in the gas phase, this would require a quite energy-demanding 4-membered transition state which leads to an unfavorable configuration of the urea group in which one side is *cis*-configured. (ii) An amino group may participate as a proton shuttle to catalyze tautomerization. However, this would require a rather

unfavorable charge separation as both hydrogen bonds to the urea group would be required to be broken. This resulted in two ammonium groups in close proximity to a deprotonated anionic urea group. (iii) The only reasonable possibility is that the secondary amine already bears one or two deuterium atoms. A mechanism would therefore proceed exactly as that one presented in the main text with the exception that a further MeOD is present. Of course, this mechanism is not excluded, but more complicated than that in the main text. Therefore, we decided to suggest the simpler one.

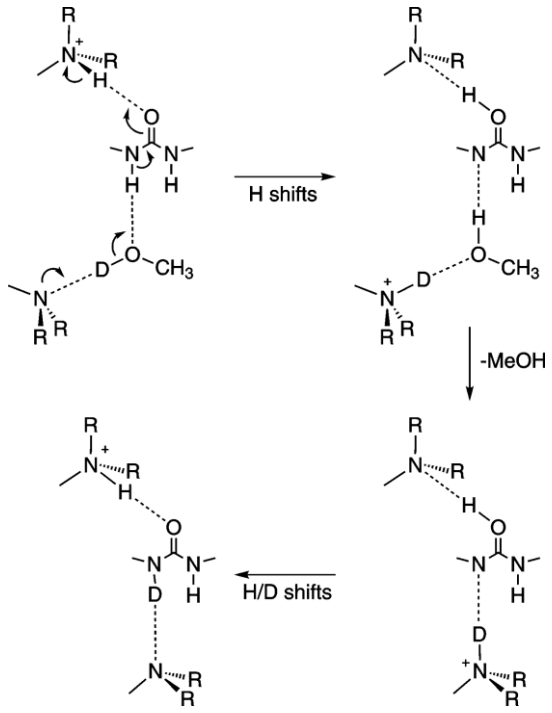

Figure S17. Insertion of a MeOD molecule between the urea NH and the ammonium ion would enable the mechanism shown, which indeed would lead to an exchange of the urea NH hydrogen atoms.

The mechanism in Figure S17, which appears to be a good alternative to the suggested one in the main text raises the question, why it should not be possible to proceed with tertiary amino and tertiary ammonium groups. As this is not observed in the experiments, the experimental results rule out this mechanism.

Likely many more potential mechanisms exist. For the time being, we decided to suggest the simplest one following Occam's razor.

7. Synthesis and characterization of the compounds under study

All reagents were commercially available and used as supplied without further purification. Di-*tert*-butyl tricarbonate (**1**) and 4'-aminomethylbenzo[21]crown-7 (**2**) were prepared according to published procedures.[2] Solvents were either employed as purchased or dried prior to use by usual laboratory methods. ^{1}H NMR and ^{13}C NMR spectra were recorded on Bruker ECX 400 MHz, Jeol Eclipse 500 MHz, or Bruker AVANCE III 700 MHz NMR spectrometers.

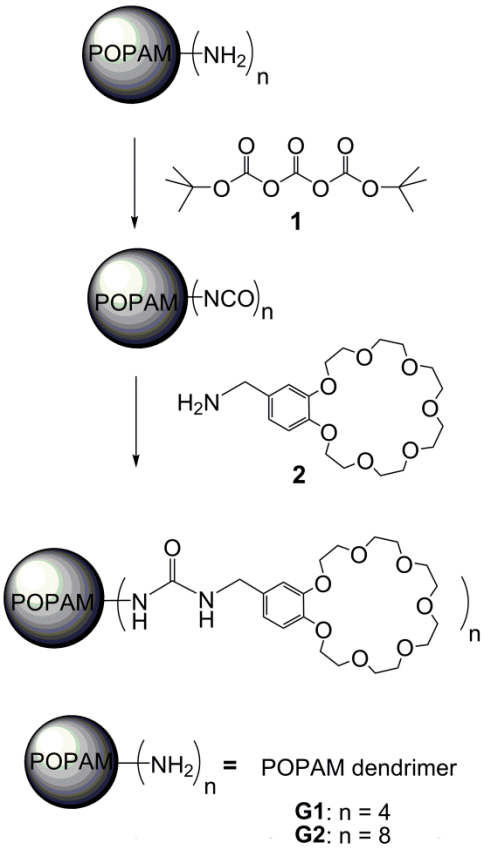

Scheme S1. The synthetic scheme of crown-functionalized POPAM dendrimers (**G1C7** and **G2C7**).

Synthesis of GnC7

The synthesis of the crown-substituted POPAM dendrimers followed a slightly modified literature protocol.[3] The polyamine (30 mg) in CH_2Cl_2 (5 mL) was injected into a stirred CH_2Cl_2 solution (15 mL) of di-*tert*-butyltricarbonate **1** (119 mg, 0.568 mmol) and stirred at room temperature for 40 min under Ar. The formation of isocyanates was checked with IR spectroscopy (ν = 2265 cm^{-1}). The excess di-*tert*-butyltricarbonate was quenched by two drops of anhydrous pyridine. Afterwards,

4’-aminomethyl-benzo[21]crown-7 **2** (578 mg) was added to the reaction mixture. After 16 hours, the crude product was precipitated with ice-cold heptane (250 mL). After column chromatography on Al_2O_3 (EtOAc/MeOH, 30:1 and CH_2Cl_2/MeOH, 20:1), pale yellowish oils of **G1C7** and **G2C7,** respectively, were obtained and characterized as follows.

G1C7. Yield: 179 mg (96 %). **^{1}H NMR** (400 MHz, $CDCl_3$, 298 K) δ [ppm] = 1.37 (br s, 4H), 1.53-1.56 (m, 8H), 2.28-2.34 (m, 12H), 3.14 (br t, 8H), 3.62 (br s, 32H), 3.68-3.76 (m, 16H), 3.73-3.76 (m, 16H), 3.84-3.87 (m, 16H), 4.06-4.09 (m, 24H), 6.78 (br s, 8H), 6.79 (br s, 4H). **^{13}C NMR** (175 MHz, $CDCl_3$, 298 K) δ [ppm] = 24.5, 27.4, 38.4, 43.6, 51.1, 53.3, 69.2, 69.4, 69.7, 70.3, 70.4, 70.8, 70.9, 113.8, 114.3, 120.2, 133.5, 147.7, 148.8, 159.0. **ESI-TOF-HRMS**: *m/z* calcd for $[M+H]^+$ $C_{96}H_{156}N_{10}O_{32}$, 1963.0997; found, 1963.0974.

G2C7. Yield: 140 mg (89 %). **^{1}H NMR** (400 MHz, $CDCl_3$, 298 K): δ [ppm] = 1.37 (br s, 4H), 1.48 (br m, 8H), 1.55 (br, 16H), 2.27-2.32 (m, 36H), 3.15 (br q, 16H), 3.62 (br s, 64H), 3.68 (m, 32H,), 3.74 (m, 32H), 3.84 (m, 32H), 4.0 (m, 48H), 6.6 - 6.8 (m, 24H, Ar). **^{13}C NMR** (175 MHz, $CDCl_3$, 298 K) δ [ppm] = 24.4, 27.7, 38.1, 43.6, 50.7, 51.6, 52.3, 69.2, 69.4, 69.8, 70.5, 70.8, 71.0, 113.6, 114.3, 120.2, 133.6, 147.8, 148.9, 159.3. **ESI-TOF-HRMS**: m/z calcd for $[M+2H]^{2+}$ $C_{96}H_{156}N_{10}O_{32}$, 2033.1677; found, 2033.1610.

Synthesis of UBC7

A solution of aminomethylbenzo[21]crown-7 **2** (200 mg, 0.52 mmol) in dry CH_2Cl_2 (3 mL) was injected into a solution of ethyl isocyanate (134 mg, 0.52 mmol) in dry CH_2Cl_2 (6 mL) under argon atmosphere, and stirred for 16 hours at room temperature. After the reaction, the solvent was removed in vacuo. The crude product was purified by column chromatography over silica gel to afford **UBC7** (273 mg) in 82 % yield as a white powder.

^{1}H NMR (700 MHz, $CDCl_3$, 298 K): δ [ppm] = 6.83 (s, 1H), 6.80 (s, 2H), 4.78 (s, 1H), 4.51 (s, 1H), 4.25 (d, *J* = 5.7 Hz, 2H), 4.13 (dd, *J* = 9.0, 3.8 Hz, 4H), 3.89 (dd, *J* = 9.2, 5.4 Hz, 4H), 3.77 (dd, *J* =

5.7, 3.5 Hz, 4H), 3.71 (dt, *J* = 6.5, 3.1 Hz, 4H), 3.68 – 3.63 (m, 8H), 3.21 – 3.16 (m, 2H), 1.10 (t, *J* = 7.2 Hz, 3H).**^{13}C NMR** (175 MHz, $CDCl_3$, 298 K): δ = 158.28, 149.23, 148.24, 132.82, 120.53, 114.50, 113.90, 77.34, 77.16, 76.98, 71.22, 71.18, 71.15, 71.10, 70.67, 70.63, 69.94, 69.54, 69.38, 44.42, 35.47, 15.63. **ESI-TOF-HRMS**: *m/z* calcd for $[M+H]^+$ $C_{13}H_{19}N_2O$, 219.1492; found, 219.1495.

8. References

1 a) S. A. Hofstadler, K. A. Sannes-Lowery, R. H. Griffey, *Rapid Commun. Mass. Spectrom.* 1999, **13**, 1971-1979; b) S. A. Hofstadler, K. A. Sannes-Lowery, R. H. Griffey, *J. Mass. Spectrom.* 2000, **35**, 62-70. The same approach was used in earlier HDX studies: (*a*) D. P. Weimann, H. D. F. Winkler, J. A. Falenski, B. Koksch and C. A. Schalley, *Nat. Chem.*, 2009, **1**, 573-577; (*b*) H. D. F. Winkler, D. P. Weimann, A. Springer and C. A. Schalley, *Angew. Chem. Int. Ed.*, 2009, **48**, 7246-7250; (*c*) H. D. F. Winkler, E. V. Dzyuba, A. Springer, L. Losensky and C. A. Schalley, *Chem. Sci.* 2012, **3**, 1111-1120.

2 Z. Qi, P. Malo de Molina, W. Jiang, Q. Wang, K. Nowosinski, A. Schulz, M. Gradzielski, C. A. Schalley, *Chem. Sci.* 2012, **3**, 2073-2082.

3. J. W. Jones, W. S. Bryant, A. W. Bosman, R. A. J. Janssen, E. W. Meijer and H. W. Gibson, *J. Org. Chem.*, 2003, **68**, 2385-2389.

9. Pseudorotaxanes with self-sorted sequence and stereochemistry

This chapter was published in the following journal:

C. Talotta, C. Gaeta, Z. Qi, C.A. Schalley, P. Neri, *Angew. Chem. Int. Ed.*, **2013**, *52*, accepted (DOI: 10.1002/anie.201301570)

http://dx.doi.org/10.1002/anie.201301570

Declaration on the personal contribution in this work

Z. Qi contributed the mass spectrometric characterization and analysis of the *pseudo*rotaxane systems.

Content and summary of the work

This article presents a study of the threading of two calix[6]arene macrocycles of differing steric hindrance of the large rim on various molecular threads incorporating secondary ammonium recognition sites in different chemical environments (benzyl or alkyl). Through proton NMR and mass spectrometry, we disclosed a set of self-sorting rules which govern the threading sequence (which macrocycle goes where) and stereochemistry (head-to-head, head-to-tail, and tail-to-tail) of the resultant *pseudo*rotaxanes. Self-sorting served as a programmable code (the constitution of the subunits), which can be complied by the algorithm (the preferred interactions between the subunits). This is the first example of an integrative self-sorting system able to discriminate species simultaneously isomeric at the sequence and stereochemical level.

10. Summary

The present research contains two parts: The first explores the macrocycle functionalized supramolecular gels and the second part investigates the host-guest chemistry of dendrimers by mass spectrometry. Although these two parts of the research were investigated under different conditions, one in the condensed phase and one in the gas phase, the same crown ether macrocycle was used as the basic building block in both cases. Herein, we reported the usefulness of macrocycle chemistry, how it benefits the construction of novel soft materials with multiple responsiveness, and how the molecular motion can be investigated in the gas phase by tandem mass spectrometric experiments. The detailed achievements can be summarized as follows:

Part A: Construction of macrocycle functionalized supramolecular gels

1. We designed and synthesized a new type of crown ether-functionalized bis(urea) organogelators which were equipped with two benzo[21]crown-7 moiety at both terminals. The host-guest chemistry of the crown ether plus the urea unit endow the gel with multiple chemical responsiveness: its gel-sol transition can be switched by several different molecular recognition events: K^+ binding to the crown ether, formation of *pseudo*rotaxane with secondary amine and the interaction of Cl^- anion with urea unit. The most intriguing part of this research is that we took advantage by exploring chemical stimuli to disclose the sophisticated signal networks when several of these chemical signals exist in the gel system. Through rational design of the gel system as well as the inputs of stimuli (type, amount, sequence), we realized seven types of chemical logic gates (including OR, AND, XOR, NOT, NOR, XNOR and INHIBIT gates), which controlled the macroscopic gel-sol transition operated in a logical manner. The resulting supramolecular gels system showed great potential by simply choosing and arranging the known responsive properties to endow the gel materials with ‘smart thinking’.

2. We further extended the crown-functionalized gels system to a large extent. One direction was to propose a strategy to utilize the selective responsive supramolecular gel as an immobilization and recycling media for Pickering emulsion. We designed and

synthesized new crown ether-appended chiral gelators which show impressive gelation ability in a variety of organic solvents, particularly in acetonitrile. Due to the crown ether, the resultant supramolecular gel remains sensitive to multiple chemical stimuli and the sol-gel phase transitions can be reversibly triggered by host-guest interactions. We demonstrated that the 3D network in the gel can entrap an enzyme (CalB, lipase B from *Candida antarctica*) and released it upon addition of potassium ions. The obtained environmental responsive gel system was extended to be utilized as a novel matrix for Pickering emulsion as a proof of concept. The newly developed gel matrix not only contributes to solving the phase problem that frequently occurs when enzymes are used to catalyze organic reactions in unpolar organic media, but also makes the recycling of the entrapped enzyme possible by chemical stimuli.

3. The crown ether-appended chiral gelator shows much broader gelation abilities, even in ionic liquids. The detailed gelation ability in different ionic liquids was evaluated, as well as the thermal stability. The ionogels showed impressive a high thermal stability. In comparison with conventional organic solvents, ionic liquids significantly increase the mechanical strength of the corresponding gels. The storage modulus G´is impressively high and is even comparable with cross-linked protein fibers. Moreover, all the ionogels displayed rare rheopexy (shear thickening) phenomenon instead of thixotropy at low shear rates. Intriguingly, the ionogel even possesses a rapid self-recovery ability.

Part B: Investigation of host-guest chemistry of dendrimers in the gas phase

1. Mass spectrometry aided by hydrogen/deuterium exchange (HDX) experiments provides evidence to a molecular motion occurring within a complex composed of a partly protonated amino-terminated polypropylene amin (POPAM) and POPAM dendrimer fully functionalized with benzo[21]-crown-7 on all branches. The multiple molecular recognition events make the complex system suitable for a multivalent study, particularly from the molecular dynamic motion aspect. Since the crown ethers can efficiently protect the ammonium group against HDX, the complete exchange of all labile N-H hydrogen atoms in the dendritic complex unravel the highly dynamic binding motion inside. Each appended crown is mobile enough to move from one ammonium

binding site to another, thus driving the two dendrimers swirling around each other without completely losing all contact at any time. Schematically, such an intracomplex motion is quite similar to two “rock ‘n roll” dancers. So far, this is the first study providing evidence for the microdynamics within multivalent complexes.

Accordingly, the marriage of macrocycle and supramolecular gels bring numerous opportunities for designing novel supramolecular gels which would be difficult to achieve by other building blocks. Even for matured dendrimer chemistry, new insights are available when the host-guest chemistry of crown macrocycle is introduced. Consequently, the future of macrocycles is bright.

11. Zusammenfassung

Die vorliegende Arbeit kann in zwei verschiedene Bereiche eingeteilt werden. Der erste Teil thematisiert die Untersuchung von mit Makrozyklen funktionalisierten supramolekularen Gelen. Der zweite Teil befasst sich mit der Erforschung der Wirt-Gast-Chemie von Dendrimeren mit Hilfe von Massenspektrometrie.

Obwohl die Untersuchungen der beiden Teile in zwei verschiedenen Phasen, in Lösung und in der Gasphase, durchgeführt wurden, haben diese etwas gemeinsam. In beiden Studien werden Kronenether als Makrozyklen und Basis-Bausteine verwendet. Wir zeigen hier, wie nützlich Makrozyklus-Chemie ist, wie diese die Entwicklung von neuartiger weicher Materie vorantreibt und wie mit Hilfe von Massenspektrometrie und Tandem-Massenspektrometrie molekulare Bewegung entschlüsselt werden kann. Die ausführlichen Studien können wie folgt zusammengefasst werden:

Teil A: Bildung von Makrozyklen-basierten supramolekularen Gelen

1. Es wurden neuartige Kronenether-funktionalisierte Bis(urea)-Organogelatoren entworfen und synthetisiert. Durch Interaktion der terminalen Benzo[21]Krone-7- und den integrierten Urea-Einheiten kommt es zu Gelbildung. Das entstandene Gel reagiert auf eine Vielzahl von äußeren Stimuli. Sein Gel-Sol-Übergang kann durch den Einfluss von unterschiedlichen auf molekulare Erkennung basierenden Schaltungsprozessen beeinflusst werden. Dies bezieht sich unter anderem auf die Bindung von K^+ an die Kronenether-Einheiten, die Bildung von *Pseudo*rotaxanen mit sekundären Aminen und die Interaktion von Cl^- mit den Urea-Einheiten. Das Faszinierendste dabei ist, dass wir nicht länger darauf fokussiert sind weitere Stimuli zur Schaltung zu entwickeln und zu erforschen, sondern unser Interesse an der Offenlegung der zugrundeliegenden Signal-Verknüpfungen, also die Reaktion auf den Einfluss mehrerer gleichzeitig eingesetzter Stimuli. Durch das bewusste Design der Gelsysteme mitsamt der entsprechenden Stimuli (Typ, Menge, Sequenz), war es uns möglich sieben Typen von chemischen Logikgattern (OR, AND, XOR, NOT, NOR, XNOR und INHIBIT) zu entwickeln und für kontrollierte makroskopische Gel-Sol-Übergänge zu nutzen.

   Die resultierenden supramolekularen Gelsysteme besitzen ein großes Potential, welches durch das bewusste Auswählen und Arrangieren der bekannten

Schaltungseigenschaften die Gele mit „Verstand“ ausstattet.

2. Des Weiteren erfolgte die Ausweitung der Studie über die Kronenether-funktionalisierten Gelsysteme. Eine Richtung ist die Ausarbeitung einer Strategie zur Nutzung von selektiven schaltbaren supramolekularen Gelen als Immobilisations- oder Recyclingmedium für Pickering-Emulsionen. Wir designten und synthetisierten einen neuartigen Kronenether-basierten chiralen Gelator mit beeindruckenden Gelierungseigenschaften in einer Vielzahl von organischen Lösungsmitteln, besonders in Acetonitril. Durch den Kronenether reagiert das resultierende supramolekulare Gel äußerst sensitiv auf verschiedene chemische Einflüsse und der Sol-Gel-Übergang kann reversibel durch Wirt-Gast-Interaktionen geschaltet werden.

   Wir demonstrierten, dass das 3D-Netzwerk im Gel ein Enzym (CalB, Lipase B des *Candida antarctica*) einfangen und durch die Zugabe von K^+ wieder freilassen kann. Das resultierende auf seine Umgebung reagierende Gelsystem wurde ausgeweitet um dieses als neue Matrix für Pickering-Emulsionen einzusetzen. Der Vorteil einer solchen Gelmatrix ist nicht nur sein Beitrag zur Lösung von Phasenproblemen, die häufig auftreten, wenn Enzyme dafür genutzt werden, um Reaktionen in unpolaren organischen Lösungsmitteln zu katalysieren, sondern auch um diese durch das gezielte Einfangen und Freilassen zu recyceln.

3. Der Kronenether-basierte chirale Gelator zeichnet sich durch seine breit gefächerten Geliereigenschaften aus. Dies bezieht sich nicht nur auf organische Lösungsmittel, sondern auch auf ionische Flüssigkeiten. Die Fähigkeit zur Gelbildung und die thermische Stabilität der Gele wurden mit Hilfe von ausführlichen Studien mit verschiedenen ionischen Flüssigkeiten evaluiert. Die resultierenden Ionogele zeigten im Vergleich zu Gelen aus konventionellen organischen Lösungsmitteln eine beachtliche mechanische Stärke. Das Speichermodul ist ebenfalls erstaunlich hoch und ist vergleichbar mit kreuzverlinkten Proteinfasern. Zudem zeigten alle Ionogele schwache Rheopexiephänomene (“*shear thickening”*) anstelle von Thixotropie bei niedrigen Scherungsraten. Faszinierenderweise zeigen sogar die Ionogele eine schnelle

Selbstheilungsfunktion.

Teil B: Untersuchung der Wirt-Gast-Chemie von Dendrimeren in der Gasphase

1. Massenspektrometrie und Wasserstoff/Deuterium-Austauschexperimente (HDX) liefern Hinweise auf eine auftretende molekulare Bewegung in Komplexen aus teilweise protonierten Amino-terminierten Polypropylenaminen (POPAM) und vollständig an jeder Abzweigung mit Benzo[21]-Krone-7 funktionalisierten POPAM-Dendrimeren. Durch die multiple molekulare Erkennung eignet sich dieses System zur Untersuchung von Multivalenz, im speziellen der Aspekt der molekularen Dynamik. Durch die Tatsache, dass Kronenether effektiv Ammoniumeinheiten gegen HDX schützen können, sollte ein vollständiger Austausch aller labilen N-H Wasserstoffatome im verzweigten Komplex zur Entwirrung des hochdynamischen internen Bewegung beitragen. Jeder gebundene Kronenether ist mobil genug um von einem Ammonium zum Nächsten zu wandern. Dies führt dazu, dass die beiden Dendrimere aneinander entlangrollen ohne vollständig den Kontakt zueinander zu verlieren. Schematisch kann diese intrakomplexe Bewegung mit der Bewegung von zwei “Rock ‘n‘ Roll”-Tänzern verglichen werden. Mit Hilfe der Studie konnten Belege für mikrodynamische Prozesse im multivalenten Komplex gesammelt werden.

Dementsprechend ergibt sich aus dem Zusammenbringen von Makrozyklen und supramolekularen Gelen eine Vielzahl von Möglichkeiten im Design derartiger Gele. Eine Vielzahl, die ohne diese Zusammenkunft nur schwer zu erreichen wäre. Sogar für die bereits gut erforschte Dendrimerchemie entwickeln sich durch den Einsatz von Wirt-Gast-Chemie neuartige und innovative Zugänge und Möglichkeiten. Die Zukunft für Makrozyklen ist offensichtlich groß.

12. Appendix

12.1 References

1. J. A. Foster and J. W. Steed, *Angew. Chem. Int. Ed.*, 2010, **49**, 6718-6724.
2. Y. Suzaki, T. Taira and K. Osakada, *J. Mater. Chem.*, 2011, **21**, 930-938.
3. A. Brizard, M. Stuart, K. van Bommel, A. Friggeri, M. de Jong and J. van Esch, *Angew. Chem. Int. Ed.*, 2008, **47**, 2063-2066.
4. A. M. Brizard and J. H. van Esch, *Soft Matter*, 2009, **5**, 1320-1327.
5. D. P. Weimann, H. D. F. Winkler, J. A. Falenski, B. Koksch and C. A. Schalley, *Nat. Chem.*, 2009, **1**, 573-577.
6. H. D. F. Winkler, D. P. Weimann, A. Springer and C. A. Schalley, *Angew. Chem. Int. Ed.*, 2009, **48**, 7246-7250.
7. P. Terech and R. G. Weiss, *Chem. Rev.*, 1997, **97**, 3133-3160.
8. L. A. Estroff and A. D. Hamilton, *Chem. Rev.*, 2004, **104**, 1201-1218.
9. N. M. Sangeetha and U. Maitra, *Chem. Soc. Rev.*, 2005, **34**, 821-836.
10. S. Banerjee, R. K. Das and U. Maitra, *J. Mater. Chem.*, 2009, **19**, 6649-6687.
11. E. A. Appel, J. del Barrio, X. J. Loh and O. A. Scherman, *Chem. Soc. Rev.*, 2012, **41**, 6195-6214.
12. J. H. v. Esch and B. L. Feringa, Gels in *Encyclopedia of Supramolecular Chemistry*, Taylor & Francis, 2007, pp. 586-596.
13. L. E. Buerkle and S. J. Rowan, *Chem. Soc. Rev.*, 2012, **41**, 6089-6102.
14. A. Noro, M. Hayashi and Y. Matsushita, *Soft Matter*, 2012, **8**, 6416-6429.
15. M. de Loos, B. L. Feringa and J. H. van Esch, *Eur. J. Org. Chem.*, 2005, **2005**, 3615-3631.
16. F. Fages, ed., *Low Molecular Mass Gelator*, Springer, Berlin, 2005.
17. http://a.rgbimg.com/cache1nUkdF/users/n/na/nazreth/600/mlCu7tg.jpg
18. S. Seiffert and J. Sprakel, *Chem. Soc. Rev.*, 2012, **41**, 909-930.
19. D. Diaz Diaz, D. Kuhbeck and R. J. Koopmans, *Chem. Soc. Rev.*, 2011, **40**, 427-448.
20. S.-k. Ahn, R. M. Kasi, S.-C. Kim, N. Sharma and Y. Zhou, *Soft Matter*, 2008, **4**, 1151-1157.
21. J. Hu, G. Zhang and S. Liu, *Chem. Soc. Rev.*, 2012, **41**, 5933-5949.
22. F. D. Jochum and P. Theato, *Chem. Soc. Rev.*, 2013, Advance Article.
23. O. Kuksenok, P. Dayal, A. Bhattacharya, V. V. Yashin, D. Deb, I. C. Chen, K. J. Van Vliet and A. C. Balazs, *Chem. Soc. Rev.*, 2013, Advance Article.
24. M. D. Segarra-Maset, V. J. Nebot, J. F. Miravet and B. Escuder, *Chem. Soc. Rev.*, 2013, Advance Article.
25. Q. Wang and M. Y. J. L. Mynar, E. Lee, M. Lee, K. Okuro, K. Kinbara, T. Aida, *Nature*, 2010, **463**, 339-343.
26. S. Dong, B. Zheng, D. Xu, X. Yan, M. Zhang and F. Huang, *Adv. Mater.*, 2012, **24**, 3191-3195.
27. J.-M. Lehn, *Supramolecular Chemistry*, Verlag Chemie, Weinheim/Germany, 1995.
28. J. W. Steed and J. L. Atwood, *Supramolecular Chemistry*, 2nd ed., Wiley, Chichester, 2009.
29. L. F. Lindoy, *The Chemistry of Macrocyclic Ligand Complexes*, Cambridge University Press, Cambridge, 1989.
30. K. Ariga and T. Kunitake, *Supramolecular Chemistry - Fundamentals and Applications*, Springer, Berlin, 2006.
31. C. M. Drain, A. Varotto and I. Radivojevic, *Chem. Rev.*, 2009, **109**, 1630-1658.
32. W.-S. Li and T. Aida, *Chem. Rev.*, 2009, **109**, 6047-6076.
33. M. G. Walter, A. B. Rudine and C. C. Wamser, *J. Porphyrins Phthalocyanines*, 2010, **14**, 759-792.
34. A. Yella, H.-W. Lee, H. N. Tsao, C. Yi, A. K. Chandiran, M. K. Nazeeruddin, E. W.-G.

Diau, C.-Y. Yeh, S. M. Zakeeruddin and M. Grätzel, *Science*, 2011, **334**, 629-634.
35. F. Vögtle, E. Weber, J. L. Toner, I. Goldberg, D. A. Laidler, J. F. Stoddart, R. A. Bartsch and C. L. Liotta, Crown ethers—complexes and selectivity in *Crown Ethers and Analogs (1989)*, eds. Fritz Vögtle and E. Weber, John Wiley & Sons, Inc., 1989, pp. 207-304.
36. J. S. Bradshaw and R. M. Izatt, *Acc. Chem. Res.*, 1997, **30**, 338-345.
37. G. W. Gokel, W. M. Leevy and M. E. Weber, *Chem. Rev.*, 2004, **104**, 2723-2750.
38. F. Huang and H. W. Gibson, *Prog. Polym. Sci.*, 2005, **30**, 982-1018.
39. A. L. Sisson, M. R. Shah, S. Bhosale and S. Matile, *Chem. Soc. Rev.*, 2006, **35**, 1269-1286.
40. T. M. Fyles, *Chem. Soc. Rev.*, 2007, **36**, 335-347.
41. B. Zheng, F. Wang, S. Dong and F. Huang, *Chem. Soc. Rev.*, 2012, **41**, 1621-1636.
42. L. Baldini, A. Casnati, F. Sansone and R. Ungaro, *Chem. Soc. Rev.*, 2007, **36**, 254-266.
43. S. Sameni, C. Jeunesse, D. Matt and J. Harrowfield, *Chem. Soc. Rev.*, 2009, **38**, 2117-2146.
44. D.-S. Guo and Y. Liu, *Chem. Soc. Rev.*, 2012, **41**, 5907-5921.
45. H. J. Kim, M. H. Lee, L. Mutihac, J. Vicens and J. S. Kim, *Chem. Soc. Rev.*, 2012, **41**, 1173-1190.
46. J. W. Steed, *Chem. Commun.*, 2013, **49**, 114-117.
47. J. W. Lee, S. Samal, N. Selvapalam, H.-J. Kim and K. Kim, *Acc. Chem. Res.*, 2003, **36**, 621-630.
48. J. Lagona, P. Mukhopadhyay, S. Chakrabarti and L. Isaacs, *Angew. Chem. Int. Ed.*, 2005, **44**, 4844-4870.
49. K. Kim, N. Selvapalam, Y. H. Ko, K. M. Park, D. Kim and J. Kim, *Chem. Soc. Rev.*, 2007, **36**, 267-279.
50. Rolf Gleiter and H. Hopf, *Modern Cyclophane Chemistry*, Wiley-VCH, Weinheim, 2005.
51. H. Dodziuk, *Cyclodextrins and Their Complexes: Chemistry, Analytical Methods, Applications*, Wiley-VCH, Weinheim, 2006.
52. E. Engeldinger, D. Armspach and D. Matt, *Chem. Rev.*, 2003, **103**, 4147-4174.
53. J. M. Haider and Z. Pikramenou, *Chem. Soc. Rev.*, 2005, **34**, 120-132.
54. S. Loethen, J. M. Kim and D. H. Thompson, *Polym. Rev.*, 2007, **47**, 383-418.
55. T. Ogoshi and A. Harada, *Sensors*, 2008, **8**, 4961-4982.
56. A. Harada, Y. Takashima and H. Yamaguchi, *Chem. Soc. Rev.*, 2009, **38**, 875-882.
57. Y. Chen and Y. Liu, *Chem. Soc. Rev.*, 2010, **39**, 495-505.
58. G. Chen and M. Jiang, *Chem. Soc. Rev.*, 2011, **40**, 2254-2266.
59. A. Hashidzume and A. Harada, *Polym. Chem.*, 2011, **2**, 2146-2154.
60. C. O. Mellet, J. M. G. Fernandez and J. M. Benito, *Chem. Soc. Rev.*, 2011, **40**, 1586-1608.
61. L. Zang, Y. Che and J. S. Moore, *Acc. Chem. Res.*, 2008, **41**, 1596-1608.
62. M. Iyoda, J. Yamakawa and M. J. Rahman, *Angew. Chem. Int. Ed.*, 2011, **50**, 10522-10553.
63. P. J. Cragg and K. Sharma, *Chem. Soc. Rev.*, 2012, **41**, 597-607.
64. M. Xue, Y. Yang, X. Chi, Z. Zhang and F. Huang, *Acc. Chem. Res.*, 2012, **45**, 1294-1308.
65. S. T. Schneebeli, C. Cheng, K. J. Hartlieb, N. L. Strutt, A. A. Sarjeant, C. L. Stern and J. F. Stoddart, *Chem. Eur. J.*, 2013, **19**, 3860-3868.
66. P. D. Frischmann and M. J. MacLachlan, *Chem. Soc. Rev.*, 2013, **42**, 871-890.
67. E. M. Driggers, S. P. Hale, J. Lee and N. K. Terrett, *Nat. Rev. Drug Discovery*, 2008, **7**, 608-624.
68. M. Albrecht, Supramolecular Containers: Host-Guest Chemistry and Reactivity in *Activating Unreactive Substrates*, Wiley-VCH Verlag GmbH & Co. KGaA, 2009, pp. 411-425.
69. J. M. Lehn, *Prix Nobel*, 1988, **1988**, 129.
70. C. J. Pedersen, *Angew. Chem. Int. Ed.*, 1988, **27**, 1021-1027.
71. R. J. Hooley and J. Rebek, Jr., *Chem. Biol.*, 2009, **16**, 255-264.
72. J. Zhou and H. Ritter, *Poly. Chem.*, 2010, **1**, 1552-1559.
73. G. Hettiarachchi, D. Nguyen, J. Wu, D. Lucas, D. Ma, L. Isaacs and V. Briken, *PLoS One*,

2010, **5**, e10514.
74. S. Walker, R. Oun, F. J. McInnes and N. J. Wheate, *Isr. J. Chem.*, 2011, **51**, 616-624.
75. H. J. Buschmann and E. Schollmeyer, *J. Cosmet. Sci.*, 2002, **53**, 185-191.
76. V. Schurig and H.-P. Nowotny, *Angew. Chem. Int. Ed. Engl.*, 1990, **29**, 939-957.
77. R. E. Mewis and S. J. Archibald, *Coord. Chem. Rev.*, 2010, **254**, 1686-1712.
78. C. A. Schalley, *Analytical Methods in Supramolecular Chemistry*, 2 ed., John Wiley and Sons Ltd, 2012.
79. J. J. van Gorp, J. A. J. M. Vekemans and E. W. Meijer, *J. Am. Chem. Soc.*, 2002, **124**, 14759-14769.
80. M. R. Hicks, J. Kowalski and A. Rodger, *Chem. Soc. Rev.*, 2010, **39**, 3380-3393.
81. J. Becerril, B. Escuder, J. F. Miravet, R. Gavara and S. V. Luis, *Eur. J. Org. Chem.*, 2005, **2005**, 481-485.
82. M. Lescanne, A. Colin, O. Mondain-Monval, F. Fages and J. L. Pozzo, *Langmuir*, 2003, **19**, 2013-2020.
83. M. Lescanne, P. Grondin, A. d'Aléo, F. Fages, J. L. Pozzo, O. M. Monval, P. Reinheimer and A. Colin, *Langmuir*, 2004, **20**, 3032-3041.
84. C. Chassenieux and L. Bouteiller, Rheology in *Supramolecular Chemistry: From Molecules to Nanomaterials*, eds. P. Gale and J. Steed, John Wiley & Sons, Ltd, 2012.
85. P. Terech, C. Rossat and F. Volino, *J. Colloid Interface Sci.*, 2000, **227**, 363-370.
86. W. Deng, H. Yamaguchi, Y. Takashima and A. Harada, *Angew. Chem. Int. Ed.*, 2007, **46**, 5144-5147.
87. Z. Ge, J. Hu, F. Huang and S. Liu, *Angew. Chem. Int. Ed.*, 2009, **48**, 1798-1802.
88. S.-Y. Hsueh, C.-T. Kuo, T.-W. Lu, C.-C. Lai, Y.-H. Liu, H.-F. Hsu, S.-M. Peng, C.-h. Chen and S.-H. Chiu, *Angew. Chem. Int. Ed.*, 2010, **49**, 9170-9173.
89. Y.-S. Su, J.-W. Liu, Y. Jiang and C.-F. Chen, *Chem. Eur. J.*, 2011, **17**, 2435-2441.
90. F. Cai, J.-S. Shen, J.-H. Wang, H. Zhang, J.-S. Zhao, E.-M. Zeng and Y.-B. Jiang, *Org. Biomol. Chem.*, 2012, **10**, 1418-1423.
91. H. Maeda, *Chem. Eur. J.*, 2008, **14**, 11274-11282.
92. B. Verdejo, F. Rodriguez-Llansola, B. Escuder, J. F. Miravet and P. Ballester, *Chem. Commun.*, 2011, **47**, 2017-2019.
93. M.-O. M. Piepenbrock, G. O. Lloyd, N. Clarke and J. W. Steed, *Chem. Rev.*, 2009, **110**, 1960-2004.
94. X. Yan, D. Xu, X. Chi, J. Chen, S. Dong, X. Ding, Y. Yu and F. Huang, *Adv. Mater.*, 2012, **24**, 362-369.
95. S. Tamesue, Y. Takashima, H. Yamaguchi, S. Shinkai and A. Harada, *Angew. Chem. Int. Ed.*, 2010, **49**, 7461-7464.
96. H. Xu and D. M. Rudkevich, *J. Org. Chem.*, 2004, **69**, 8609-8617.
97. H. Xu and D. M. Rudkevich, *Chem. Eur. J.*, 2004, **10**, 5432-5442.
98. Y.-L. Zhao and J. F. Stoddart, *Langmuir*, 2009, **25**, 8442-8446.
99. I. Hwang, W. S. Jeon, H.-J. Kim, D. Kim, H. Kim, N. Selvapalam, N. Fujita, S. Shinkai and K. Kim, *Angew. Chem. Int. Ed.*, 2007, **46**, 210-213.
100. X. Liao, G. Chen, X. Liu, W. Chen, F. Chen and M. Jiang, *Angew. Chem. Int. Ed.*, 2010, **49**, 4409-4413.
101. M. Nakahata, Y. Takashima, H. Yamaguchi and A. Harada, *Nat. Commun.*, 2011, **2**, 511.
102. A. l. Gasnier, G. Royal and P. Terech, *Langmuir*, 2009, **25**, 8751-8762.
103. T. Oku, Y. Furusho and T. Takata, *Angew. Chem. Int. Ed.*, 2004, **43**, 966-969.
104. J.-L. Zhou, X.-J. Chen and Y.-S. Zheng, *Chem. Commun.*, 2007, 5200-5202.
105. K. Maeda, H. Mochizuki, K. Osato and E. Yashima, *Macromolecules*, 2011, **44**, 3217-3226.
106. D. K. Smith, *Chem. Soc. Rev.*, 2009, **38**, 684-694.
107. S. Yagai and A. Kitamura, *Chem. Soc. Rev.*, 2008, **37**, 1520-1529.

108. J. W. Steed, *Chem. Soc. Rev.*, 2010, **39**, 3686-3699.
109. X. Yang, G. Zhang and D. Zhang, *J. Mater. Chem.*, 2011, **22**, 38-50.
110. H. Danjo, K. Hirata, S. Yoshigai, I. Azumaya and K. Yamaguchi, *J. Am. Chem. Soc.*, 2009, **131**, 1638-1639.
111. K. Tanaka, S. Hayashi and M. R. Caira, *Org. Lett.*, 2008, **10**, 2119-2122.
112. S. Dong, Y. Luo, X. Yan, B. Zheng, X. Ding, Y. Yu, Z. Ma, Q. Zhao and F. Huang, *Angew. Chem. Int. Ed.*, 2011, **50**, 1905-1909.
113. J. Liu, G. Chen, M. Guo and M. Jiang, *Macromolecules*, 2010, **43**, 8086-8093.
114. P. Du, J. Liu, G. Chen and M. Jiang, *Langmuir*, 2011, **27**, 9602-9608.
115. J. Liu, G. Chen and M. Jiang, *Macromolecules*, 2011, **44**, 7682-7691.
116. T. Nakagaki, A. Harano, Y. Fuchigami, E. Tanaka, S. Kidoaki, T. Okuda, T. Iwanaga, K. Goto and T. Shinmyozu, *Angew. Chem. Int. Ed.*, 2010, **49**, 9676-9679.
117. T. Kato, Y. Hirai, S. Nakaso and M. Moriyama, *Chem. Soc. Rev.*, 2007, **36**, 1857-1867.
118. A. R. Hirst, B. Escuder, J. F. Miravet and D. K. Smith, *Angew. Chem. Int. Ed.*, 2008, **47**, 8002-8018.
119. A. Ajayaghosh and V. K. Praveen, *Acc. Chem. Res.*, 2007, **40**, 644-656.
120. A. Ajayaghosh, V. K. Praveen and C. Vijayakumar, *Chem. Soc. Rev.*, 2008, **37**, 109-122.
121. S. S. Babu, S. Prasanthkumar and A. Ajayaghosh, *Angew. Chem. Int. Ed.*, 2012, **51**, 1766-1776.
122. P. Terech, G. Gebel and R. Ramasseul, *Langmuir*, 1996, **12**, 4321-4323.
123. S.-i. Tamaru, M. Nakamura, M. Takeuchi and S. Shinkai, *Org. Lett.*, 2001, **3**, 3631-3634.
124. M. Shirakawa, N. Fujita and S. Shinkai, *J. Am. Chem. Soc.*, 2003, **125**, 9902-9903.
125. M. Shirakawa, S.-i. Kawano, N. Fujita, K. Sada and S. Shinkai, *J. Org. Chem.*, 2003, **68**, 5037-5044.
126. T. Kishida, N. Fujita, K. Sada and S. Shinkai, *J. Am. Chem. Soc.*, 2005, **127**, 7298-7299.
127. M. Shirakawa, N. Fujita and S. Shinkai, *J. Am. Chem. Soc.*, 2005, **127**, 4164-4165.
128. J. Sly, P. Kasak, E. Gomar-Nadal, C. Rovira, L. Gorriz, P. Thordarson, D. B. Amabilino, A. E. Rowan and R. J. M. Nolte, *Chem. Commun.*, 2005, **0**, 1255-1257.
129. T. Akutagawa, K. Kakiuchi, T. Hasegawa, S.-i. Noro, T. Nakamura, H. Hasegawa, S. Mashiko and J. Becher, *Angew. Chem. Int. Ed.*, 2005, **44**, 7283-7287.
130. Y. Tatewaki, T. Hatanaka, R. Tsunashima, T. Nakamura, M. Kimura and H. Shirai, *Chem. Asian J.*, 2009, **4**, 1474-1479.
131. A. A. Sobczuk, S.-i. Tamaru and S. Shinkai, *Chem. Commun.*, 2011, **47**, 3093-3095.
132. A. A. Sobczuk, Y. Tsuchiya, T. Shiraki, S.-i. Tamaru and S. Shinkai, *Chem. Eur. J.*, 2012, **18**, 2832-2838.
133. K. Balakrishnan, A. Datar, W. Zhang, X. Yang, T. Naddo, J. Huang, J. Zuo, M. Yen, J. S. Moore and L. Zang, *J. Am. Chem. Soc.*, 2006, **128**, 6576-6577.
134. K. Cantin, S. Rondeau-Gagne, J. R. Neabo, M. Daigle and J.-F. Morin, *Org. Biomol. Chem.*, 2011, **9**, 4440-4443.
135. T. Ide, D. Takeuchi and K. Osakada, *Chem. Commun.* , 2012, **48**, 278-280.
136. S. Rondeau-Gagné, J. R. Néabo, M. Desroches, J. Larouche, J. Brisson and J.-F. Morin, *J. Am. Chem. Soc.*, 2012, **135**, 110-113.
137. J. Vollmeyer, S.-S. Jester, F. Eberhagen, T. Prangenberg, W. Mader and S. Höger, *Chem. Commun.*, 2012, **48**, 6547-6549.
138. S. Rondeau-Gagne, J. R. Neabo, M. Desroches, K. Cantin, A. Soldera and J.-F. Morin, *J. Mater. Chem. C*, 2013, **1**, 2680-2687.
139. J. H. Jung, Y. Ono and S. Shinkai, *Langmuir*, 1999, **16**, 1643-1649.
140. J. Hwa Jung, Y. Ono and S. Shinkai, *J. Chem. Soc., Perkin Trans. 2*, 1999, 1289-1292.
141. J. H. Jung, H. Kobayashi, M. Masuda, T. Shimizu and S. Shinkai, *J. Am. Chem. Soc.*, 2001, **123**, 8785-8789.
142. M. Llusar and C. Sanchez, *Chem. Mater.*, 2008, **20**, 782-820.

143. B. Escuder, F. Rodriguez-Llansola and J. F. Miravet, *New J. Chem.*, 2010, **34**, 1044-1054.
144. J. H. Jung, M. Park and S. Shinkai, *Chem. Soc. Rev.*, 2010, **39**, 4286-4302.
145. K. Murata, M. Aoki, T. Nishi, A. Ikeda and S. Shinkai, *J. Chem. Soc. Chem. Commun.*, 1991, 1715-1718.
146. T. D. James, H. Kawabata, R. Ludwig, K. Murata and S. Shinkai, *Tetrahedron*, 1995, **51**, 555-566.
147. J. H. Jung, Y. Ono and S. Shinkai, *Tetrahedron Lett.*, 1999, **40**, 8395-8399.
148. J. H. Jung, Y. Ono, K. Sakurai, M. Sano and S. Shinkai, *J. Am. Chem. Soc.*, 2000, **122**, 8648-8653.
149. J. H. Jung and S. Shinkai, *J. Incl. Phenomena Macrocyc. Chem.*, 2001, **41**, 53-59.
150. GRAS Notice No. GRN 000046, gamma-cyclodextrin, 2000.
151. GRAS Notice No. GRN 000074, beta-cyclodextrin, 2001.
152. GRAS Notice No. GRN 000155, alpha-cyclodextrin, 2004.
153. A. H. Jun Li, Mikiharu Kamachi, *Polym. J.*, 1994, **26**, 1019–1026.
154. J. Li, X. P. Ni and K. W. Leong, *J. Biomed. Mater. Res. A* 2003, **65A**, 196.
155. J. Li, *NPG Asia Mater*, 2010, **2**, 112-118.
156. J. Li, X. Li, Z. Zhou, X. Ni and K. W. Leong, *Macromolecules*, 2001, **34**, 7236-7237.
157. J. Li, X. Li, X. Ni and K. W. Leong, *Macromolecules*, 2003, **36**, 2661-2667.
158. Y. Chen, X.-H. Pang and C.-M. Dong, *Adv. Funct. Mater.* , 2010, **20**, 579-586.
159. D.-Q. Wu, T. Wang, B. Lu, X.-D. Xu, S.-X. Cheng, X.-J. Jiang, X.-Z. Zhang and R.-X. Zhuo, *Langmuir*, 2008, **24**, 10306-10312.
160. K. M. Huh, T. Ooya, W. K. Lee, S. Sasaki, I. C. Kwon, S. Y. Jeong and N. Yui, *Macromolecules*, 2001, **34**, 8657-8662.
161. J. Li and X. J. Loh, *Adv. Drug Delivery Rev.*, 2008, **60**, 1000-1017.
162. J. Li, Cyclodextrin Inclusion Polymers Forming Hydrogels in *Inclusion Polymers*, ed. G. Wenz, Springer Berlin Heidelberg, 2009, vol. 222, pp. 175-203.
163. J. Li, F. Zhao and J. Li, *Appl. Microbiol. Biotechnol.*, 2011, **90**, 427-443.
164. M. D. Moya-Ortega, C. Alvarez-Lorenzo, A. Concheiro and T. Loftsson, *Int. J. Pharm.*, 2012, **428**, 152-163.
165. J. Li, X. Li, X. Ni, X. Wang, H. Li and K. W. Leong, *Biomaterials*, 2006, **27**, 4132-4140.
166. K. Peng, I. Tomatsu and A. Kros, *Chem. Commun.*, 2010, **46**, 4094-4096.
167. K. Peng, C. Cui, I. Tomatsu, F. Porta, A. H. Meijer, H. P. Spaink and A. Kros, *Soft Matter*, 2010, **6**, 3778-3783.
168. N. i. Saleh, A. L. Koner and W. M. Nau, *Angew. Chem. Int. Ed.*, 2008, **47**, 5398-5401.
169. K. M. Park, K. Suh, H. Jung, D.-W. Lee, Y. Ahn, J. Kim, K. Baek and K. Kim, *Chem. Commun.*, 2009, **0**, 71-73.
170. V. D. Uzunova, C. Cullinane, K. Brix, W. M. Nau and A. I. Day, *Org. Biomol. Chem.*, 2010, **8**, 2037-2042.
171. E. A. Appel, X. J. Loh, S. T. Jones, F. Biedermann, C. A. Dreiss and O. A. Scherman, *J. Am. Chem. Soc.*, 2012, **134**, 11767-11773.
172. E. A. Appel, X. J. Loh, S. T. Jones, C. A. Dreiss and O. A. Scherman, *Biomaterials*, 2012, **33**, 4646-4652.
173. K. M. Park, J.-A. Yang, H. Jung, J. Yeom, J. S. Park, K.-H. Park, A. S. Hoffman, S. K. Hahn and K. Kim, *ACS Nano*, 2012, **6**, 2960-2968.
174. R. P. Wool, *Soft Matter*, 2008, **4**, 400-418.
175. B. J. Blaiszik, S. L. B. Kramer, S. C. Olugebefola, J. S. Moore, N. R. Sottos and S. R. White, *Annu. Rev. Mater. Res.*, 2010, **40**, 179-211.
176. K. Imato, M. Nishihara, T. Kanehara, Y. Amamoto, A. Takahara and H. Otsuka, *Angew. Chem. Int. Ed.*, 2012, **51**, 1138-1142.
177. M. Zhang, D. Xu, X. Yan, J. Chen, S. Dong, B. Zheng and F. Huang, *Angew. Chem. Int. Ed.*, 2012, **51**, 7011-7015.

178. G. von Kiedrowski, S. Otto and P. Herdewijn, *J. Syst. Chem.*, 2010, **1**, 1-6.
179. R. F. Ludlow and S. Otto, *Chem. Soc. Rev.*, 2008, **37**, 101-108.
180. J. Peyralans and S. Otto, *Curr. Opin. Chem. Biol.*, 2009, **13**, 705 - 713.
181. N. Giuseppone, *Acc. Chem. Res.*, 2012, **45**, 2178-2188.
182. T. Ueno, K. Bundo, Y. Akagi, T. Sakai and R. Yoshida, *Soft Matter*, 2010, **6**, 6072-6074.
183. R. Yoshida, *Adv. Mater.*, 2010, **22**, 3463-3483.
184. T. Ueno and R. Yoshida, *J. Phys. Chem. A*, 2011, **115**, 5231-5237.
185. M. M. Safont-Sempere, G. Fernández and F. Würthner, *Chem. Rev.*, 2011, **111**, 5784-5814.
186. P. Mukhopadhyay, A. Wu and L. Isaacs, *J. Org. Chem.*, 2004, **69**, 6157-6164.
187. S. Ghosh, A. Wu, J. C. Fettinger, P. Y. Zavalij and L. Isaacs, *J. Org. Chem.*, 2008, **73**, 5915-5925.
188. A. Wu and L. Isaacs, *J. Am. Chem. Soc.*, 2003, **125**, 4831-4835.
189. N. Tomimasu, A. Kanaya, Y. Takashima, H. Yamaguchi and A. Harada, *J. Am. Chem. Soc.*, 2009, **131**, 12339-12343.
190. W. Jiang and C. A. Schalley, *Proc. Natl. Acad. Sci. USA*, 2009, **106**, 10425-10429.
191. K. Sugiyasu, S.-i. Kawano, N. Fujita and S. Shinkai, *Chem. Mater.*, 2008, **20**, 2863-2865.
192. J. R. Moffat and D. K. Smith, *Chem. Commun.*, 2009, 316-318.
193. M. M. Smith and D. K. Smith, *Soft Matter*, 2011, **7**, 4856-4860.
194. L. M. Kyle, C. Lin, R. Jaclyn, R. S. Owen, C. Pepa, P. Alison, C. G. Peter, M. K. Stephen, K. O. R. Rachel, C. S. Louise and J. A. Dave, *Nat. Commun.*, 2013, **4**, 1480-1480.
195. A. Harada, R. Kobayashi, Y. Takashima, A. Hashidzume and H. Yamaguchi, *Nat. Chem.*, 2011, **3**, 34-37.
196. H. Yamaguchi, R. Kobayashi, Y. Takashima, A. Hashidzume and A. Harada, *Macromolecules*, 2011, **44**, 2395-2399.
197. Y. Zheng, A. Hashidzume, Y. Takashima, H. Yamaguchi and A. Harada, *Langmuir*, 2011, **27**, 13790-13795.
198. A. Hashidzume, Y. Zheng, Y. Takashima, H. Yamaguchi and A. Harada, *Macromolecules*, 2013, **46**, 1939-1947.
199. Y. Zheng, A. Hashidzume, Y. Takashima, H. Yamaguchi and A. Harada, *ACS Macro Letters*, 2012, **1**, 1083-1085.
200. H. Yamaguchi, Y. Kobayashi, R. Kobayashi, Y. Takashima, A. Hashidzume and A. Harada, *Nat. Commun.*, 2012, **3**, 603.
201. J. B. Fenn, M. Mann, C. K. Meng, S. F. Wong and C. M. Whitehouse, *Mass Spectrom. Rev.*, 1990, **9**, 37-70.
202. P. Kebarle and L. Tang, *Anal. Chem.*, 1993, **65**, A972-A986.
203. S. J. Gaskell, *J. Mass Spectrom.*, 1997, **32**, 677-688.
204. J. B. Fenn, *Angew. Chem. Int. Ed.*, 2003, **42**, 3871-3894.
205. F. Hillenkamp, M. Karas, R. C. Beavis and B. T. Chait, *Anal. Chem.*, 1991, **63**, 1193A-1202A.
206. M. Karas, U. Bahr and U. Gießmann, *Mass Spectrom. Rev.*, 1991, **10**, 335-357.
207. Y. Tanaka, K. Otsuka and S. Terabe, *J. Pharmaceut. Biomed. Anal.*, 2003, **30**, 1889-1895.
208. A. J. Loo, *Mass Spectrom. Rev.*, 1997, **16**, 1-23.
209. J. L. Beck, M. L. Colgrave, S. F. Ralph and M. M. Sheil, *Mass Spectrom. Rev.*, 2001, **20**, 61-87.
210. P. Sarni-Manchado and V. Cheynier, *J. Mass Spectrom.*, 2002, **37**, 609-616.
211. J. A. E. Kraunsoe, R. T. Aplin, B. Green and G. Lowe, *FEBS Lett.*, 1996, **396**, 108-112.
212. C. Uetrecht and A. J. R. Heck, *Angew. Chem. Int. Ed.*, 2011, **50**, 8248-8262.
213. M. Kogej and C. A. Schalley, Mass Spectrometry and Gas Phase Chemistry of Supramolecules in *Analytical Methods in Supramol. Chem.*, ed. C. A. Schalley, Wiley-VCH, Weinheim, 2007, pp. 104-160.
214. B. Baytekin, H. T. Baytekin and C. A. Schalley, *Org. Biomol. Chem.*, 2006, **4**, 2825-2841.

215. C. A. Schalley, *Mass Spectrom. Rev.*, 2001, **20**, 253-309.
216. C. A. Schalley and A. Springer, *Mass Spectrometry of Non-Covalent Complexes: Supramolecular Chemistry in the Gas Phase*, Wiley, Hoboken, 2009.
217. H. D. Winkler, PhD thesis, Freie Universität Berlin, 2011.
218. J. V. Iribarne and B. A. Thomson, *J. Chem. Phys.*, 1976, **64**, 2287-2294.
219. B. A. Thomson and J. V. Iribarne, *J. Chem. Phys.*, 1979, **71**, 4451-4463.
220. J. B. Fenn, J. Rosell and C. K. Meng, *J. Am. Soc. Mass Spectrom.*, 1997, **8**, 1147-1157.
221. M. Dole, L. L. Mack, R. L. Hines, R. C. Mobley, L. D. Ferguson and M. B. Alice, *J. Chem. Phys.*, 1968, **49**, 2240-2249.
222. P. Kebarle and M. Peschke, *Anal. Chim. Acta*, 2000, **406**, 11-35.
223. J. H. Gross, *Mass Spectrometry - A Textbook*, Springer, Heidelberg, 2004.
224. S. A. McLuckey and D. E. Goeringer, *J. Mass Spectrom.*, 1997, **32**, 461-474.
225. M. W. Senko, J. P. Speir and F. W. McLafferty, *Anal. Chem.*, 1994, **66**, 2801-2808.
226. R. A. Zubarev, K. F. Haselmann, B. Budnik, F. Kjeldsen and F. Jensen, *Eur. J. Mass Spectrom.*, 2002, **8**, 337 - 349.
227. R. A. Zubarev, *Mass Spectrom. Rev.*, 2003, **22**, 57-77.
228. R. A. Zubarev, *Curr. Opin. Biotechnol.*, 2004, **15**, 12-16.
229. T.-Y. Huang, J. F. Emory, R. A. J. O'Hair and S. A. McLuckey, *Anal. Chem.*, 2006, **78**, 7387-7391.
230. D. L. Swaney, G. C. McAlister, M. Wirtala, J. C. Schwartz, J. E. P. Syka and J. J. Coon, *Anal. Chem.*, 2007, **79**, 477-485.
231. E. Mirgorodskaya, P. O'Connor and C. Costello, *J. Am. Soc. Mass Spectrom.*, 2002, **13**, 318-324.
232. T. E. Wales and J. R. Engen, *Mass Spectrom. Rev.*, 2006, **25**, 158-170.
233. J. Mandell, A. Baerga-Ortiz, A. Falick and E. Komives, Measurement of Solvent Accessibility at Protein-Protein Interfaces in *Protein-Ligand Interactions*, ed. G. Ulrich Nienhaus, Humana Press, 2005, vol. 305, pp. 65-79.
234. I. A. Kaltashov, C. E. Bobst and R. R. Abzalimov, Hydrogen/Deuterium Exchange Mass Spectrometry (HDX MS) in the Studies of Architecture, Dynamics, and Interactions of Biopharmaceutical Products in *Mass Spectrometry Handbook*, John Wiley & Sons, Inc., 2012, pp. 227-241.
235. H. D. F. Winkler, E. V. Dzyuba and C. A. Schalley, *New J. Chem.*, 2011, **35**, 529-541.
236. S. A. Hofstadler, K. A. Sannes-Lowery and R. H. Griffey, *J. Mass Spectrom.*, 2000, **35**, 62-70.
237. J. I. Brauman, Factors Influencing Thermal Ion-Molecule Rate Constants in *Kinetics of Ion-Molecule Reactions*, ed. P. Ausloos, Plenum Press, New York, 1979, pp. 153-164.
238. S. G. Lias, *J. Phys. Chem.*, 1984, **88**, 4401-4407.
239. P. Ausloos and S. G. Lias, *J. Am. Chem. Soc.*, 1981, **103**, 3641-3647.
240. E. Gard, M. K. Green, J. Bregar and C. B. Lebrilla, *J. Am. Soc. Mass Spectrom.*, 1994, **5**, 623-631.
241. T. Wyttenbach and M. T. Bowers, *J. Am. Soc. Mass Spectrom.*, 1999, **10**, 9-14.
242. C. Lifshitz, *Int. J. Mass Spectrom.*, 2004, **234**, 63-70.
243. U. Mazurek, O. Geller, C. Lifshitz, M. A. McFarland, A. G. Marshall and B. G. Reuben, *J. Phys. Chem. A*, 2005, **109**, 2107-2112.
244. J. E. Chipuk and J. S. Brodbelt, *Int. J. Mass Spectrom.*, 2009, **287**, 87-95.
245. S. Campbell, M. T. Rodgers, E. M. Marzluff and J. L. Beauchamp, *J. Am. Chem. Soc.*, 1995, **117**, 12840-12854.
246. X. Cheng and C. Fenselau, *Int. J. Mass Spectrom. Ion Processes*, 1992, **122**, 109-119.

12.2 Curriculum Vitae

For reasons of data protection, the Curriculum Vitae is not published in the online version.

12.3 Publications and presentations

PUBLICATIONS:

9. **Z. Qi**, C. Schlaich, C.A. Schalley*, Gas-phase multivalency: H/D-exchange reactions unravel the dynamic "rock 'n roll" motion in the dendrimer-dendrimer complexes, *Chem. Sci*., submitted
8. **Z. Qi**, C. Wu, P. M. de Molina, H. Sun, A. Schulz, C. Griesinger, M. Gradzielski, R. Haag, M.B. Ansorge-Schumacher, C.A. Schalley*, Fibrous networks with incorporated macrocycles: a chiral stimuli-responsive supramolecular supergelator and its application to biocatalysis in organic media. *Chem. Eur. J.*, **2013**, *19*, accepted
7. C. Talotta, C. Gaeta*, **Z. Qi**, C.A. Schalley*, P. Neri*, Pseudorotaxanes with self-sorted sequences and stereochemistry. *Angew. Chem. Int. Ed.*, **2013**, *52*, accepted
6. **Z. Qi**, P.M. de Molina, W. Jiang, Q. Wang, K. Nowosinski, A. Schulz, M. Gradzielski, C.A. Schalley*, Systems Chemistry: Logic gates based on the stimuli-responsive gel-sol transition of a crown-ether functionalized bis-urea-gelator. *Chem. Sci.*, **2012**, *3*, 2073-2082
5. **Z. Qi**, C.A. Schalley*, Hostguest chemistry of dendrimers in the gas phase. *Supramol. Chem.* **2010**, *22*, 672-682
4. Y. Xie, X. Wang, X. Han, X. Xue, W. Ji, **Z. Qi**, J.Q. Liu, B. Zhao,* Y. Ozaki, Sensing of polycyclic aromatic hydrocarbons with cyclodextrin inclusion complexes on silver nanoparticles by surface-enhanced Raman scattering. *Analyst*, **2010**, *135*, 1389-1394
3. Y. Ge, **Z. Qi**, Y. Wang, X. Liu, J. Li, J. Xu, J.Q. Liu*, J.C. Shen, Engineered selenium-containing glutaredoxin displays strong glutathione peroxidase activity rivaling natural enzyme. *Int. J. Biochem. Cell Biol*. **2009**, *41*, 900-906
2. X. Li, **Z. Qi**, K. Liang, X. Bai, J. Xu, J.Q. Liu*, J.C. Shen. An artificial supramolecular nanozyme based on β-cyclodextrin-modified gold nanoparticles. *Catal. Lett*. **2008**, *124*, 3-4
1. J. Li, X.M. Liu, T.Y. Ji, **Z. Qi**, Y. Ge, J.Y. Xu, J.Q. Liu*, G.M. Luo, J.C. Shen, Biosynthesis of selenosubtilisim: a novel way to target selenium into the active site of subtilisin. *Chin. Sci. Bull.* **2008**, *53*, 2454-2461

ORAL PRESENTATIONS:

1. **Z. Qi**, The recent gel story in AG Schalley, *1st combined external doctoral students workshop Graduate Schools SFB 765 and 858*, Rheinsberg, Germany, March.6-8, **2013**.
2. **Z. Qi**, The gel story in AG Schalley, *G4 Workshop 2011*, Wildenhof, Aachen, Germany, September 13-15, **2011**.
3. **Z. Qi**, Rock and Roll with my Friend: Crown-substituted Dendrimers in the Gas Phase, *G3 Workshop 2010 ,* Burg Bischofstein, Rheinland-Pfalz, Germany, July 21-24, **2010**.

POSTER PRESENTATIONS:

1. Tag der Chemie (TDC) in Technischen Universität Berlin, June. 12, **2012**
2. MESA+SFB 765 minisymposium about multivalency in chemistry and supramolecular chemistry in Berlin, Germany, June. 5, **2012**
3. 2nd Poster Prize in **DAAD-GCLB** Symposium on Life Science and Biotechnology in Bonn, Germany, Spet. 24-25, **2011**.

12.4 Acknowledgement

First of all, I thank my supervisor Prof. Dr. *Christoph A. Schalley* for offering me the opportunity to accomplish my Ph.D. thesis in his group. I am deeply indebted to his strong support in my scientific research and personal life. I appreciate he gives me freedom to explore new areas based on my own research interests, provides me with numerous scientific suggestion, and teach me with his profound knowledge and experience.

I wish to express my sincere gratitude to Prof. Dr. *Rainer Haag* for accepting to act as the second referee and spending his valuable time on reviewing my thesis. I am so grateful for his constructive suggestion in my research and collative projects, as well as generous help for my future career development.

All my former and current colleagues in the Schalley group are acknowledged for their great help in my research and personal life during the last years. Their encouragements and useful suggestions give me the power to overcome difficulties in my research. They are Dr. *Andreas Springer*, Prof. Dr. *Wei Jiang*, Dr. *Boris Brusilowskij*, Dr. *Rainer Brehme*, Dr. *Ralf Troff*, Dr. *Dominik Weimann*, Dr. *Wang Qi*, Dr. *Egor Dzyuba*, Dr. *Henrik Winkler*, Dr. *Moorthy Suresh*, Dr. *Johannes Poppenberg*, *Lena Kaufmann* M. Sc., *Dominik Sattler* M. Sc., *Christoph Traulsen* M. Sc., *Sebastian Richter* M. Sc., *Karol Nowosinski* M. Sc., *Luca Cera* M. Sc., *Nora Löw* M. Sc., *Felix Schwarz* M. Sc., *Larissa von Krbek* M. Sc., *Marc Driessen* M. Sc., *David Komaromi M. Sc.*, *Antti Senf* M. Sc., *Valentin Kunz* M. Sc, *Julian Sklorz* M. Sc., *Lee Garrett* M. Sc., *Sophia Möhl* M. Sc., *Maria Tatzke* M. Sc., *Eliza Kanaki* M. Sc., *Melanie Göth M. Sc.*, *Christoph Schlaich*, *Mehdi Hamze*, *Stefan Leisering*, *Hendrik Schroder*, *Karoline Täuber*, *Andreas Drach*.

In particular, I acknowledge my collaborators: Prof. Dr. *Michael Gradzielski*, Dr. *Paula Malo de Molina* for the rheological characterization of gel materials; Prof. Dr. *Marion B. Ansorge-Schumacher*, Dr. *Changzhu Wu* for the Pickering emulsion project; Prof. Dr. *Christian Griesinger*, Dr. *Han Sun* for the VCD measurements; *Nora Löw* M. Sc. for the ITC measurements; Prof. Dr. *Bert Meijer* (TU Eindhoven) and Dr. *Henk M. Janssen* (SyMO-Chem B.V., Eindhoven) for providing the POPAM dendrimers; Prof. Dr. *Placido Neri*, Dr. *Carmen Talotta*, Dr. *Carmine Gaeta* for the self-sorting project. They expanded

my knowledge so much, and great enrich my expertise in broader areas.

I thank Frau *Andrea Schulz* for helping me with the AFM and TEM measurements through all my research projects, and spending her valuable time on proofreading the manuscripts and providing very useful suggestions. I am also grateful for her assistance for chemical ordering and other lab techniques.

I thank Dr. *Andreas Springer*, Dipl.-Ing. *Fabian Klautzsch*, Dr. *Henrik Winkler*, and their colleagues Herrn *Thomas Kolrep* and Frau *Isolde S. Mäckle-Jentsch*, Herrn *Jürgen Lindemann* in the MS department their professional help on mass spectrometric experiments.

I appreciate Dr. *Andreas Schäfer* and his colleagues in the NMR department for their scientific help on NMR experiments.

I thank all the service and education provided by the professors and others people working in the Institut für Chemie und Biochemie of Freie Universität Berlin.

I also thank *Nora Löw* M. Sc., *Christoph Traulsen* M. Sc., *Jason Heier* M. Sc., *Sebastian Richter* M. Sc., *Karol Nowosinski* M. Sc., *Larissa von Krbek* M. Sc. spending their valuable time on proofreading my thesis and providing very useful suggestions.

I thank the Deutsche Forschungsgemeinschaft for financial support (SCHA 893/5 and SFB 765). China Scholarship Council (CSC) is acknowledged for providing me a Ph.D. fellowship.

I am very grateful to my family and friends for their care throughout all the years. They provide me so many help that encourages me to pursue my dream in Germany.

Finally, I especially thank my beloved wife Dr. Yan Ge. I don’t know how to express my gratitude. You help me so much from every aspect. Whenever I need you, you are always with me. Thank you to accompany me through all these years.